Broad or Wide Complex Regular QRS Monomorphic Ventricular Tachycardia (BCT or WCT) in young man with spontaneous Type 1 ECG Brugada pattern

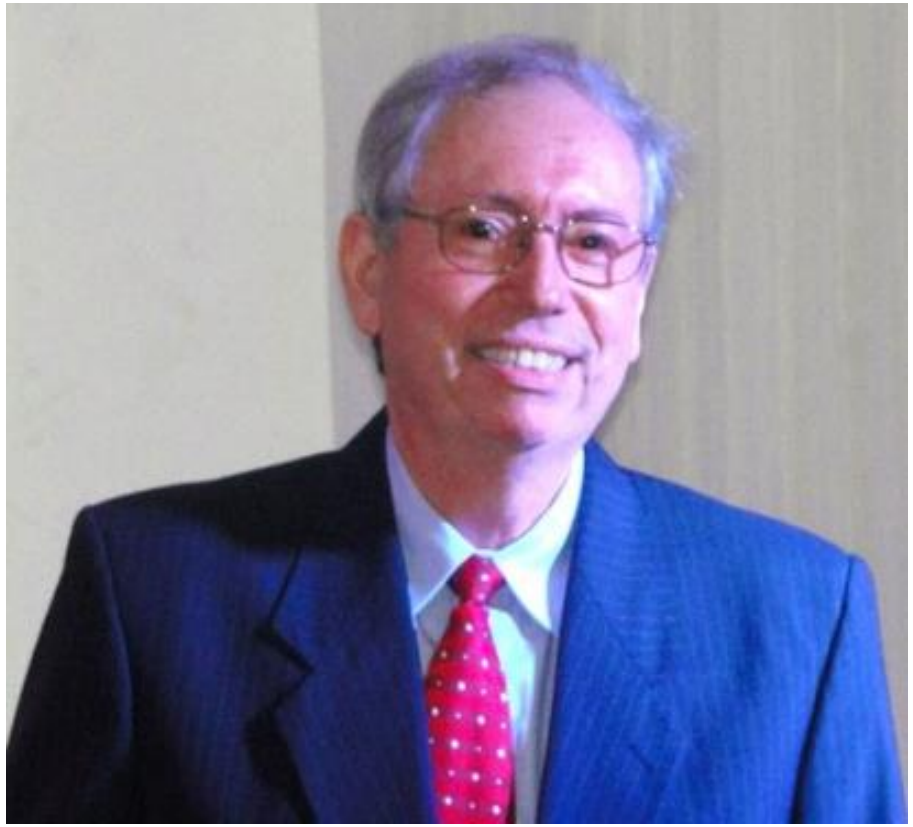

Raimundo Barbosa-Barros, MD
Chief of the Coronary Center of the Hospital de Messejana Dr. Carlos Alberto Studart Gomes. Fortaleza – CE- Brazil

Case report

English:

Male, 33-year-old patient (previously healthy) was admitted into the emergency room with oppressive chest pain.
Hemodynamically stable.
Negative family history.
He did not use any medication or illegal drugs. No previous syncope. No fever during ECG recordings.
The physician interpreted the initial ECG as Supraventricular Tachycardia with aberrancy (SVT-A) and he administered adenosine injection, unsuccessfully.
Later, 50 J electrical cardioversion was conducted, which led to VF and a short while later 200 J defibrillation was applied, successfully.
Normal troponin and electrolyte levels.
The patient was moved to the Hospital, where coronary angiography was performed (normal).
Normal echo.

Questions:

1. What is the diagnosis of ECG-1 and why?
2. What is the diagnosis of ECG-2 registered immediately after electrical cardioversion?
3. What is the diagnosis of ECG-3 performed after coronary angiography than normal result?
4. What is diagnostic ECG-4 performed 24 hours after admission?
5. What is the diagnosis ECG-5 performed 72 hours after being asymptomatic admission with high right precordial V_{1H} V2H
6. Can this patient be carrying the Brugada syndrome with monomorphic TV?

Spanish:

Reporte de caso

Hombre de 33 años (previamente sano)
Ingresó a la urgencia con dolor en el pecho opresivo
Hemodinamicamente estable
Antecedentes familiares negativos
No utiliza ningún medicamento o drogas ilícitas .Niega sincope Sin fiebre durante registros de ECG
El médico interpretó el ECG inicial como siendo una taquicardia supraventricular con aberrancia (TSV-A) y administró una inyección de adenosina sin éxito.
Posteriormente se realizó una cardioversión eléctrica (CVE) con 5OJ que degeneró en una FV revertida con 200J (bifásico).
Troponina normal.
Electrólitos normales.
El paciente fue trasladado para el Hospital donde llevan a cabo una coronariografía que resultó normal.
Ecocardiografía normal.

Preguntas:

1. ¿Cual es el diagnóstico del ECG-1 y porque?
2. ¿Cual es el diagnóstico del ECG-2 registrado inmediatamente después de la cardioversión eléctrica
3. ¿Cual es el diagnóstico del ECG-3 realizado después de la coronariografia que resultó normal?
4. ¿Cual es el diagnóstico del ECG-4 realizado 24 horas después de la admisión?
5. ¿Cual es el diagnóstico del ECG-5 realizado 72 horas después de la admisión estando asintomático con las precordiales derechas altas V_{1H} V_{2H}
6. ¿Puede este paciente ser portador del sindrome de Brugada con TV monomórfica?

ECG-1 At admission

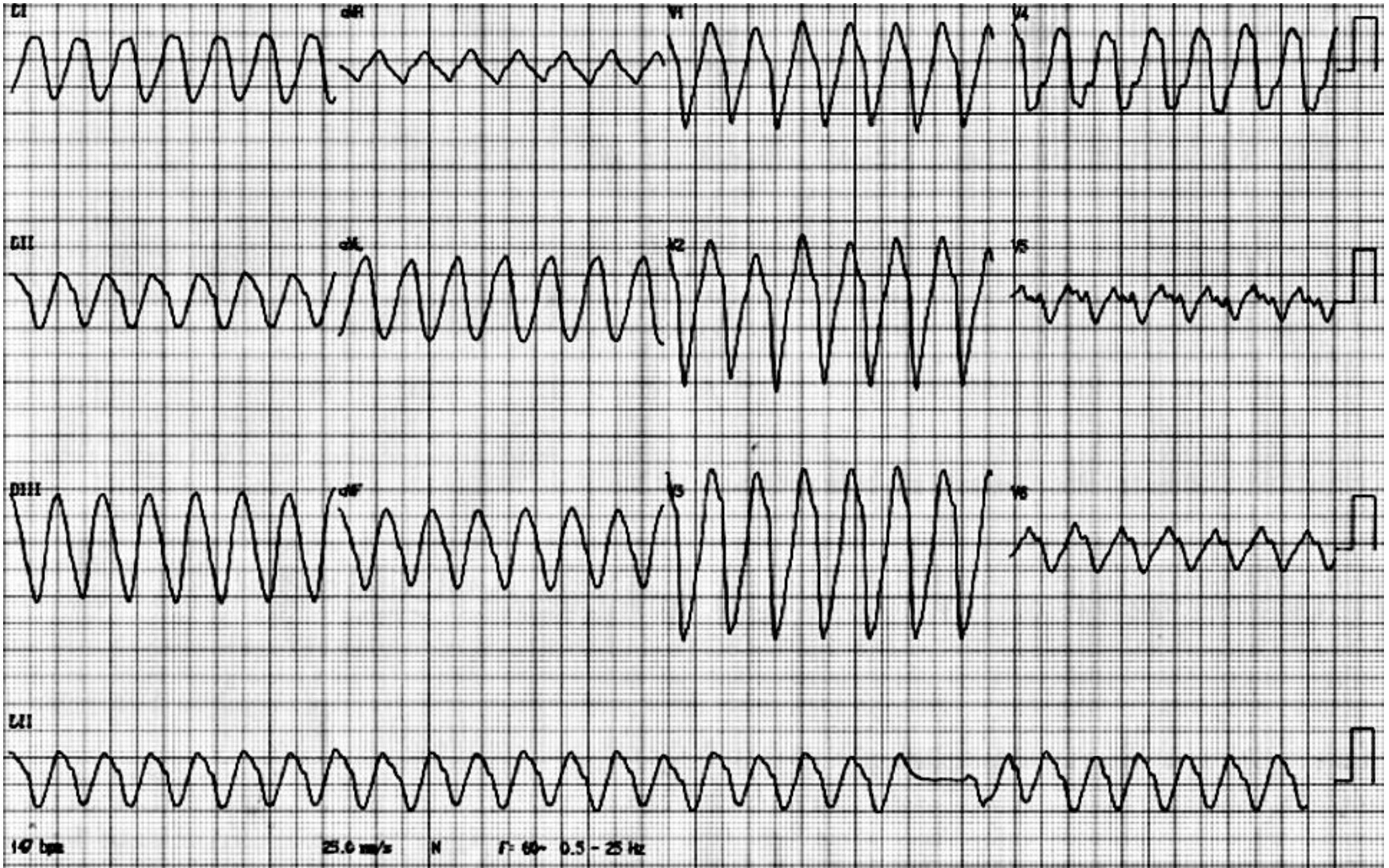

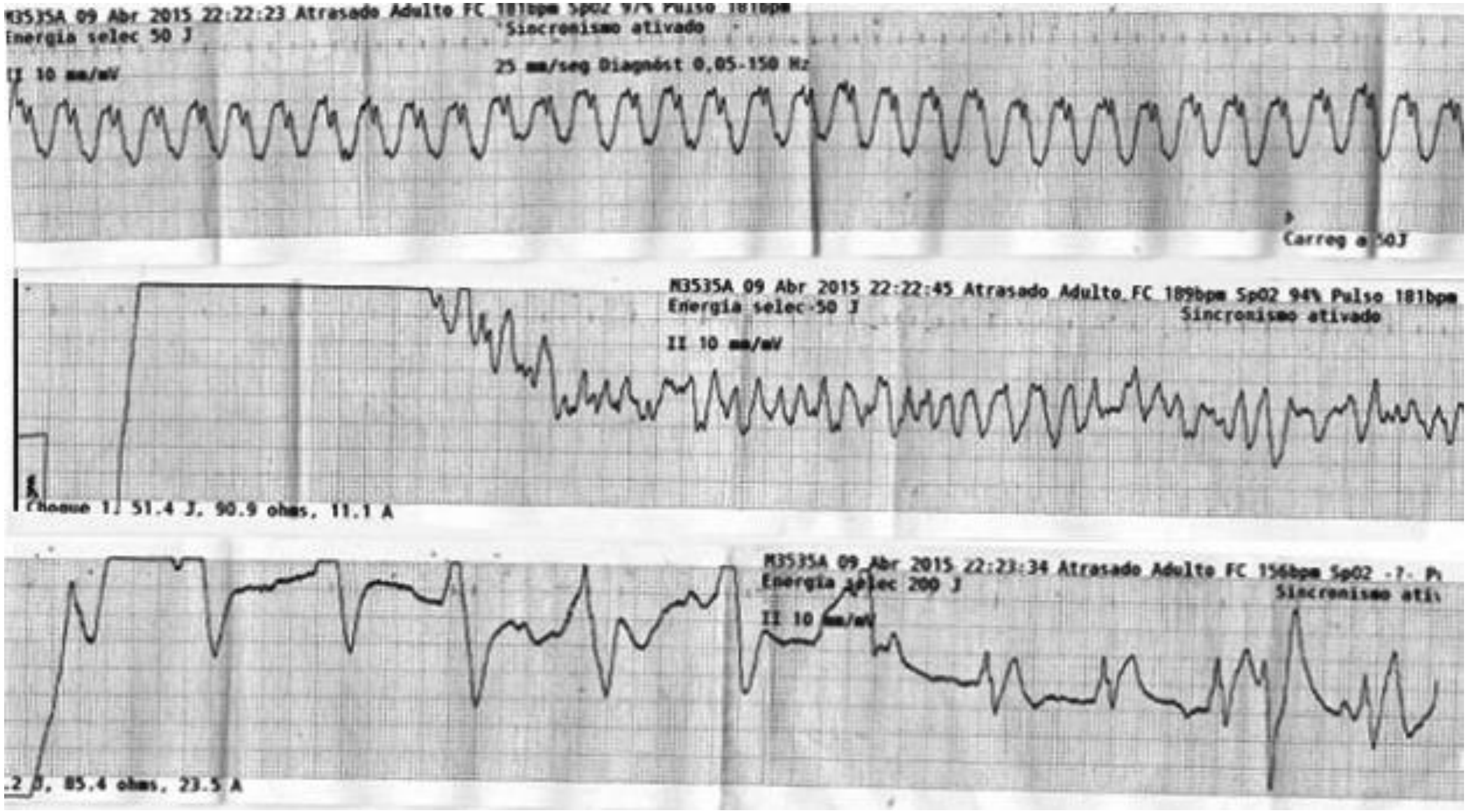
M3535A 09 Abr 2015 22:22:23 Atrasado Adulto FC 181bpm SpO2 97% Pulso 181bpm
Energia selec 50 J
Sincronismo ativado
II 10 mm/mV
25 mm/seg Diagnóst 0,05-150 Hz
Carreg a 50J
M3535A 09 Abr 2015 22:22:45 Atrasado Adulto FC 189bpm SpO2 94% Pulso 181bpm
Energia selec 50 J
Sincronismo ativado
II 10 mm/mV
Choque 1: 51.4 J, 90.9 ohms, 11.1 A
M3535A 09 Abr 2015 22:23:34 Atrasado Adulto FC 156bpm SpO2 -?- Pu
Energia selec 200 J
Sincronismo ati
II 10 mm/mV
.2 J, 85.4 ohms, 23.5 A

ECG-2 After electrical cardioversion

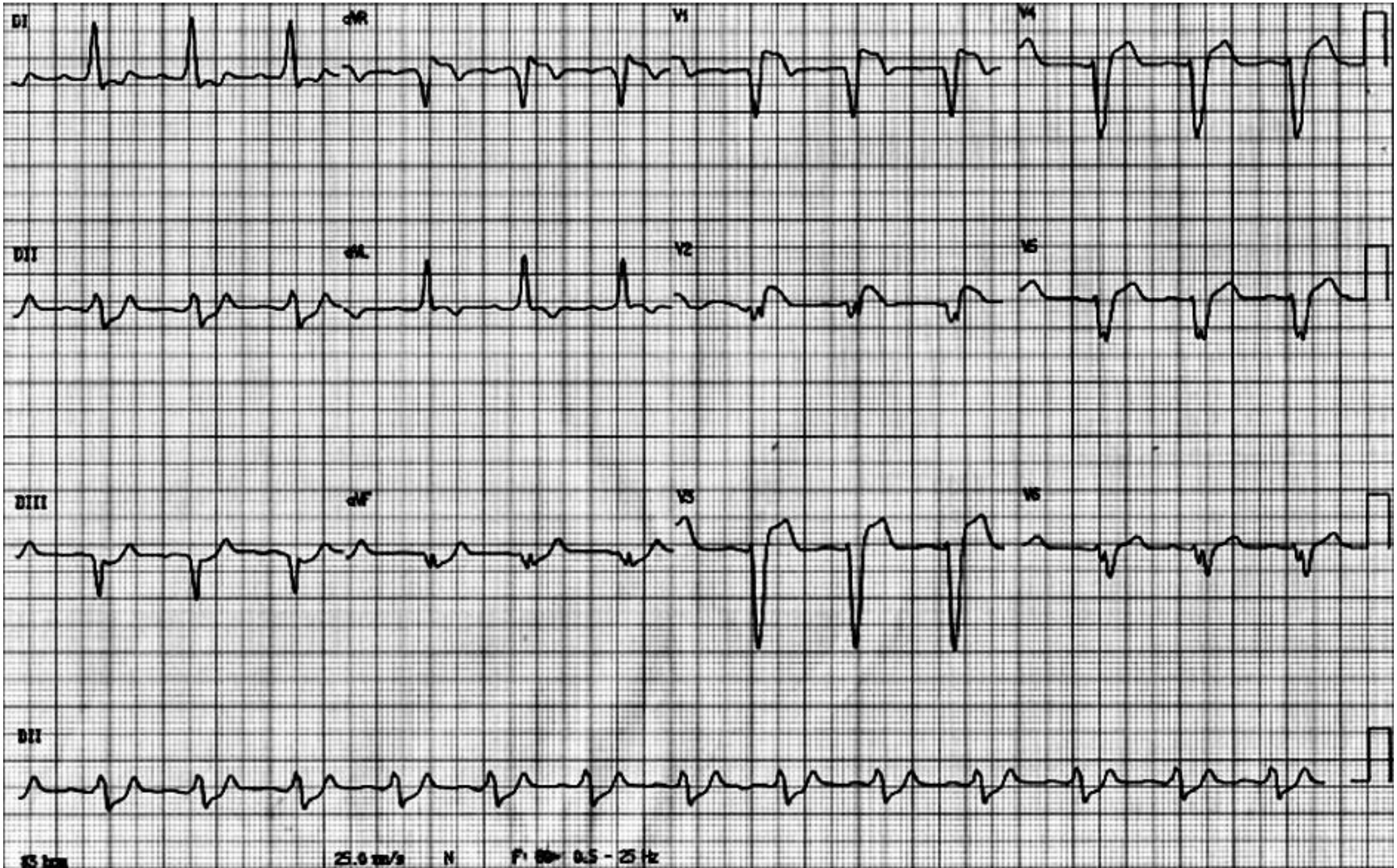

ECG-3 After coronary angiography

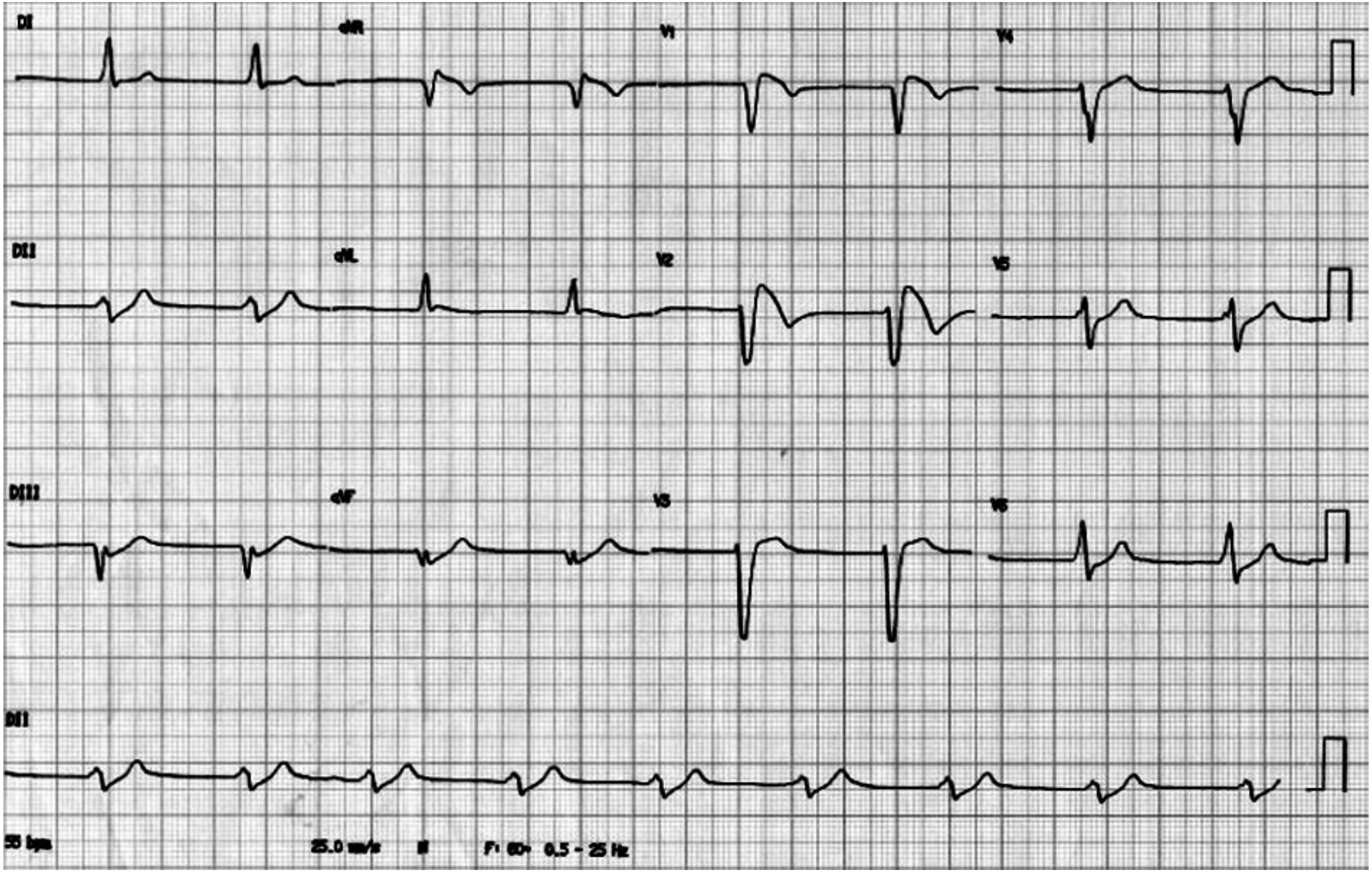

ECG-4 24 hours after admission

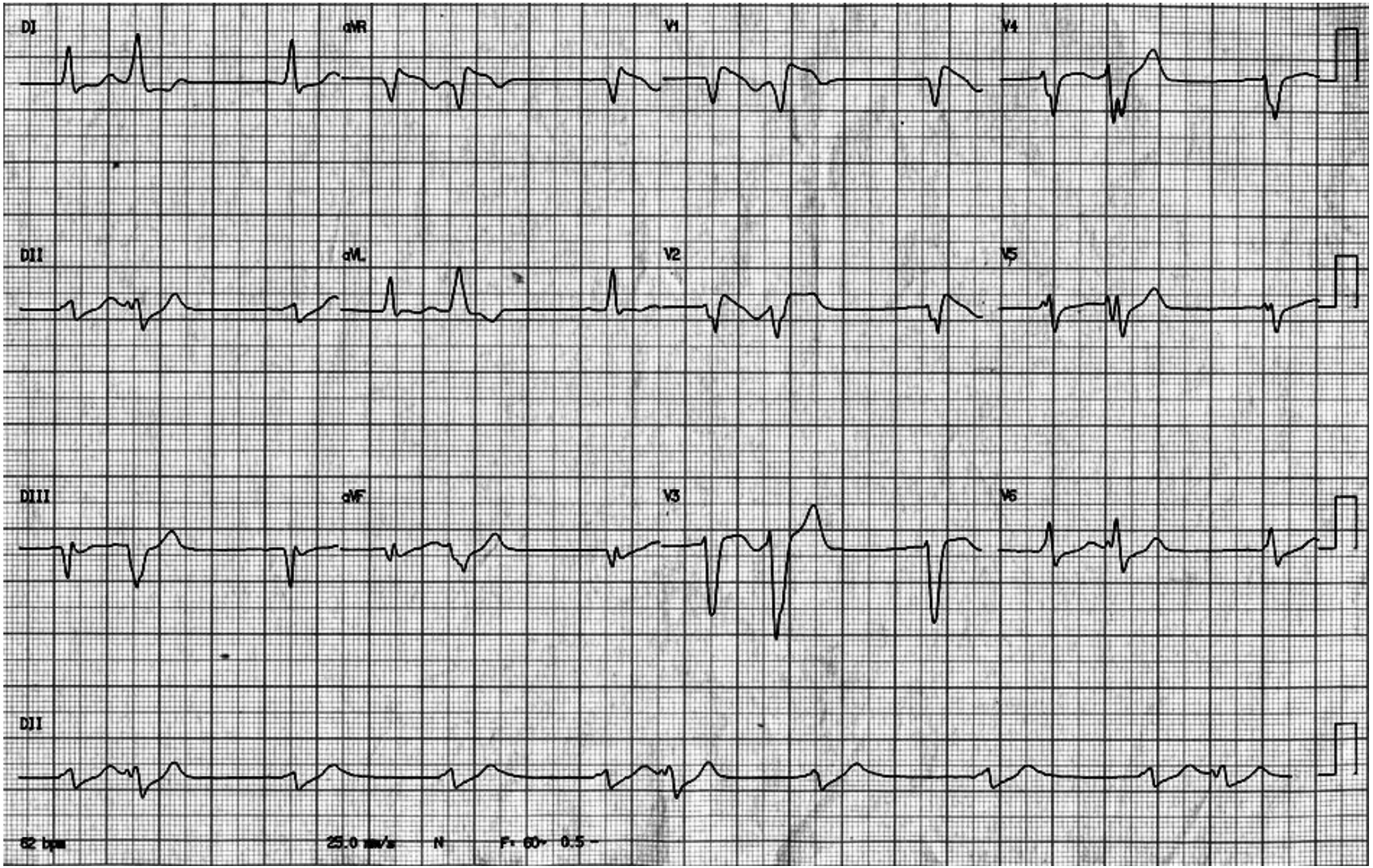

ECG-5 72 hours after admission (asymptomatic) V_{1H} V_{2H}

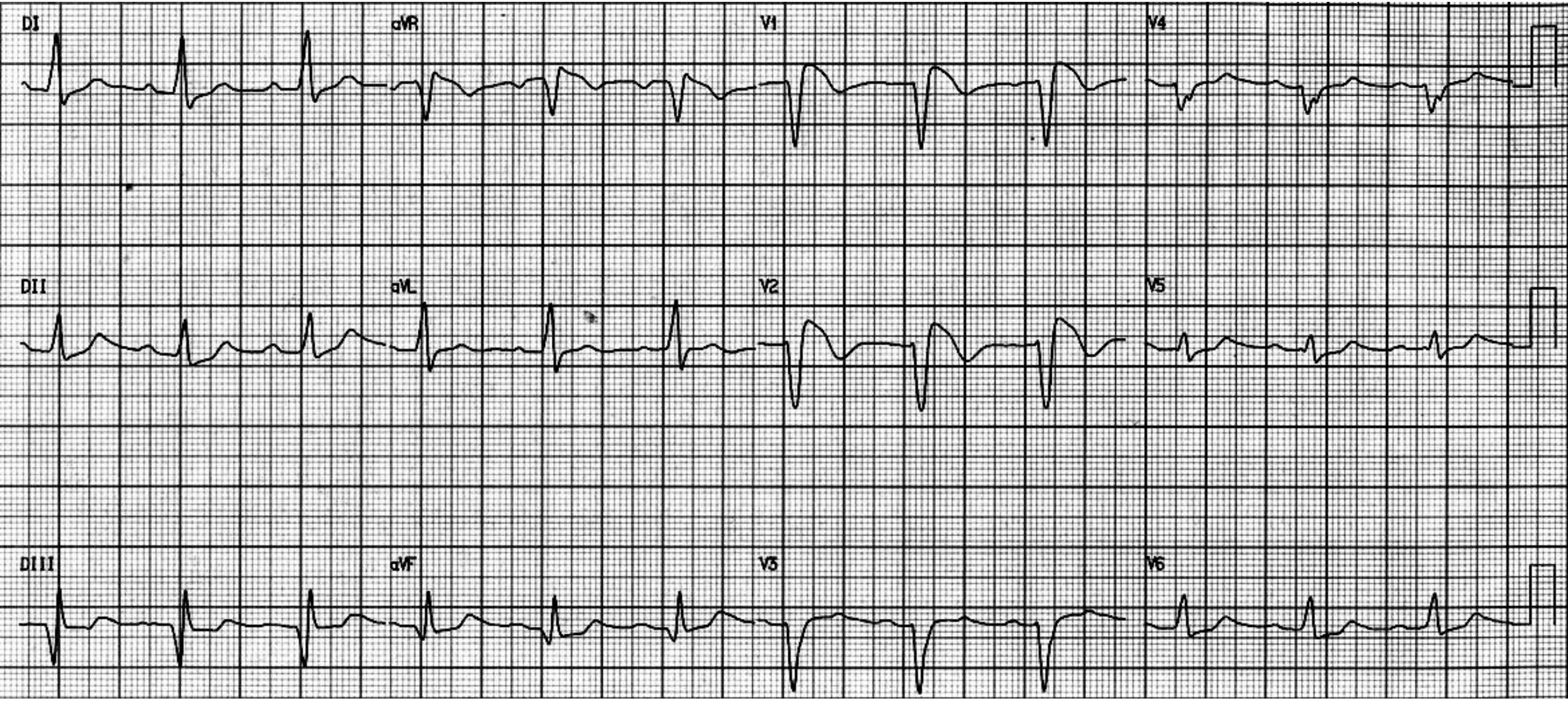

Colleagues opinions

ECG 1 classic VT from apical crux which can be seen in normal hearts.

ECG 2 Vf post shock ? synchronized shock?

ECG3 Antero lateral MI post cardioversion

ECG 4Classic Brugada pattern junctional rhythm and capture beats R now visible in V5 and V6.

ECG 5 Sinus rhythm and ventricular bigemini Brugada

Brugada most often gives rise to Polymorphous or VF,have seen Monomorphic VT while taking Quinidine.Needs AICD plus Quinidine failing this consider ablation either via MCV or over epicardium .

Melvin M **Scheinman**, Professor of Medicine
Department of Cardiac Electrophysiology, University of
California San Francisco,
San Francisco, California, USA.
Address:
UCSF
Electrophysiology Service
500 Parnassus Avenue
San Francisco, CA 94143-1354 USA

Melvin.Scheinman@ucsf.edu

Portuguese Minha impressão:

Resp. 1: TV monomórfica pelos seguintes critérios: desvio extremo do eixo do QRS, duração do QRS acima de 160ms, ausência de RS em precordiais, AVR positivo.
Resp. 2:Ritmo sinusal. Atraso inespecífico da condução intraventricular, área eletricamente inativa em parede anterior, supradesnível de ST discordante de V1-3, supra de ST em AVR, infra de ST ascendente em DIIDIIIAVF - As alterações da repolarização observadas podem ocorrer de forma transitória após a desfibrilação elétrica.
Resp. 3: Ritmo juncional.
Resp. 4: Ritmo juncional com extrassístoles ventriculares isoladas e monomórficas, fragmentadas e com transição tardia nas precordiais, sugerindo origem no VD.
Resp. 5: Ritmo sinusal, BAV 1º grau, atraso inespecífico da condução intraventricular, área eletricamente inativa em parede anterior (V1-4), supradesnivelamento de ST acima de 2mm em V1-2 sugestivo de Brugada.
Resp. 6: A síndrome de Brugada não está associada a TV monomórfica. Este tipo de taquicardia geralmente está relacionada com a presença de cardiopatia estrutural com substrato bem definido (área de fibrose e fibras viáveis de permeio com diferentes tempos de condução). A displasia arritmogênica do VD pode eventualmente apresentar um padrão eletrocardiográfico semelhante à S. de Brugada. A morfologia da TV observada neste caso sugere origem em região ínfero-apical do VD. Apesar de ecocardiograma e coronariografia sem alterações, a ressonância magnética seria fundamental para avaliar o VD e definir o a etiologia da TV neste caso.
Cordial abraço,

Acácio **Fernandes-Cardoso** M.D. Cardiologista – HBPSCS São Paulo Brazil.

My interpretation:
Reply 1: monomorphic VT by the following criteria: extreme QRS axis shift, QRS duration above 160 ms, absence of sinus rhythm in precordial leads, positive AVR.
Reply 2: sinus rhythm. Unspecific delay of intraventricular conduction, electrically inactive area in anterior wall, mismatching ST elevation in V1-V3, ST elevation in AVR, upsloping ST depression in DII, DIII, AVF. The repolarization alterations observed could occur transitorily after defibrillation.
Reply 3: Junctional rhythm.
Reply 4: Junctional rhythm with isolated monomorphic and fragmented PVC, and with late transition in precordial leads, suggesting origin in the RV.
Reply 5: sinus rhythm, 1st degree AV block, unspecific intraventricular conduction delay, electrically inactive area in anterior wall (V1-4), ST elevation above 2 mm in V1-2 suggestive of Brugada.
Reply 6: Brugada syndrome is not associated to monomorphic VT. This type of tachycardia is generally related to the presence of structural heart disease with a well-defined substrate (area of fibrosis and feasible permeable fibers with different conduction times). ARVD may possibly present an electrocardiographic pattern similar to Brugada syndrome. The VT morphology observed in this case suggests origin in the inferoapical region of the RV. In spite of echocardiogram and coronary angiography with no alterations; NMR would be essential to evaluate the RV and define the etiology of the VT in this case.
Warm regards,

Acácio F. Cardoso MD Sao Paulo Brazil

Diagnosis of

1. **ECG 1:** difficult diagnosis with DD between VT and SVT +aberration ; The very wide QRS complex supports VT; most importantly, the arrhythmia termination followed by recurrence of the same tachycardia at a slightly faster rate is very suggestive of VT.
2. **ECG 2:** NSR ; RBBB pattern; left axis deviation; high suspicion of Brugada-ECG type 1.
3. **ECG 3:** "AV junctional rhythm" 50/min with escape morphology similar in morphology to the ECG 2.
4. **ECG 4:** 2 possible diagnosis: a) junctional rhythm with intermittent atrial captures and greater degree of aberration; ; b) the second possibility (looks more likely) is short-coupled VPC's having strangely a pattern similar but not identical to the sinus beats.
5. **ECG 5:** Sinus rhythm with typical Brugada pattern; note the disappearance of the "left axis deviation" presently noted.

There is a superb multicenter study by Rodriguez-Manero(1) and coworkers that has been published on MONOMORPHIC VT in patients with Brugada syndrome. One of the mechanisms that could explain VT in this paper was bundle branch reentry VT. I do not exclude that in the present patient who showed initial LBBB-left axis VT, that this could have been the mechanism.

I recommend EPS to try to induce it and maybe ablation to cure it. As far as the management of Brugada syndrome this is another story. Most people will recommend ICD. I usually recommend EP-guided therapy with quinidine. However due to the apparently co-existent sick sinus syndrome, I would also recommend ICD if VF or non ablatable sustained monomorphic VT are induced.

Thanks for this superb case.

Reference:

1. Rodríguez-Mañero M1, Sacher F, de Asmundis C,et al. Monomorphic ventricular tachycardia in patients with Brugada syndrome: A multicenter retrospective study. Heart Rhythm. 2016 Mar;13(3):669-82.

Professor Bernard Belhassen of Tel Aviv University, Tel Aviv Israel.

Final comments

Andrés Ricardo **Pérez-Riera, M.D. Ph.D.**
Design of Studies and Scientific Writing Laboratory in the ABC School of Medicine, Santo André, São Paulo, Brazil
https://ekgvcg.wordpress.com

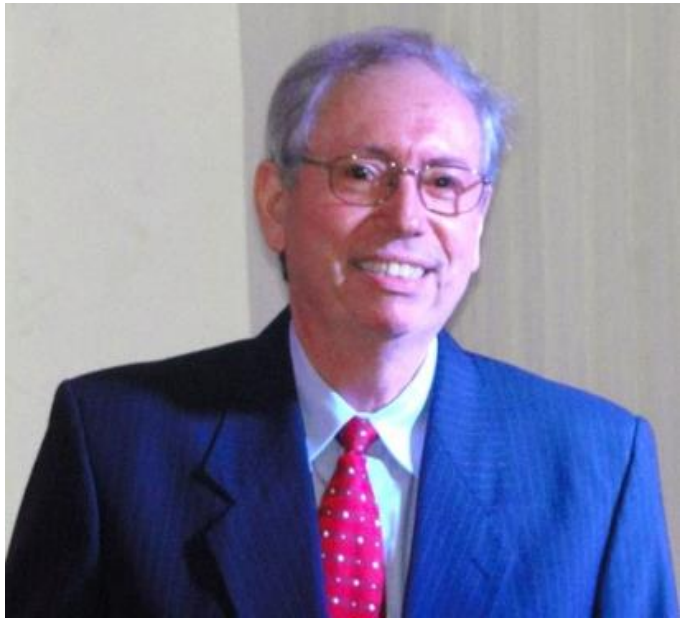

Raimundo **Barbosa-Barros, M.D.**
(nickname "Raymond, the Fox")
Chief of Coronary Center of the Hospital de Messejana Dr. Carlos Alberto Studart Gomes, Fortaleza, Ceará CE, Brazil

Luiz Carlos **de Abreu, Ph.D.**
Design of Studies and Scientific Writing Laboratory in the ABC School of Medicine, Santo André, São Paulo, Brazil

ECG-1 At admission

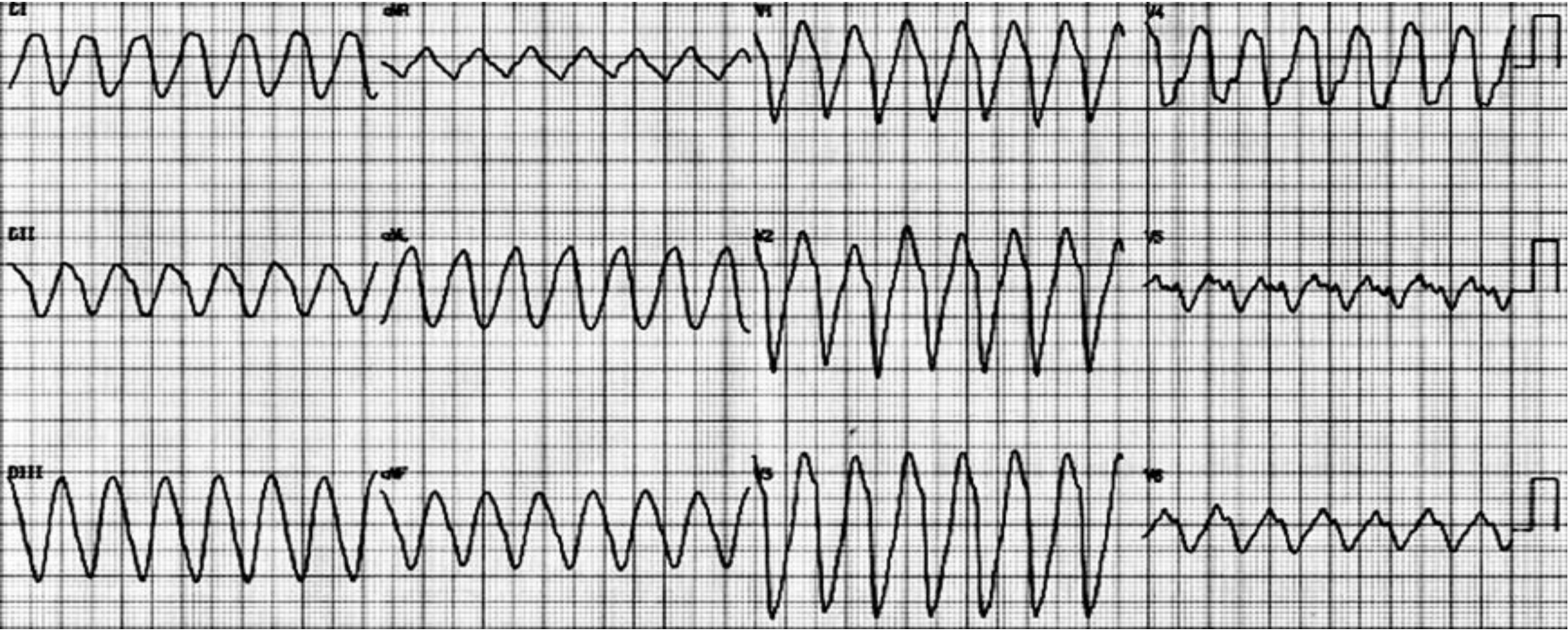

Clinical aspect: Hemodynamically stable, broad complex tachycardia in young man.

ECG diagnosis: Sustained (duration > 30 seconds) monomorphic regular complex tachycardia, rapid heart rate (> 100 bpm), 162 bpm, LBBB-like pattern, very broad complexes (≥160ms), QRS axis on upper left quadrant (positive complexes in aVL and aVR) and negative in inferior leads), distance from the onset of the QRS complex to the nadir of the S-wave is≥100ms (Brugada sign), absence of positive or negative concordance throughout the chest leads, absence of notching near the nadir of the S-wave (Josephson's sign), absence of capture or fusion beats and origin focus from apical crux (**Kawamura 2014**). See next slide.

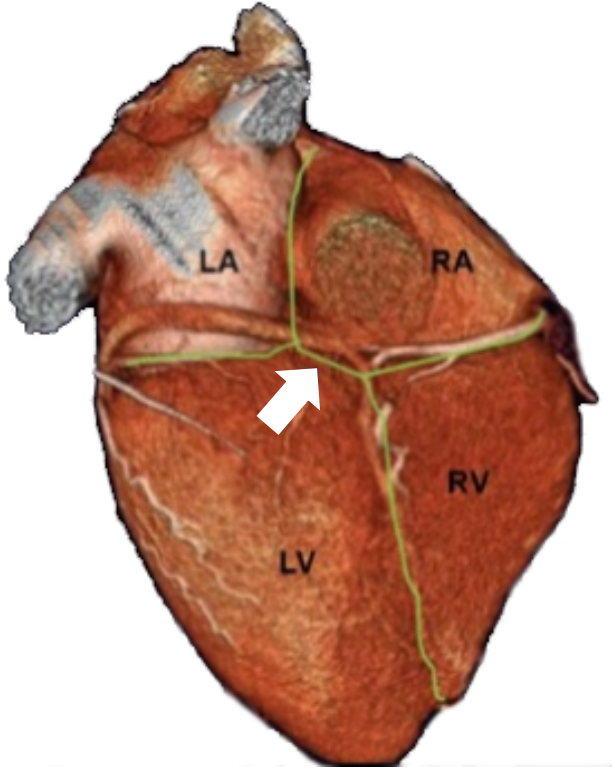

External cardiac crux is an area in the posterior aspect of the heart where cardiac chambers show their maximum proximity (arrow). This area is filled with fat. The vertical and horizontal lines in the cardiac crux are perpendicular (green lines). As seen in this inferior view of the heart, the interatrial groove meets the left AV groove at right angle, and the interventricular and the right AV grooves are perpendicular. The right AV groove is inferior to the left AV groove due to inferior position of the septal leaflet of tricuspid relative to the mitral valve.

Example of apical crux VT from literature

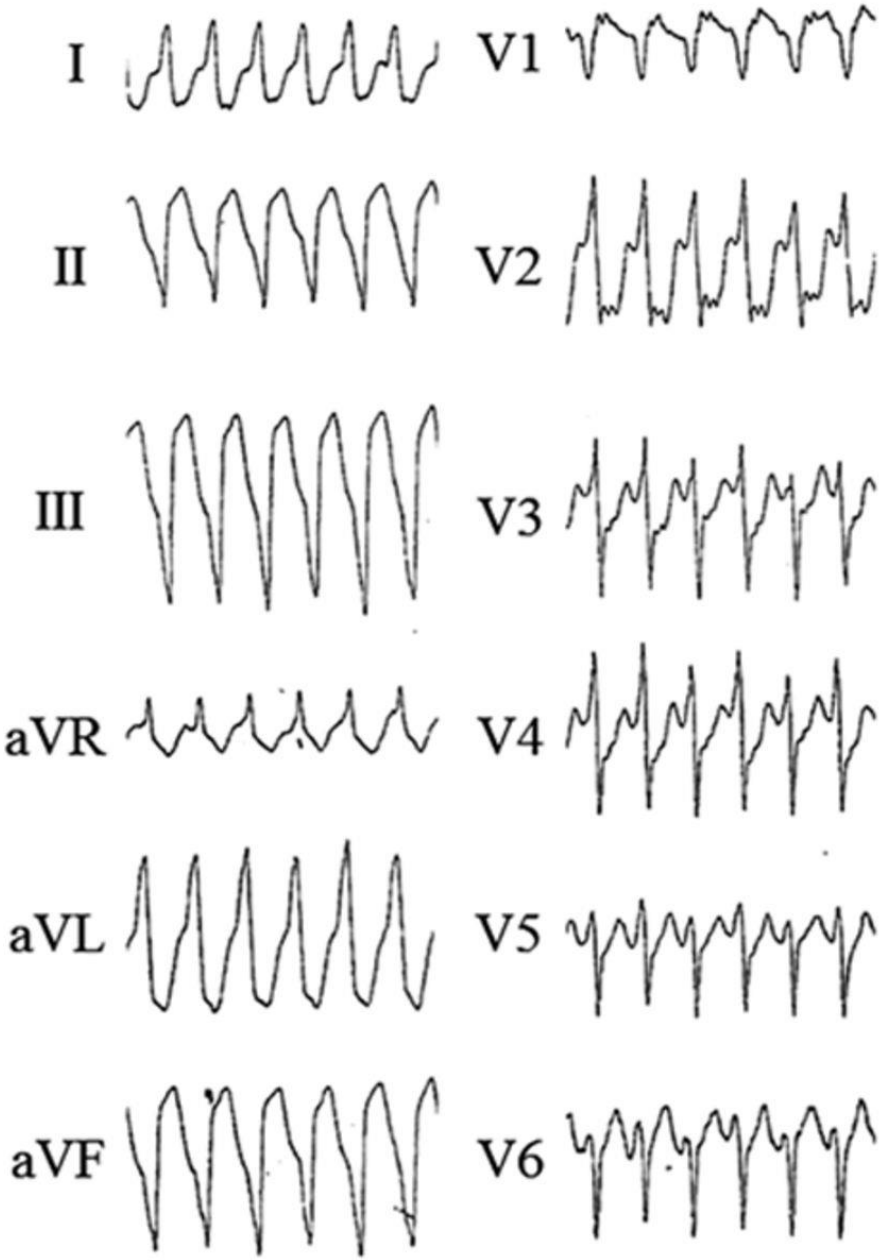

The present case: ECG-1 At admission

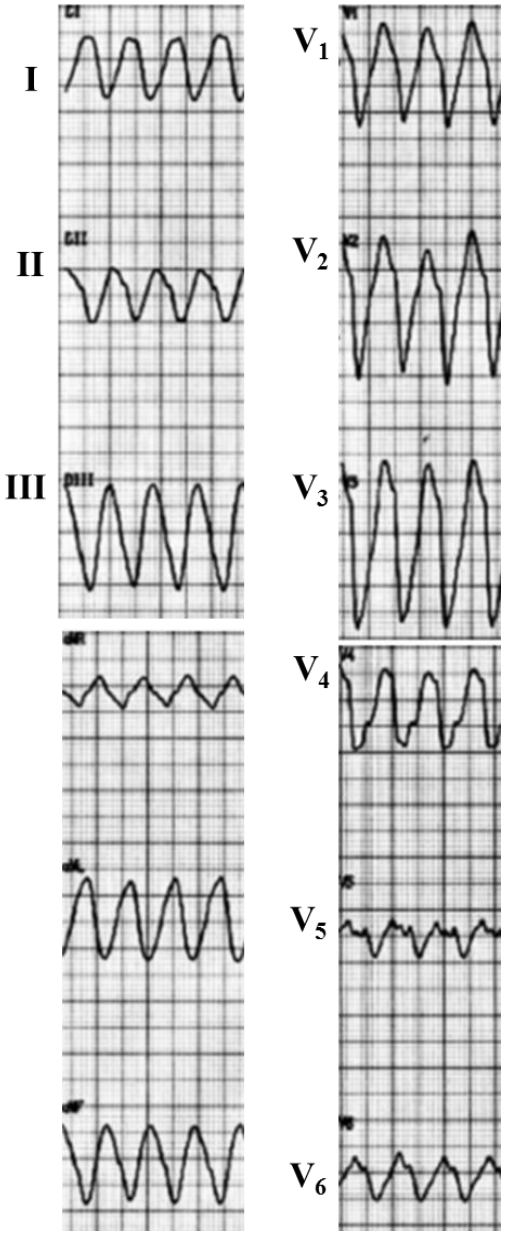

Comparison of patients with crux ventricular arrhythmia (VA) and another site of idiopathic VA

	Crux VA (n=18)	Idiopathic VA (n=251)	Pvalue
Age (y/o)	53±12	48±21	0.07
Men	8 (44%)	115 (46%)	0.81
History of syncope	8 (44%)	50 (20%)	0.001
History of VT	15 (83%)	83 (33%)	0.0001
QRS duration (ms)	150±27	138±19	0.04
LV ejection fraction (%)	60±5	58±8	0.26
ICD implantation	3 (17%)	7 (3%)	0.02

Baseline characteristics and outcomes of apical crux VA	
Age (y/o)	Between 53-64
Sex	50% each
LVEF (%)	55-75
Symptoms	Palpitation, syncope, cardiac arrest
VT pattern	RBBB or LBBB
QRS axis of VT	100% superior
Ventricular tachycardia cycle length (ms)	Between 220-300
Pseudodelta duration (ms)	Between 38-75

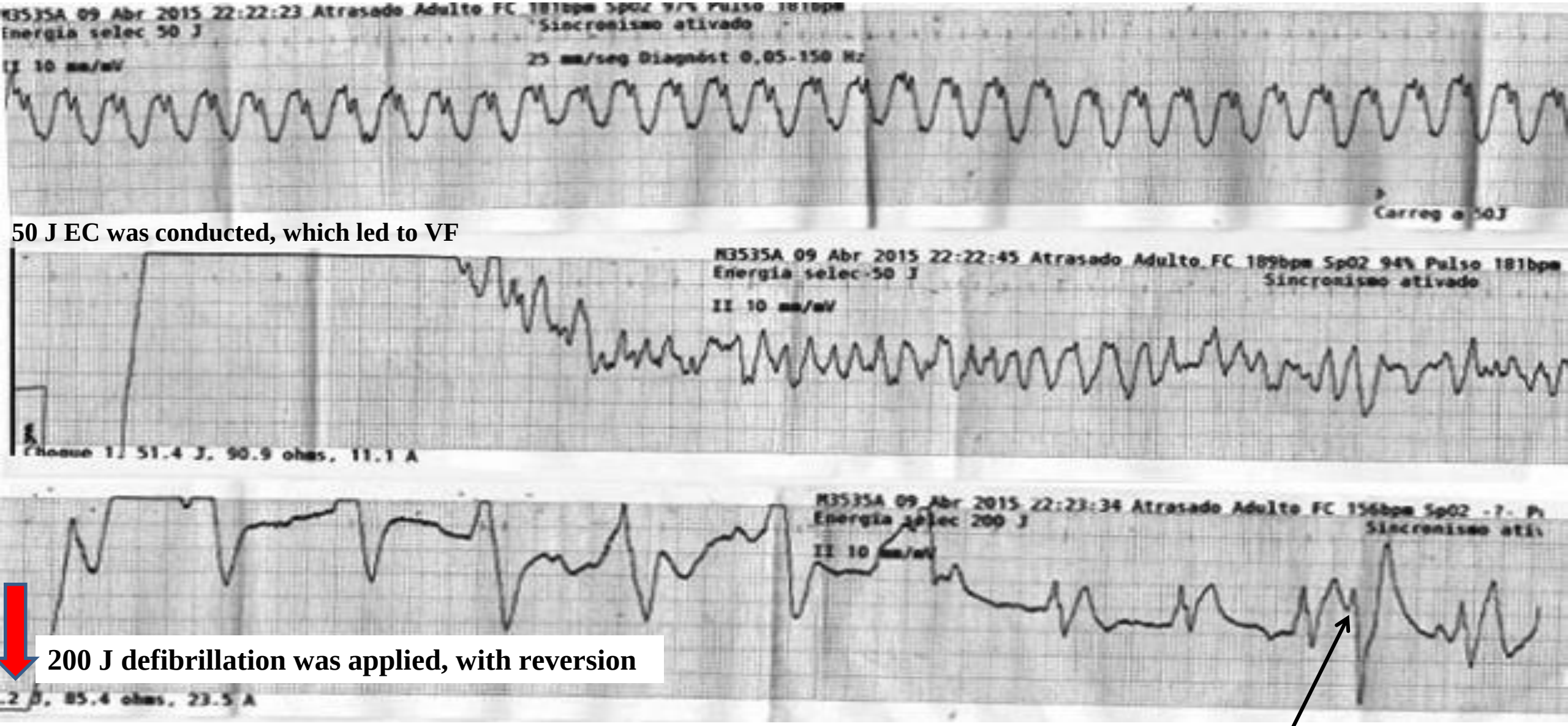
Energia selec 50 J
II 10 mm/mV
25 mm/seg Diagnóst 0,05-150 Hz
Carreg a 50J
50 J EC was conducted, which led to VF
M3535A 09 Abr 2015 22:22:45 Atrasado Adulto FC 189bpm SpO2 94% Pulso 181bpm
Energia selec 50 J
Sincronismo ativado
II 10 mm/mV
51.4 J, 90.9 ohms, 11.1 A
M3535A 09 Abr 2015 22:23:34 Atrasado Adulto FC 156bpm SpO2
Sincronismo ati
II 10
200 J defibrillation was applied, with reversion
85.4 ohms, 23.5 A
PVC with very short coupling interval

ECG-2 After electrical cardioversion

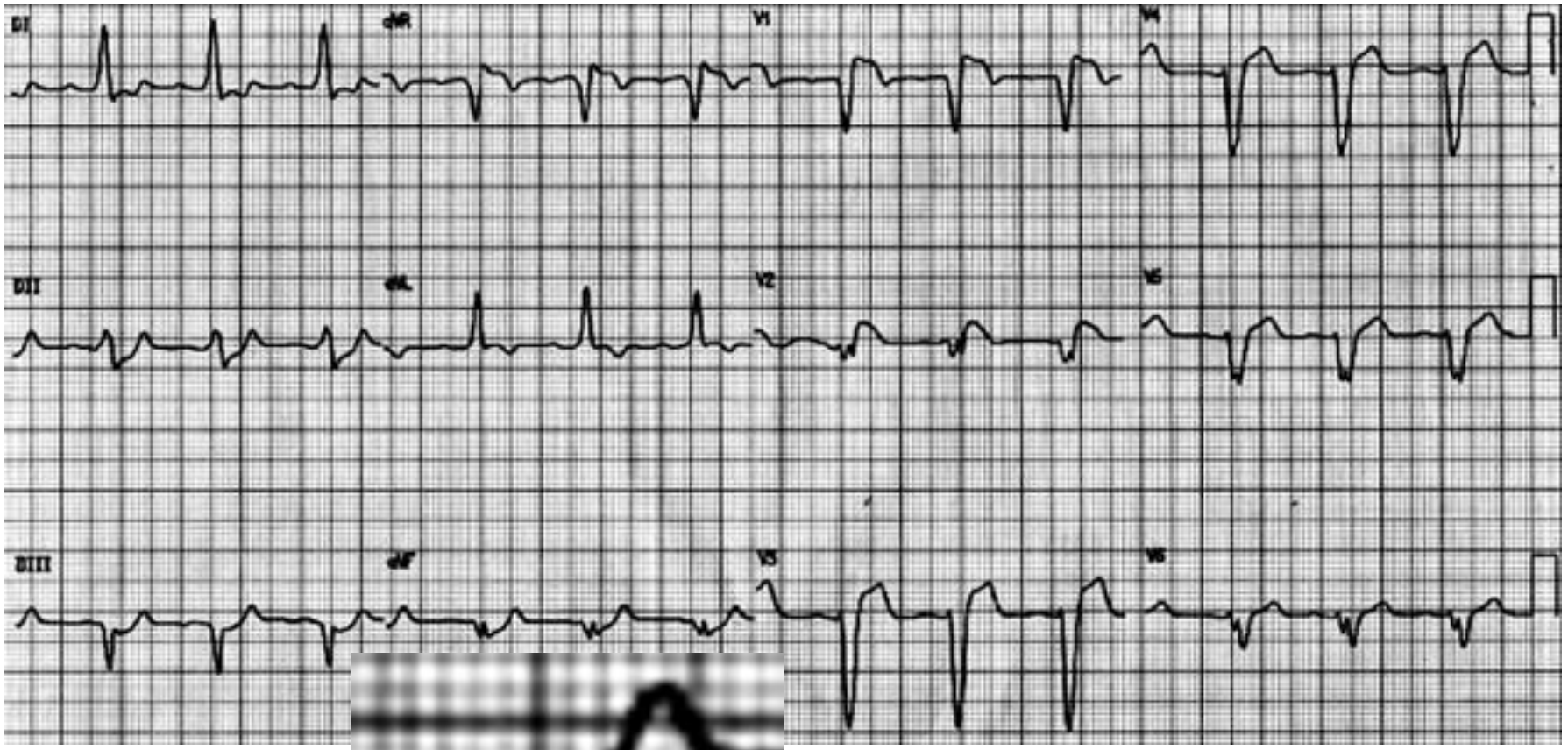

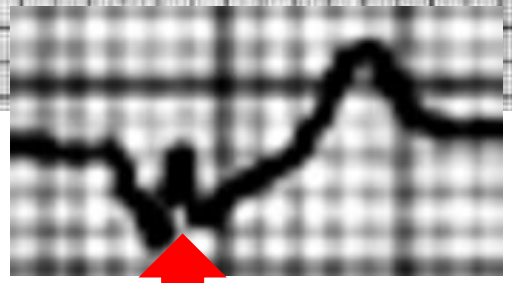

aVF

f-QRS

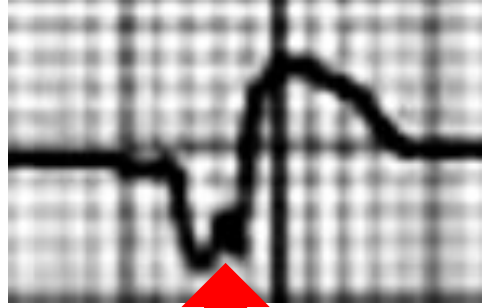

V2

f-QRS

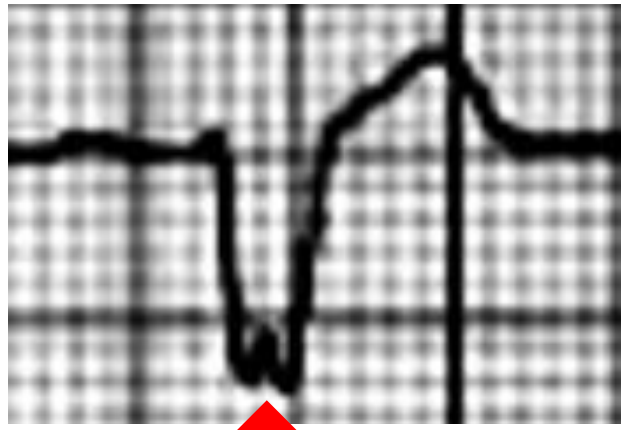

V5

f-QRS

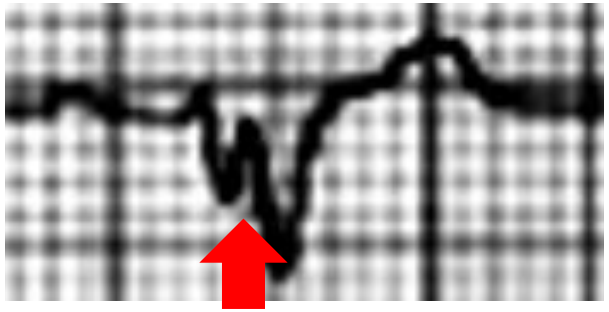

V6

f-QRS

Clinical aspect: Immediately after electrical synchronized cardioversion.
ECG diagnosis: Clear fragmented QRS in V2, V4, V5, and aVF. Low QRS voltage in V2, V5 and V6.
Fragmented QRS and ERP are common ECG findings in high-risk BrS patients, occurring in up to 27% of cases. When combined, f-QRS and early repolarization pattern (ERP) confer a higher risk of appropriate ICD interventions during a very long-term follow-up (**Conte 2016**).

ECG-3 After coronary angiography

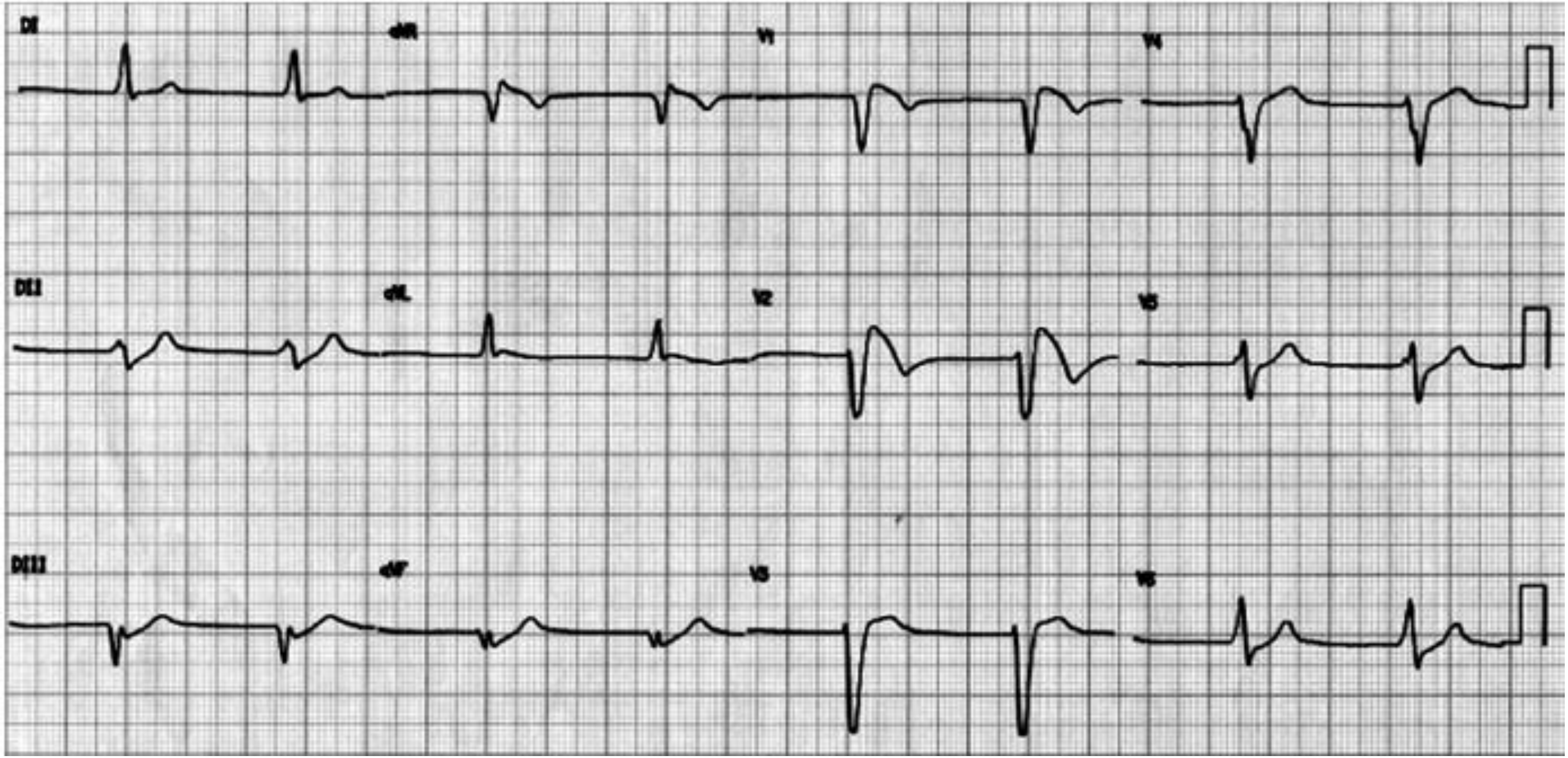

ECG diagnosis: junctional rhythm It is an escape mechanism HR 53bpm. This rhythm is usually asymptomatic ECG features are: rate is slower than sinus rhythm, regular, no preceding P wave, infrequently P wave may precede or be just after the QRS (the P waves are inverted in II) In the present case absence of P wave because concomitant with QRS complexes. Type 1 Brugada pattern.

ECG-4 24 hours after admission

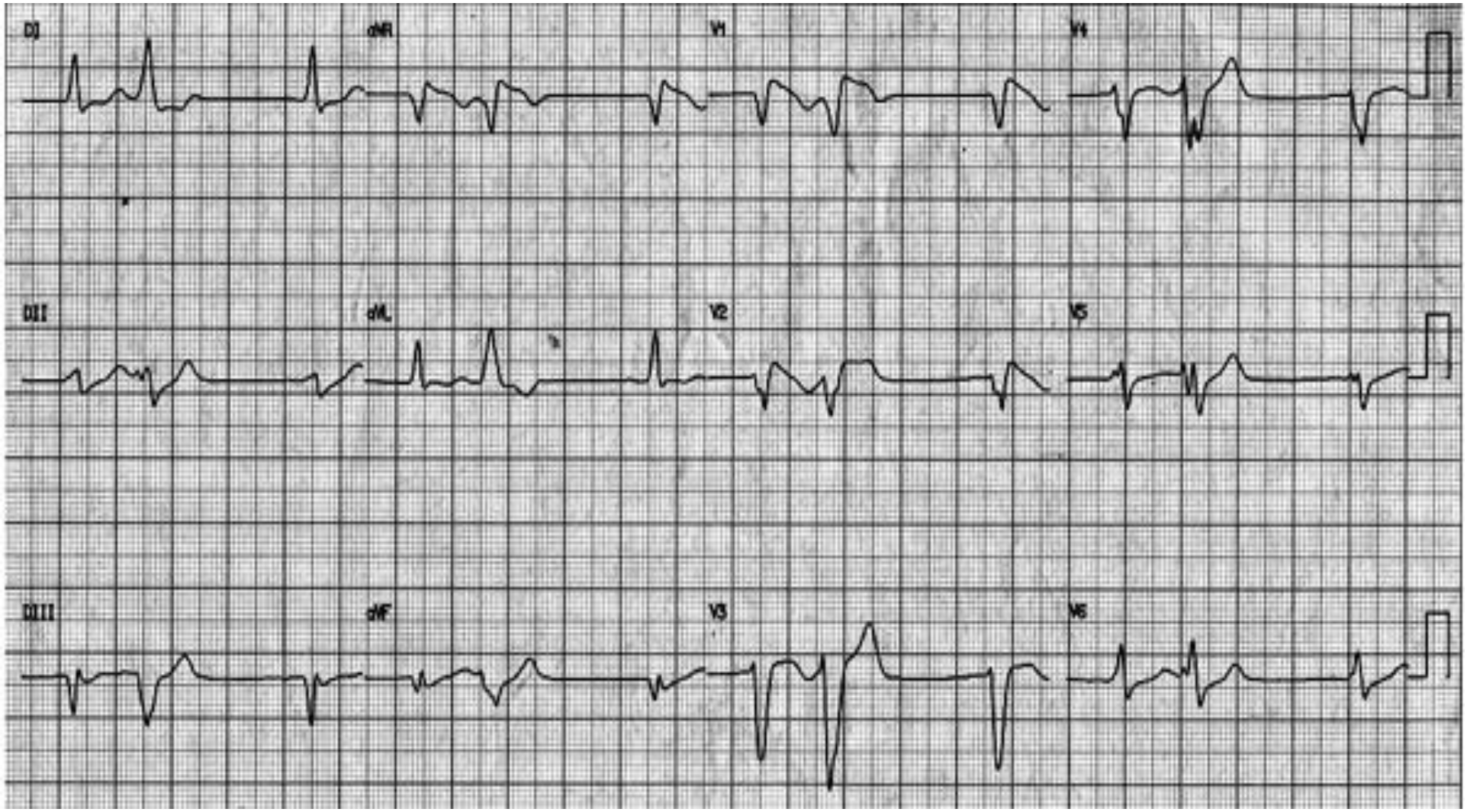

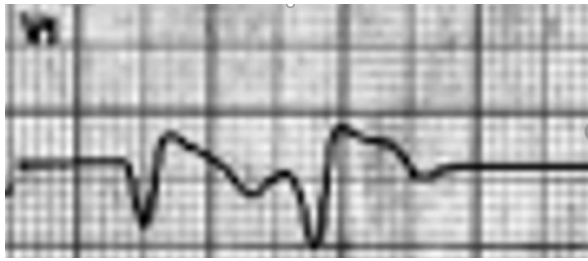

PVCs with short coupling interval (PVCSCI)

ECG diagnosis: Type 1 Brugada patter and very frequent monomorphic PVCs with short coupling interval from right ventricle. Monomorphic fragmented PVCs with inferior axis (RVOT) and short coupling interval (PVCSCI) are electrical predictors and may trigger malignant ventricular arrhythmias and episodes of SD in patients with and without structural heart disease. To a lesser degree of coupling of these contractions, worse is the prognosis; therefore, it is one important factor for the risk stratification, but by no means is the only one. The PVCs of Purkinje of the right or left side are characterized by lower duration of the QRS and short coupling intervals.

ECG-5 72 hours after admission (asymptomatic) V_{1H} V_{2H}

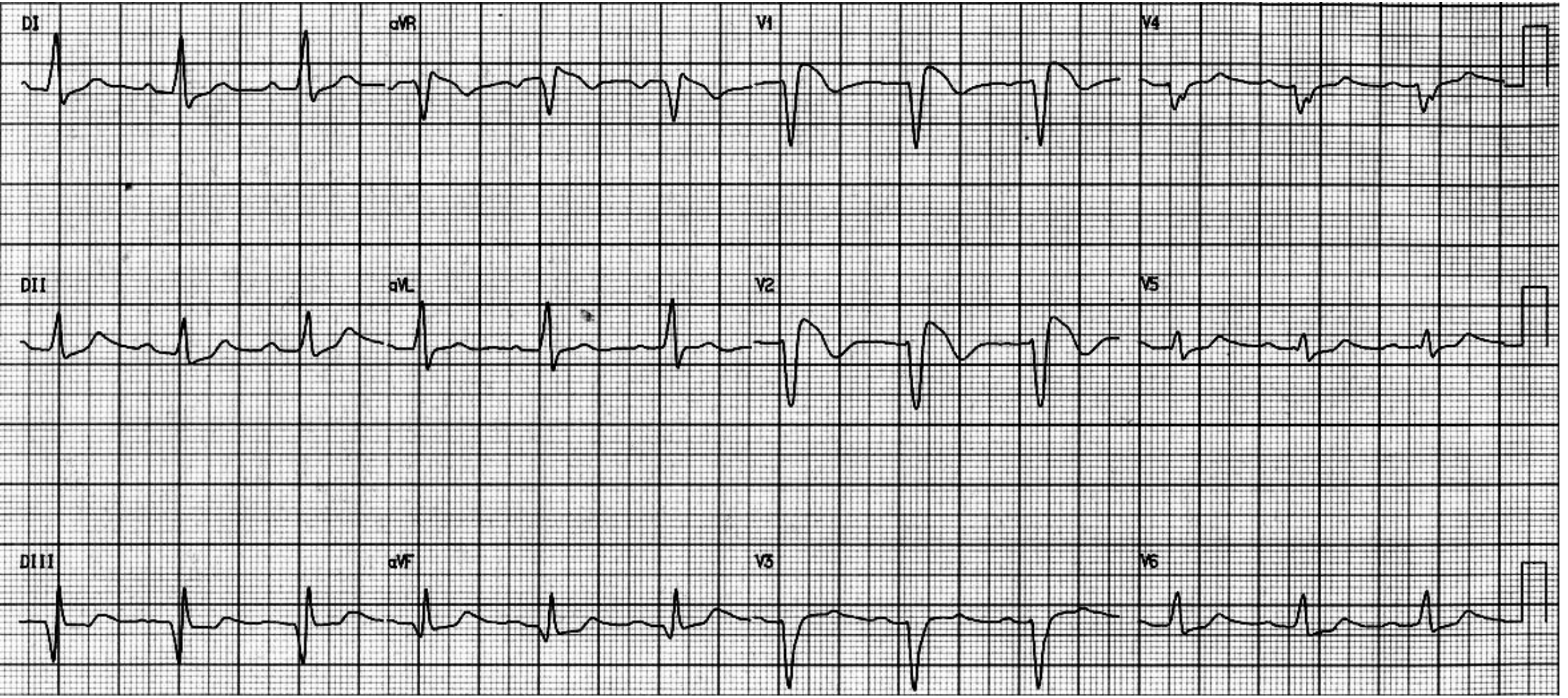

ECG: sinus rhythm, HR 61bpm, prolonged PR interval (PR= 250ms) normal QRS axis (+ 20°), spontaneous type 1 Brugada pattern (V_{1H} V_{2H}), broad QRS duration in V2 (QRS duration ≥120 ms is a powerful depolarization marker for VF/SCD). Fragmented QRS only in V4 (It is necessary at least 2 consecutive leads ≥ 2 notches of the R wave or in the nadir of the S wave), low QRS voltage in left precordial leads V4-6 and deep Q wave in III and aVF.(normal variant?).

Broad QRS Complex Tachycardia (BCT)

The typical presentation of Brugada syndrome(BrS) is either or polymorphic ventricular tachycardia (PVT) / ventricular fibrillation (VF) that may result in syncope or sudden cardiac death (SCD) in patients without apparent structural heart disease. Usually, BrS patients are affected by PVT. PVT in BrS are postulated to be a circus movement tachycardia initiated by an early coupled premature ventricular contractions (PVCs) following a phase-2 reentry due to a transmural dispersion of repolarization in the right ventricular outflow tract (RVOT) (**Antzelevitch 2001**). Both triggered automaticity and phase-2 reentry have been suggested to underlie monomorphic VTs (MVTs) in BrS, but the reason for the predominance of this type of arrhythmia in children remains unclear (**Shimada 1996**; **Sastry 2001; Dinckal; Pinar-Bermudez 2000**). Human action potentials (APs) in the BrS have been characterized by delayed or even complete loss of dome formation, especially in the right ventricular epicardial layers of RVOT. Such a repolarization pattern is believed to trigger phase-2 reentry (P2R). Not only does P2R induction by BrS require regions of AP with delayed-dome and lost-dome, but in order to generate a sustained reentry from a triggered wave back multiple factors are necessary, including heterogeneity in AP distribution, tissue coupling, direction of stimulation, the shape of the late plateau, the duration of lost-dome APs, and recovery of tissue excitability, which is predominantly modulated by tissue coupling (**Bueno-Orovio 2015**).

In a retrospective multicenter select cohort of patients, Rodríguez-Mañero et al (**Rodríguez-Mañero 2016**) examined the incidence and characteristics of MVT in a population of patients with BrS implanted with an ICD. All patients diagnosed with BrS and implanted with an ICD in 15 hospitals since 1993 until 2014 were included. The diagnosis was made after an episode of aborted SCD, during evaluation of syncope in asymptomatic patients with a suggestive ECG pattern recorded during routine examination, or as a consequence of family screening after the diagnosis of BrS in a family member. The main finding was that MVT occurred in 4.2%, QRS width was an independent predictor of MVT. In patients where a VT was captured on ECG, the predominant origin of MVT was in the RVOT (n=6), although it was occasionally due to BBRVT (n=2). Accordingly, endocardial ablation (on one occasion combined with epicardial ablation) was effective in controlling the symptoms in almost all patients. These data imply that the occurrence of MVT should not rule out the diagnosis of BrS. Moreover, this information may be relevant to ICD model selection and programming. The repolarization theory postulates that the VF in BrS is a re-entrant VT initiated by an early-coupled PVC following phase-2 reentry due to a dispersion of repolarization in the RVOT epicardium20. BrS have been linked to transmural and subepicardial dispersion of repolarization, which facilitates phase 2 reentry between endocardial and epicardial layers, or between RV epicardial regions.

Early repolarization mechanism in Brugada syndrome repolarization mechanism

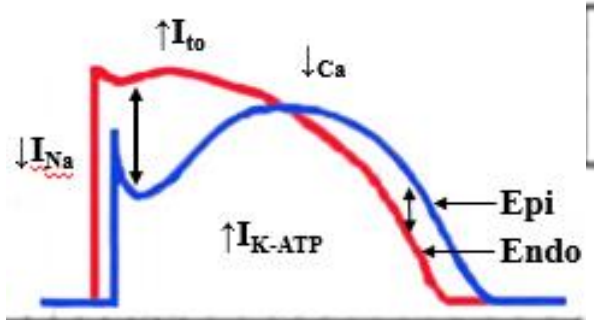

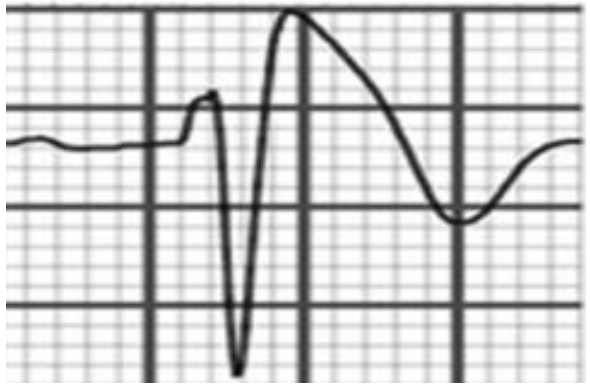

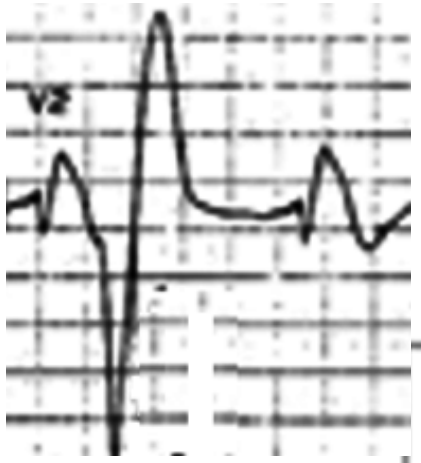

Gene mutations SCN5A and other

↓I_{Na}; ↓I_{Ca}

I_{to}; ↑I_{K-ATP}

Fever
Ischaemia
Multiple Drugs
Cocaine
Alcohol
Hypokalaemia
Hypothermia

Type 1 Brugada Pattern

Short-coupled PVCs/ Polymorphic VT
Phase 2 reentry VT

Self-terminating VT/VF

Sustained VF

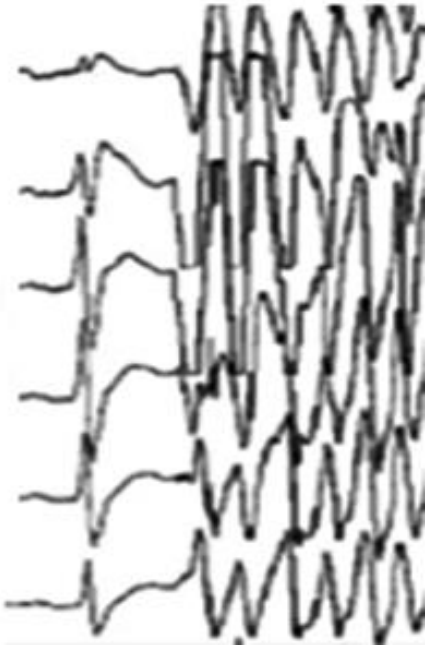

Repolarization mechanism

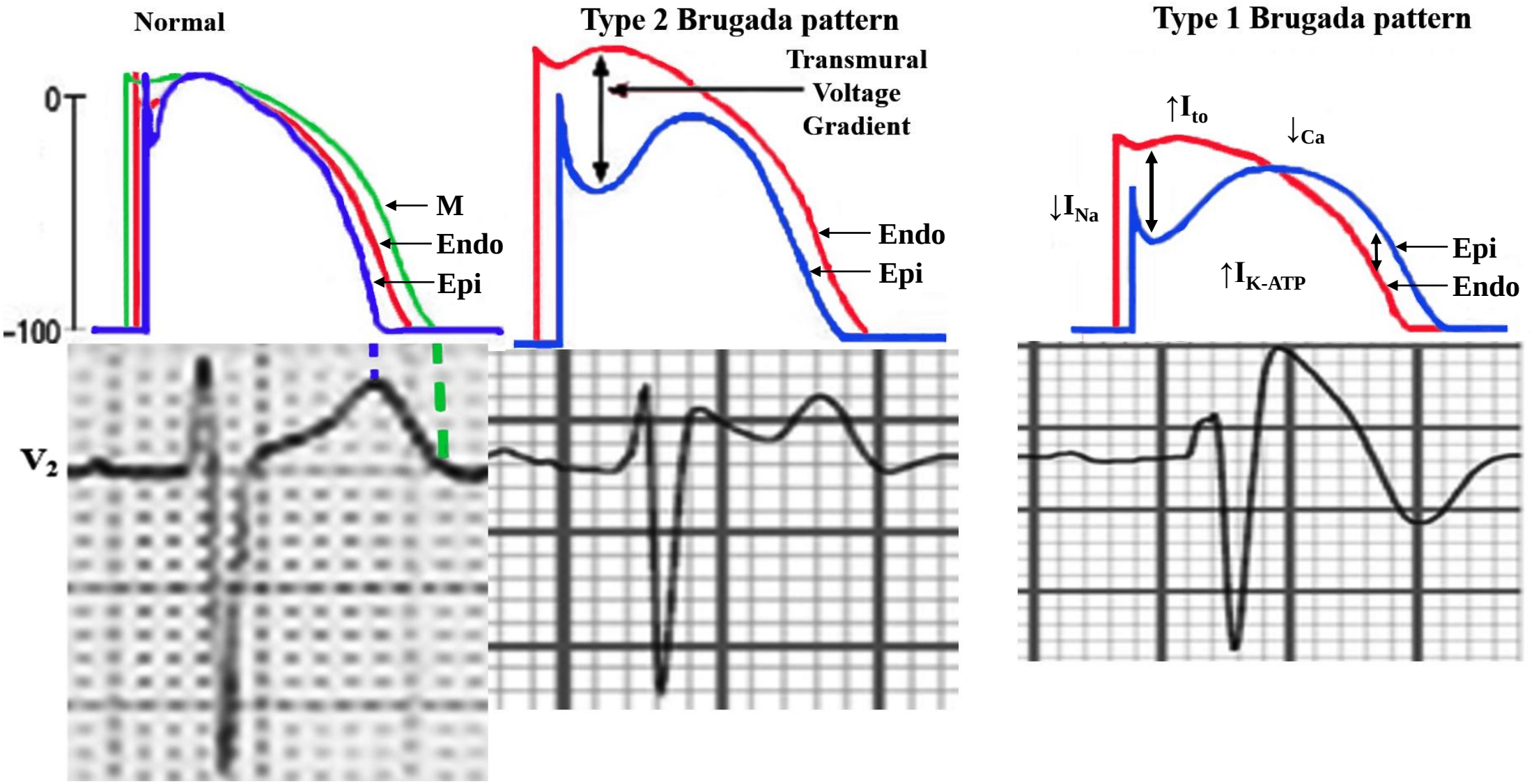

Proposed mechanism of ST-SE in BrS. The appearance of a notch in certain regions of the epicardium, but not in the endocardium, creates a transmural voltage gradient, which produces J-point elevation. If the notch is marked, the AP in the epicardium is lengthened compared to the endocardium, which causes ST-SE and appearance of negative T-waves Endo indicates endocardium; Epi, epicardium; M, myocardium (**Antzelevitch 2006**).

Ventricular arrhythmia mechanism in Brugada syndrome following the repolarization concept: Phase 2 reentry

Brugada Syndrome (Phase 2 Reentry)

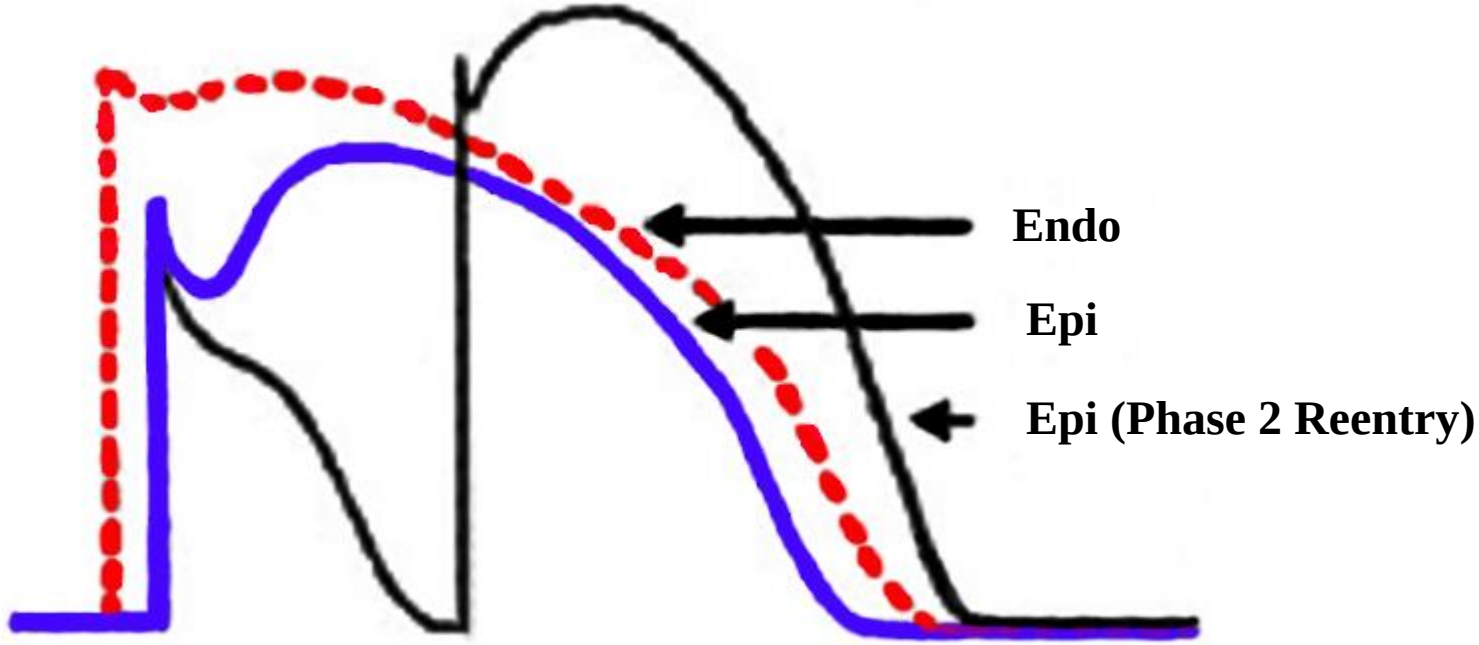

The mechanisms of arrhythmogenesis in BrS can be explained by the heterogeneous shortening of the APD on the RV epicardium (**Antzelevitch 2006; Rossenbacker 2007**). Insufficient Na^+ current and Ca^{2+} current coupled with strong Ito can result in the loss of AP dome and early repolarization in some of the epicardial cells. The same reduction of Na^+ current, however, can also lead to a delayed onset of phase 2 and paradoxically prolongs the AP. The electrophysiological heterogeneity creates an electrical gradient between epicardium AP and endocardium AP, resulting in phase 2 re-entry. Mechanism 2 is phase 3 early afterdepolarization (**Burashnikov 2006; Patterson 2005**). The figure above shows a schematic of this mechanism. Acute shortening of the APD allows the intracellular Ca^{2+} to be elevated during the late phase 3 of the AP and activates the Na^+-Ca^{2+} exchange current. Because the Na^+-Ca^{2+} exchange current exchanges 3 Na^+ with 1 Ca^{2+} ion, there is a net inward (depolarizing) current that promotes the early after depolarization (EAD) and triggered activity (**Patterson 2006**). This hypothesis is best documented in the atria, where vagal activation strongly shortens the AP. Because of an association between AF and VF in BrS patients (**Kusano 2008**), it is possible that the same mechanism is operative in both the atria and the ventricles.

Correlation of PVCs Site of Origin With ECG Morphology

Correlation of the site of origin of PVCs with the ECG morphology in V_1. The anatomy of the outflow tract region is such that areas on the right and left sides of the heart can be in close proximity to each other. This can give similar ECG patterns in several leads. However, note that in V_1, there is a gradual increase in the amplitude of the r-wave as the site of origin of the ventricular ectopy moves leftward.

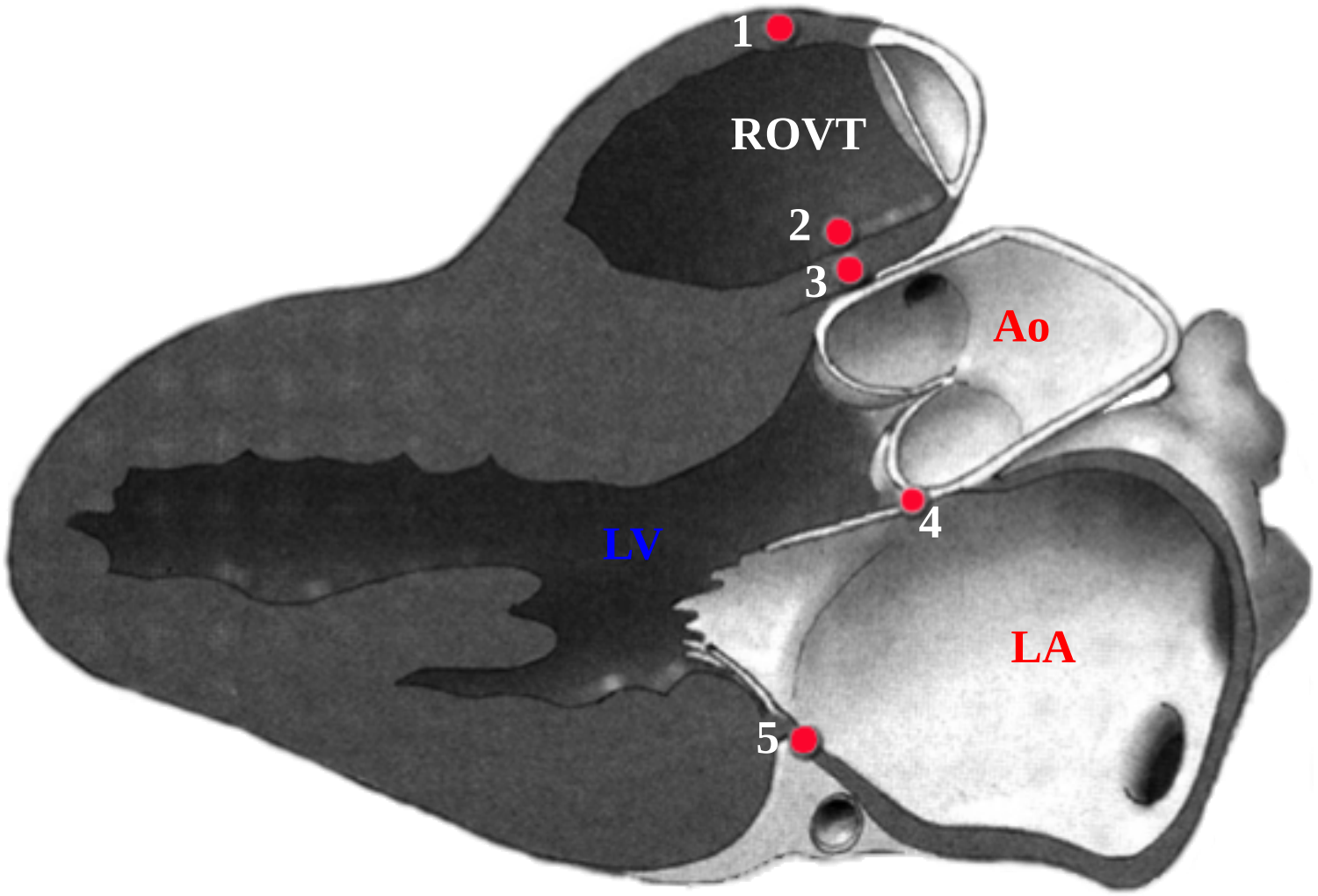

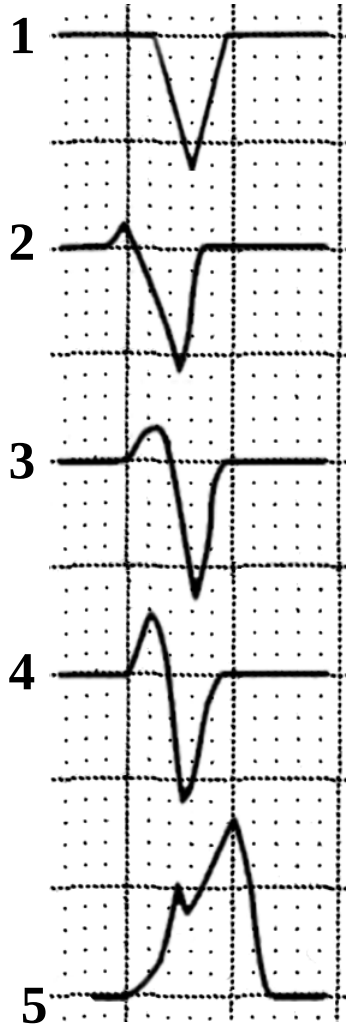

Ao = aorta; LA = left atrium; LV = left ventricle; RVOT = right ventricular outflow tract.

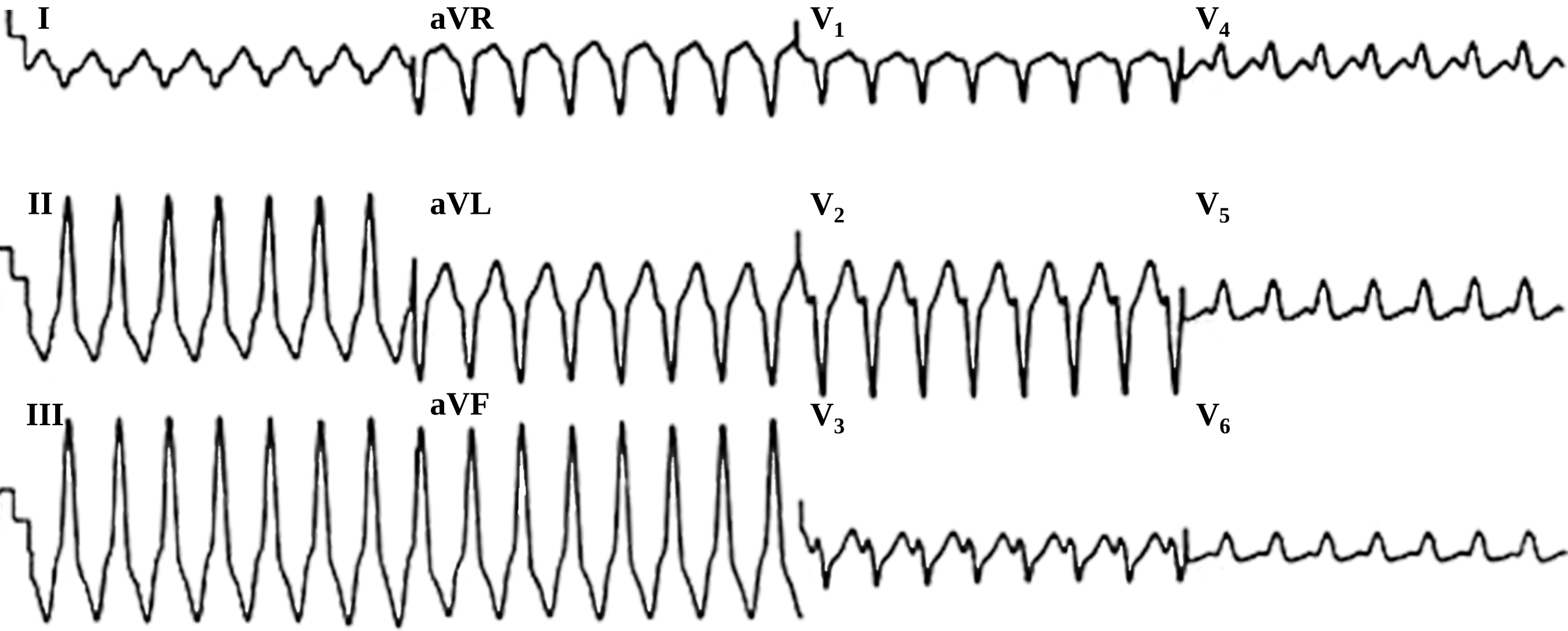

On this 12-lead ECG of RVOT-VT, note that there is a LBBB pattern in the precordial leads with transition from a small r-wave to a large R-wave in V_3 to V_4, consistent with a right-sided site of origin. Also consistent with inferior QRS axis.

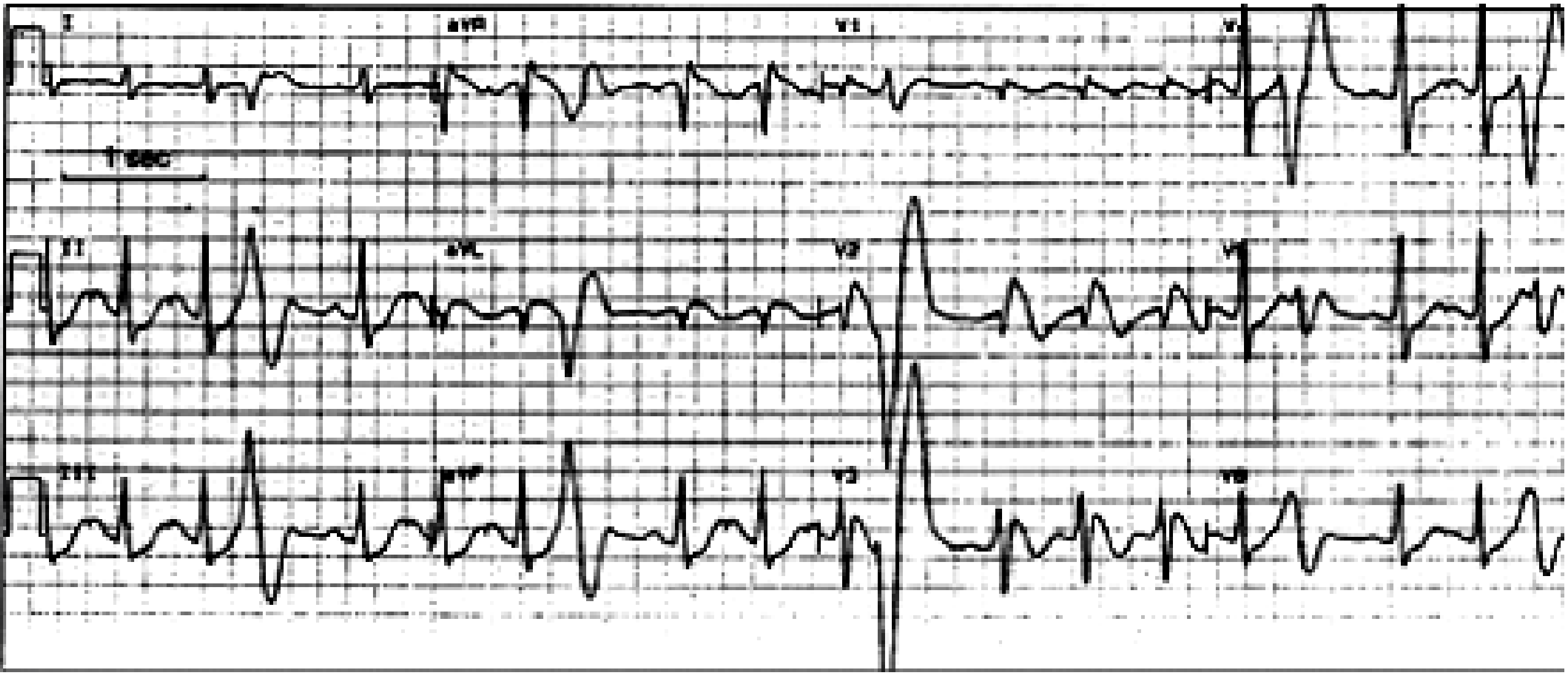

Clinical diagnosis: Patient with symptomatic BrS and repetitive episodes of electrical storm

ECG diagnosis: Type 1 BrP is present despite sinus tachycardia repeated isolated monomorphic very short-coupled PVCs (R on T phenomenon) from the RVOT are observed (inferior axis), consequently QRS negative in aVL and positive in inferior leads.

Differential diagnosis between type 1 ECG phenotype of BrS and PVCs with idiopathic right ventricular outflow tract: LBBB/inferior axis morphology with a negative QRS complex in lead aVL (Letsas 2014)

	Type 1 ECG phenotype of BrS and PVCs	idiopathic right ventricular outflow tract (RVOT) PVCs
QRS duration in inferior and right precordial leads	Is significantly longer in subjects with BrS phenotype.	Lesser
RS interval in lead V2	Significantly prolonged (epicardial conduction delay)	No prolonged
R-peak time in right V1-V3	46.0 ± 7.6	27.2 ± 9.5 ms
Pseudo-delta wave in precordial leads	Frequent suggesting epicardial focus	

Idiopathic PVCs can originate in more than 1 area of the heart but are most common in the outflow tract area, nearly 80% of which originate from the RVOT. Other common outflow tract sites include LVOT, the aortic sinuses of Valsalva, the area of aortomitral continuity, the superior basal septum near the His bundle, the pulmonary artery, and the epicardial surface of the outflow tracts (pseudo delta waves on ascending R ramp). The RVOT is leftward and anterior to the LVOT, and the pulmonic valve is superior to the aortic valve. The RVOT is a muscular infundibulum circumferentially whereas LVOT is part muscular and part fibrous. A large of part of right and some part of left aortic sinuses of Valsalva overlie the muscular LVOT and are in close proximity to the AV node and His bundle. The PVCs arising from these areas may show early activation near the His bundle region. The non-coronary cusp and posterior aspect of left coronary cusp are continuous with the fibrous aortomitral continuity, explaining the lack of PVCs related to the non-coronary cusp. The PVCs from the aortic sinuses of Valsalva arise from muscular extensions of the LVOT to areas above the base of the aortic valve cusps. These muscle fibers often exhibit slow conduction and fractionated electrograms. Localization of site of VA origin can be predicted using the QRS morphology on surface ECG, and the anatomic relationships help to explain the shared ECG patterns and subtle differences. The RVOT PVCs present with a distinct ECG pattern of LBBB and inferior axis. In general, LVOT PVCs manifest an early precordial R-wave transition (in V_2 or V_3) because of its more posterior location compared with the RVOT (See next slide).

2. Depolarization mechanism

Clinical studies in humans have also shown evidence of depolarization abnormalities over the anterior RVOT epicardium such as areas of low-voltage and fragmented QRS (f-QRS) defined as ≥ 2 notches of the R wave or in the nadir of the S wave in at least 2 consecutive leads have been described in patients with BrS (**Nademanee 2011**) (I) . QRS duration ≥120 ms in V2 and II, f-QRS are powerful depolarization marker for VF/SCD is a significant S-wave (≥0.1 mV and/or ≥40 ms) in lead I in patients with BrS (**Calò 2016**) (II); QT-interval prolongation in right precordial leads (**Pitzalis 2003**)(III) Presence of LPs on SAECG: 1) Total filtered QRS duration (f-QRS) ≥114 ms; 2) Root Mean Square voltage (RMS40) of the terminal 40 ms of the f-QRS complexes ≥20 μV; and 3) Duration of low-amplitude signals 40 μV of the f-QRS complexes (LAS_{40}) ≥38 ms. LP is identified when 2 of the criteria are satisfied. (IV); Right End Conduction Delay on vector cardiogram (**Pérez-Riera 2012**).

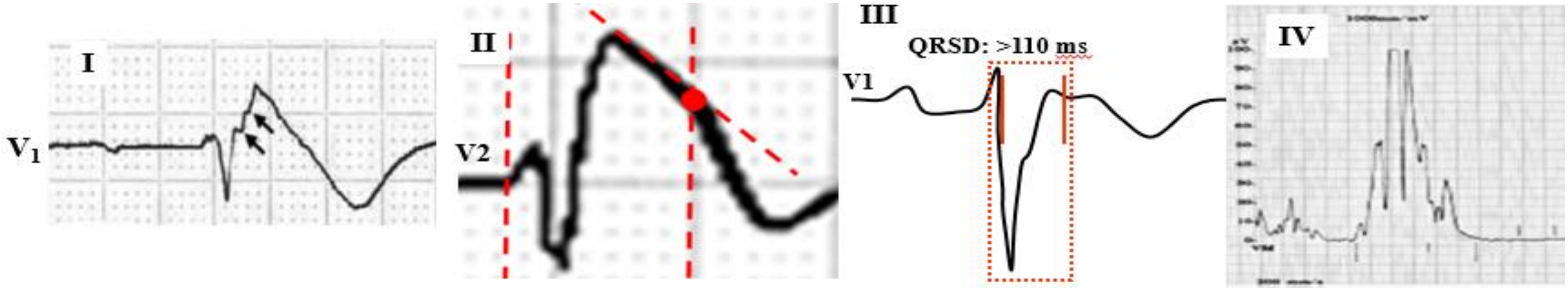

Marked regional endocardial conduction delay and heterogeneities in repolarization is observed in BrS. Wave break in areas of maximal conduction delay appears to be critical in the initiation and maintenance of VT. Slow-conduction zones should be considered to determine their role in spontaneous VTs (**Lambiase 2009**). Structural abnormalities probably are intrinsic to the BrS, and limited sensitivity of our diagnostic modalities may render these structural discontinuities difficult to distinguish from normal. None of the proposed mechanisms of the BrS has so far been irrefutably demonstrated in patients. To date, right ventricular conduction disturbances by current-to-load mismatch is the only mechanism that unifies the often observed structural abnormalities with the functional modulation of the Brugada ECG pattern and associated arrhythmias by changes in I_{Na}, I_{CaL}, and I_{to}. (**Hoogendijk 2010; Sacher 2014**). In this setting, occur structural reentry around these areas. This is further reinforced by the fact that quinidine was unable to reduce the arrhythmia burden in certain cases. Thus, depolarization abnormalities may also be a relevant causative mechanism in BrS. Sodium channel abnormalities have been linked to these structural changes either by inducing fibrosis or apoptosis.

Frigo et al by the first time described an homozygous missense mutation in SCN5A associated with atypical monomorphic ventricular tachycardia s and right structural abnormalities (**Frigo 2007**). Bezzina et al observed compound heterozygosity for mutations (W156X and R225W) in SCN5A associated with severe cardiac conduction disturbances and degenerative changes in the conduction system and dilated cardiomyopathy. The occurrence of compound heterozygosity for these two mutations implies that the proband carries solely severely dysfunctional cardiac Na^+ channels.. The morphological changes within the heart may have occurred secondary to the Na^+ channel abnormality and contributed to the severity of the disorder in this individual (**Bezzina 2003**). Coronel et al studied a BrS patient without clinically detected cardiac structural abnormalities underwent cardiac transplantation for intolerable numbers of ICD discharges. The patient's explanted heart was studied electrophysiologically and histopathologically. Whole-cell currents were measured in HEK293 cells expressing wild-type or mutated sodium channels from the patient. The RVOT endocardium showed activation slowing and was the origin of VF without a transmural repolarization gradient. Conduction restitution was abnormal in the RVOT but normal in the LV. Right ventricular hypertrophy and fibrosis with epicardial fatty infiltration were present. HEK293 cells expressing a G1935S mutation in the gene encoding the cardiac sodium channel exhibited enhanced slow inactivation compared with wild-type channels. Computer simulations demonstrated that conduction slowing in the RVOT might have been the cause of the ECG changes. In this patient with BrS, conduction slowing based on interstitial fibrosis, but not transmural repolarization differences, caused the ECG signs and was the origin of VF (**Coronel 2005**). In a multicenter retrospective study (**Rodríguez-Mañero 2016**), (mean age 45.3 ± 13.9; 200 patients, 24% women). During a mean follow-up of 69.4 ± 54.3 months, 114 patients (13.7%) experienced at least one appropriate ICD intervention, with MVT recorded in 35 patients (4.2%) (sensitive to antitachycardia pacing in 15 (42,8%)). Only QRS width was an independent predictor of MVT in the overall population. six patients presented with RVOT-VT successfully ablated from the endocardium in 4 and epi + endocardial ablation, two patients with MVT arising from the LV) one successfully ablated in the supra lateral mitral annulus) and two patients with bundle branch reentry VT (BBRVT). Significant structural heart disease was ruled out by echo and/or CMR. The authors also found that two patients experienced MVT post epicardial VT ablation for RVOT-VT. One case manifested acutely during the procedure and the other presented 12 months subsequent to it. The authors believe the underlying mechanism of MVT in these patients may be different from that seen in patients without epicardial ablation. It could be in part attributable to scar homogenization with the possibility of promoting reentry after RFCA. Three patients were receiving quinidine at the time of the observed VT episodes. Quinidine is known to be highly effective in preventing VF induction and spontaneous VF in BrS. It may exert its beneficial effects in BrS by inhibiting *Ito*, thereby restoring electrical homogeneity29. On the other hand, it also prolongs ventricular refractoriness, which may have organized the ventricular arrhythmia, giving rise to the MVT. It should be noted that in patient, quinidine was very effective in controlling the episodes of MVT, with no further events documented after the introduction of this drug.

Quinidine was also very effective in two previously reported BrS patients presenting with MVT. However, due to the limited number of patients receiving quinidine in this series (n=8), these findings need to be viewed with caution and will need further validation in future studies. Finally, BBRVT is a well-known mechanism of VT in patients with abnormal His- Purkinje conduction. Significant conduction delay within the His-Purkinje system is commonly found in patients with BrS. Mutations in the SCN5A gene encoding the voltage-gated Na^+ channel -*subunit* have been associated with both BrS and isolated Lenègre disease phenotypes (**Schott 1999**) is plausible therefore, that the electrophysiological substrates for BBRVT and BrS may share a common genotype. BBRVT may be a potential mechanism of arrhythmia in patients with BrS. The mechanism underlying the presentation of MVT is not completely understood and merits further consideration. Most likely, the mechanism will prove to be heterogeneous and will not be generalizable to the whole BrS population. It could also be argued that such cases may represent a subclinical cardiomyopathic process akin to ARVC. These disorders exist on a pathophysiological spectrum initially manifesting as an arrhythmia before structural changes become apparent (**Gomes 2012**). An individual evaluation will then be required when faced with BrS patients with MVT in order to determine the most suitable treatment.

Although that the authors did not identify overt structural heart disease in this series, microscopic structural changes could be diffuse and beyond the resolution of current imaging techniques. Moreover, sodium channel abnormalities have also been shown to be associated with conduction system disease. In this study, QRS width was found to be an independent predictor of MVT while the same was not true for presence of the SCN5A mutation. Previous existing literature does not provide much information to rule in or rule out an association with the SCN5A mutation, since only two of the aforementioned patients with MVT and BrS for whom genetic testing was performed, exhibited this mutation.

VT configuration-Electrophysiological considerations: 10 patients in this series for whom an ECG was obtained during a VT episode were confirmed on EPS to have MVT arising from a focal origin, such as the RVOT and LVOT or mitral annulus, or due to reentry involving both bundle branches. Regarding the coexistence of outflow tract VT and BrS, it remains to be elucidated whether the electrophysiological heterogeneity within the RVOT (**Morita 2008**) could provide a substrate for MVT arising in BrS. In such cases, ventricular arrhythmias in patients with BrS can be prevented by catheter ablation over the anterior aspect of the RVOT21. Moreover, in our experience and in previous studies endocardial ablation has also proven to be effective in this setting. This raises the question of whether thorough endocardial mapping and induction of the VT should be undertaken before contemplating an epicardial approach. This concept was already pointed out by Haïssaguerre et al (**Haïssaguerre 2003**). They reported 3 highly symptomatic patients in which endocardial ablation allowed the suppression of recurrences. In the 2 cases, VPBs exhibited RVOT morphology and long coupling intervals. Nonetheless, although the RVOT seems to be the predominant origin of the MVT both in this cohort and in some other cases previously reported, various configurations including RBBB morphology have also been described.

Clinical relevance Young patients with BrS, based on their low risk of bradycardia and MVT, have been considered as a subgroup where the subcutaneous ICD (S-ICD) may be recommended (**Olde 2013**). Given the finding that a small proportion of patients with BrS as shown in this study may develop MVT. The use of the S-ICD should be carefully evaluated to make sure such patients have no documented MVT prior to implant or a high burden of isolated RVOT ectopy which could trigger MVT. Although intriguing, the findings of this study do not provide enough evidence to change the current recommendations for ICD programming in patients with BrS and an ICD. In authors opinion, to do so would be imprudent based on the higher rate of inappropriate shocks reported in this population (**Sacher 2006**). However, they do believe that programming of ATP could be useful in those patients where a MVT has been recorded in order to minimize the occurrence of ICD shocks in BrS trans venous ICD recipients (**Rodríguez-Mañero 2015**).

Although MVT should raise the suspicion of ARVC rather than BrS, it does not exclude the possibility of the latter. Moreover, in those situations where no clear etiology is identified, an ajmaline test should be performed in order to rule out BrS. These findings could have relevance not only for the diagnostic work-up of patients with MVT but also for their medical treatment. Class IC, are often prescribed in patients with RVOT-VT, but maybe contraindicated in the setting of underlying BrS. The occurrence of MVT in patients with BrS and ICD implantation is not a negligible one. In this multicenter retrospective study, 4.2% of this population demonstrated MVT, 15 (42.8%) of whom were successfully treated by ATP. Wide QRS was an independent predictor of MVT in the overall population. In those patients where an ECG captured the VT episode, the predominant origin of MVT was from the RVOT. Endocardial RFCA or combined with epicardial was successful in controlling the symptoms at short-term follow-up. Consequently, BrS should be part of the differential diagnosis of patients with MVT. The possibility of BrS in patients with MVT should be taken into account at the time of ICD model selection and programming.

3. **Eclectic theory**

We demonstrate using ECG/VCG that in the BrS both mechanism depolarization and repolarization are operative. The following cases of our series demonstrate both mechanism Right End Conduction Delay (**RECD**) on RVOT area and primary T wave: velocity of inscription of afferent and efferent limbs of the T loop (circular, small, of symmetrical limbs) and with a 1:1 length/width ratio (**Pérez-Riera 2008**).

BrS was originally described by Osher and Wolff in 1953 (**Osher 1953**) and further elucidated by Josep and Pedro Brugada in 1991. Osher and Wolff speculated that the ECG pattern "simulating acute myocardial injury" is apparently due to prolongation of the depolarization process by RBBB or possibly **focal block with delayed activation of a portion of the right ventricle**. Surprisingly fifty-one years later we verified that Osher and Wolff were right!!!! This verification of focal block with delayed activation of a portion of the RV we denominate Right End Conduction Delay located in free wall of RV at the region of the RVOT best registered in unipolar aVR lead. Ours II guidelines on analysis and issuance of electrocardiographic reports of the Brazilian Society of Cardiology call this focal block **Right Superior Divisional Block (RSDB) (Luna Filho 1989), superior or subpulmonary fascicular block** (**Pastore 2016**) or **Right anterior subdivision block (RASB)**. This fascicle is located inside of RVOT in front of aVR lead and consequently better recorded in this lead: "The forgotten lead".

Distribution of the three fascicles of the right bundle branch of the His bundle in the right ventricle free wall (Pérez-Riera 2005)

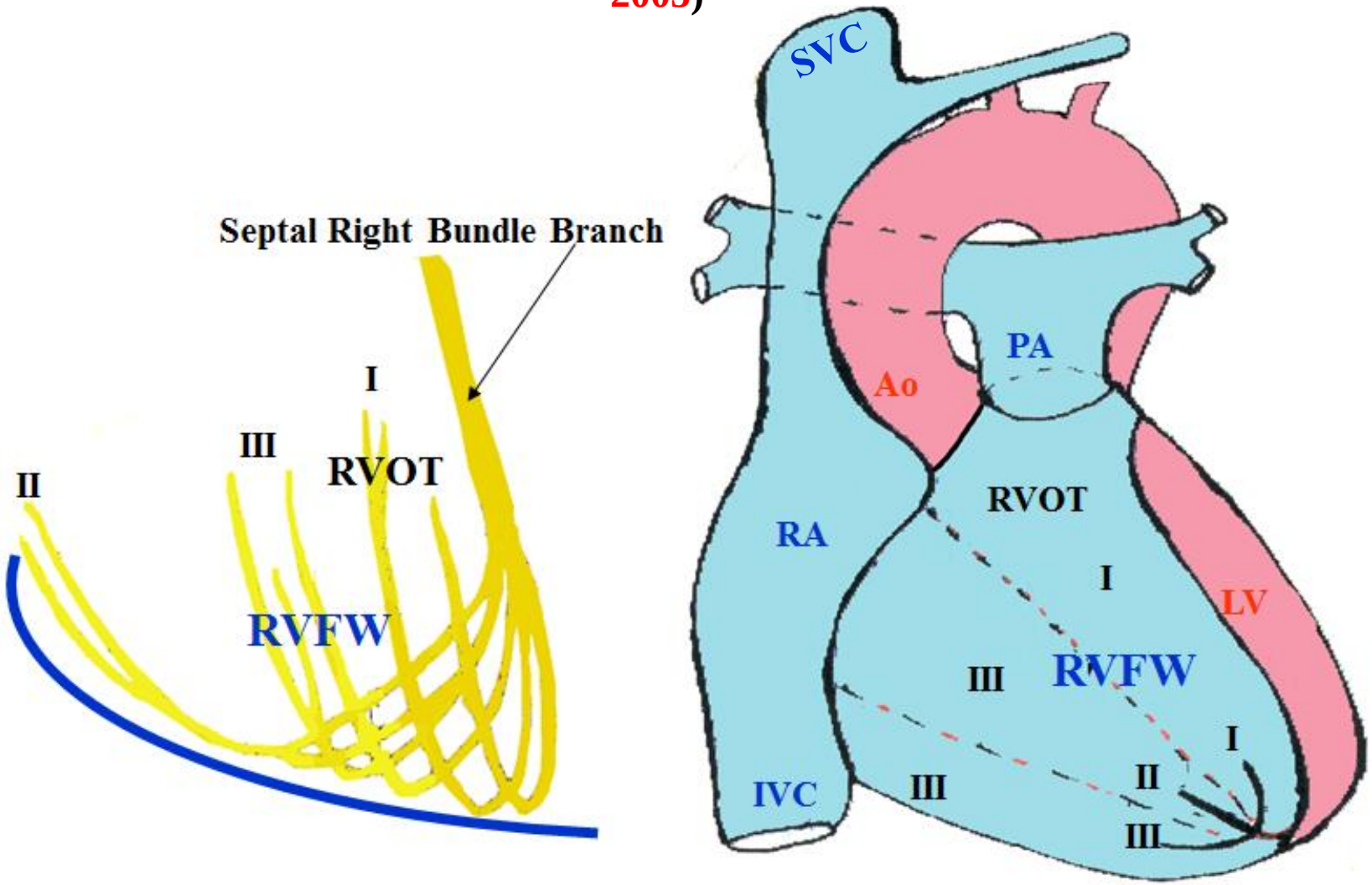

I - Territory of superior or subpulmonary fascicle(Right superior division or subpulmonary fascicle inside of RVOT
II – Territory of inferior or posteroinferior fascicle
III – Territory of middle fascicle: Do it exist?
RVFW: Right Ventricular Free Wall; **SVC:** Superior Vena Cava; **IVC:** Inferior Vena Cava; **RVOT:** Right Ventricular Outflow Tract; PA: Pulmonary Artery; **Ao:** Aorta; **RA:** Right Atrium; LV: Left Ventricle.

The cardionector system and the hexafascicular concept of intraventricular Hisian system demonstrated by Vectorcardiography

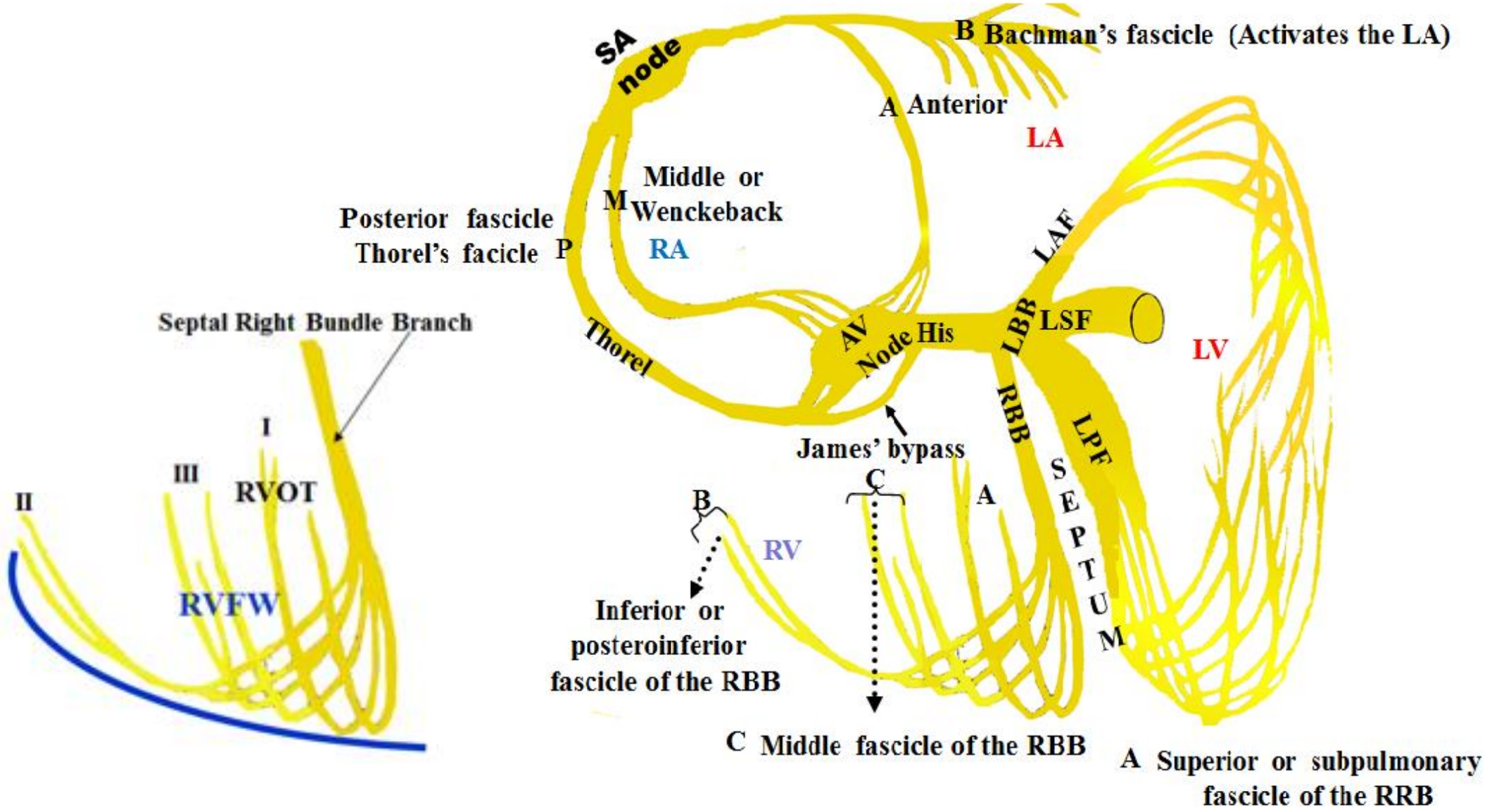

Right End Conduction Delay (RECD) concept: These are the electrovectorcardiographic conduction changes, secondary to physiological delay or to true dromotropic disturbance in the territory of one of the three hypothetical fascicles (or contingents) of the right bundle branch (right fascicular block of the His bundle or RASB (**de Micheli 1988**), in isolation in right ventricular free wall. We divided the right divisional blocks according the location of the **RECD** in the frontal plane in three types: **Type I (right anterior subdivision block (RASB)), Type II (Right posteroinferior subdivision block (RPSB)) and Type III (right middle fascicle block (RMFB). Does it exist?).** The type I is the variant observed in the Brugada syndrome (**Pérez Riera 2008**) and in concealed forms of arrhythmogenic right ventricular cardiomyopathy/dysplasia (ARVC/D) (**Corrado 1996; Corrrado 2001**).

Classification of right divisional blocks according the location of the RECD in the Frontal Plane

Right Anterior Subdivision Block (RASB) Type I

Right Middle Fascicle Block (RMFB) Type III

Right Posteroinferior Subdivision Block (RPSB) Type II

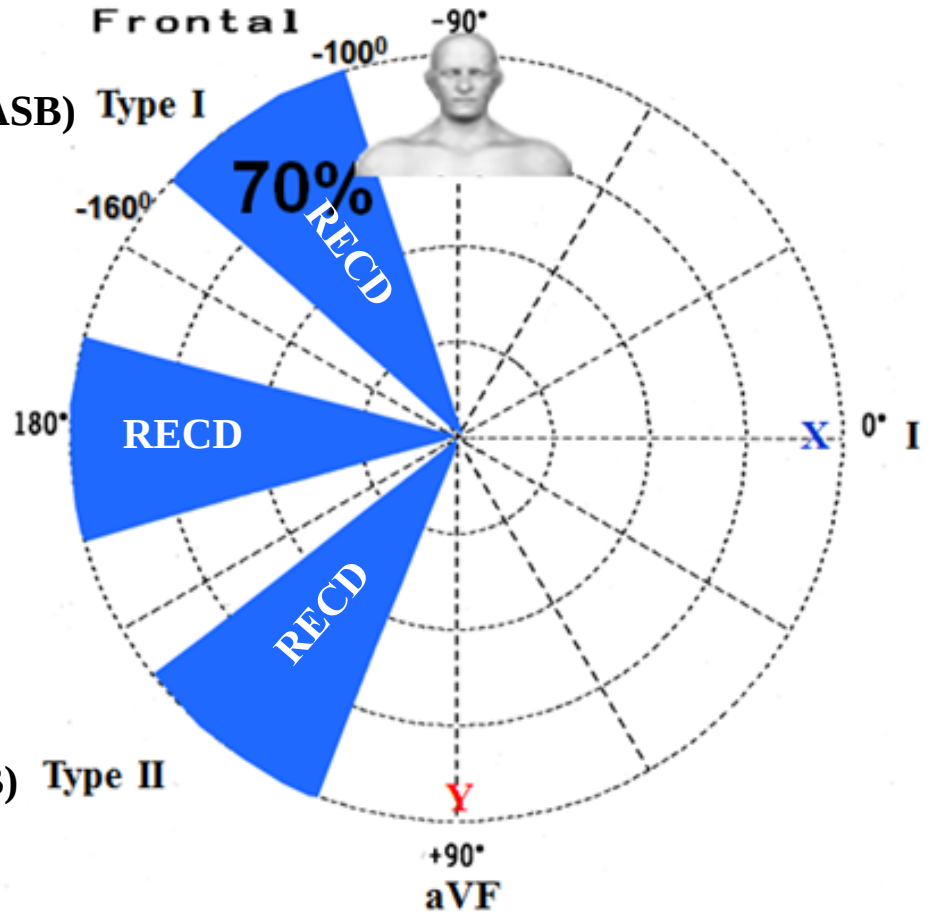

I) Right anterior subdivision block (RASB) or type I: Vectorcardiographic types (following the QRS rotation in the FP)

Only type IA variant has differential diagnosis with LAFB

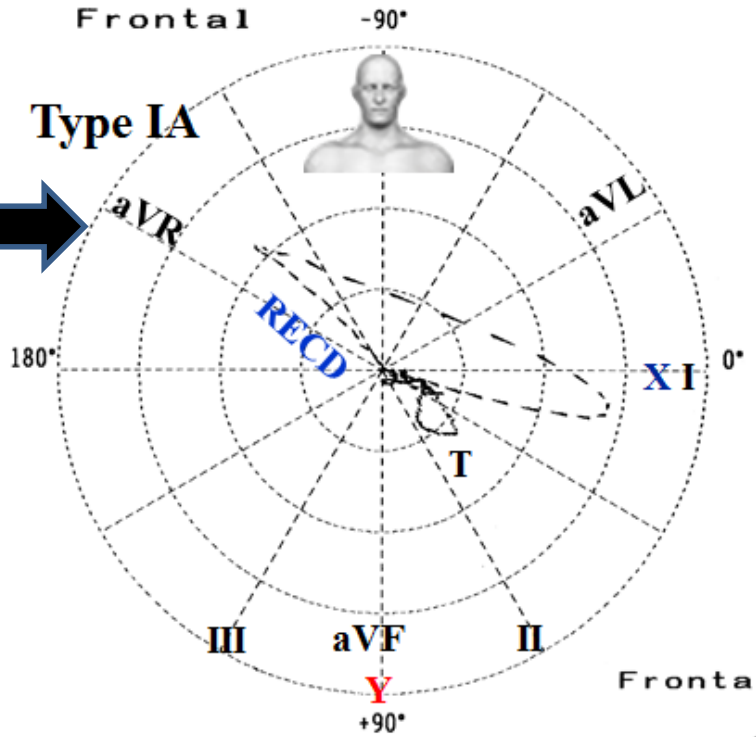

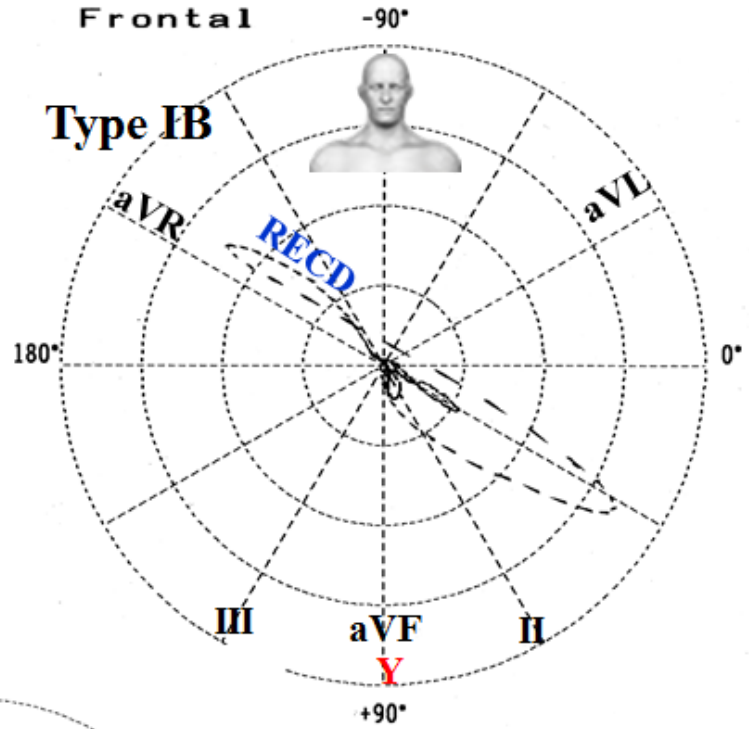

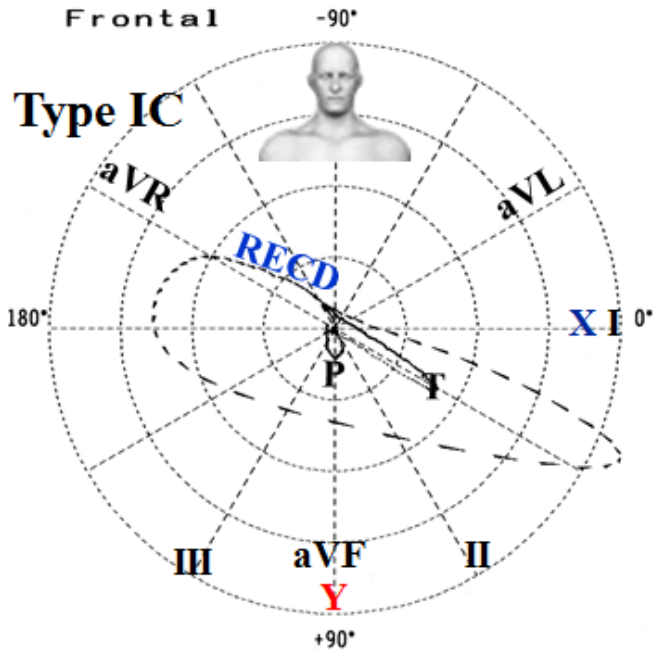

Clinical features: Syncope. Positive familiar background of sudden death in young (≤35yo) first-degree relative. Genetic research performed: negative.

Name: MK **Age:** 38 y.o; **Gender:** Male; **Ethnic Group:** Asian; **Weight:** 68kg; **Height:** 1,70m

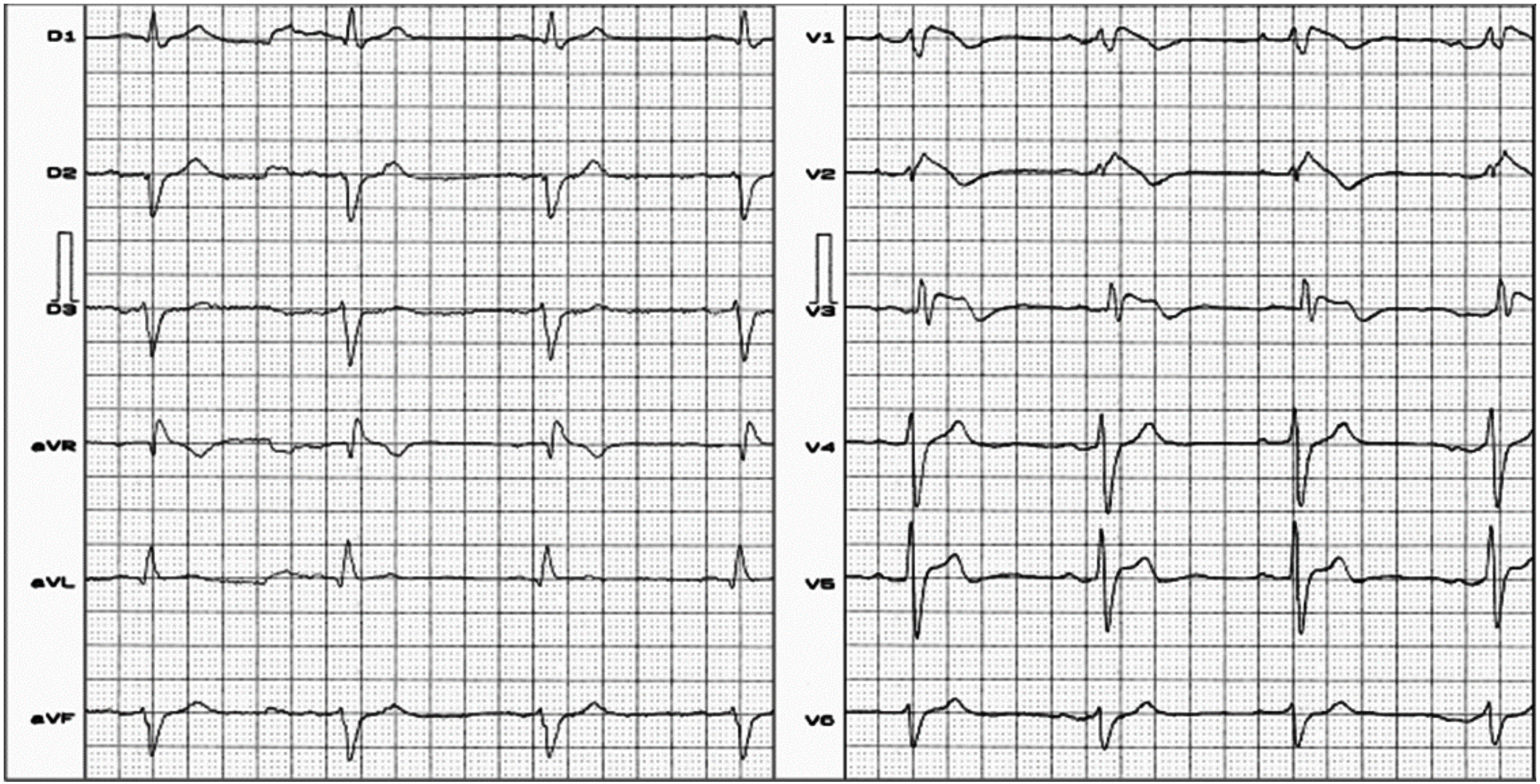

ECG diagnosis: Sinus bradycardia (heart rate under 60 bpm) Brugada type 1 ECG pattern Prolonged QRS duration, aVR signal: final R wave of aVR lead >3mm. fQRS in V1-V2. Extreme left axis deviation: Left anterior fascicular block? or Right superior fascicular block or RECD Type IA?

ECG/VCG correlation in the Frontal Plane

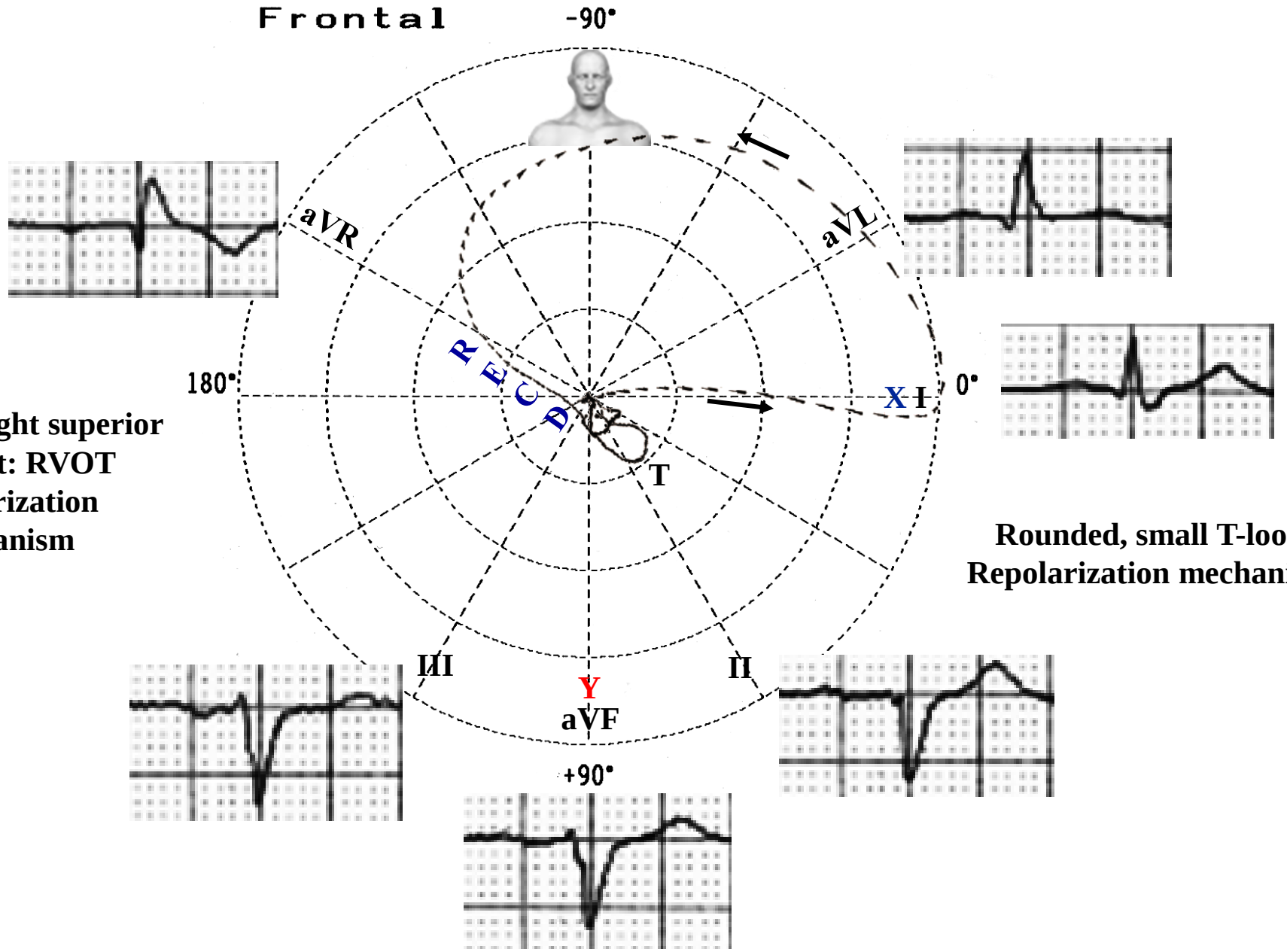

RECD on right superior quadrant: RVOT Depolarization mechanism

Rounded, small T-loop Repolarization mechanism

Initial 20 ms QRS forces directed to left, SII>SIII, extreme left axis deviation, CCW, **RECD** located near -150°: prominent final R wave in aVR.

ECG/VCG correlation in the Horizontal Plane

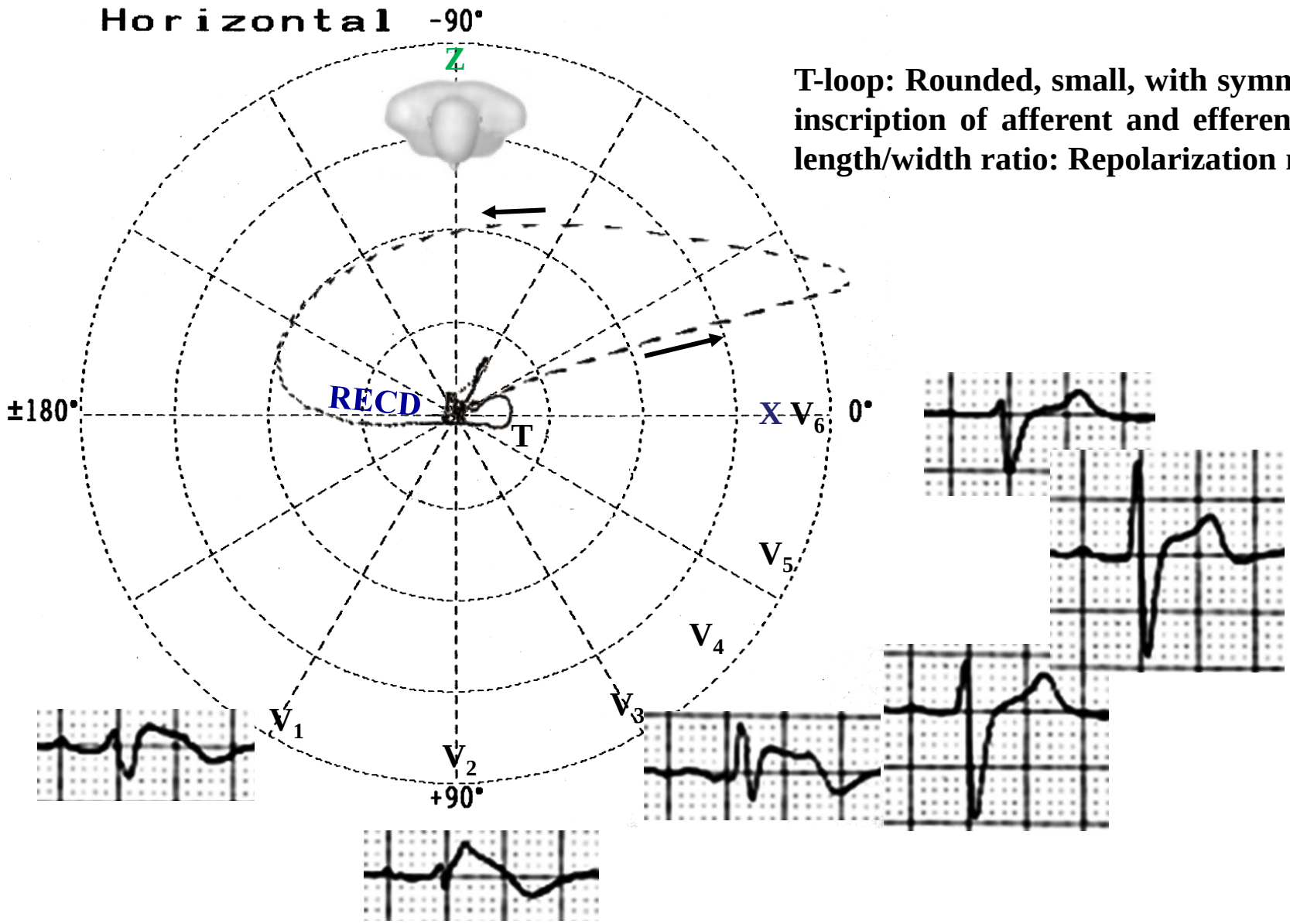

T-loop: Rounded, small, with symmetrical velocity of inscription of afferent and efferent limbs and a 1:1 length/width ratio: Repolarization mechanism.

Type 1 BrP, initial forces directed to left and backward, **RECD** on orthogonal X lead (±180°), rS/RS in left leads with S > R, primary T-loop.

ECG/VCG correlation in the Right Sagittal Plane

RECD on upper posterior quadrant: Depolarization mechanism

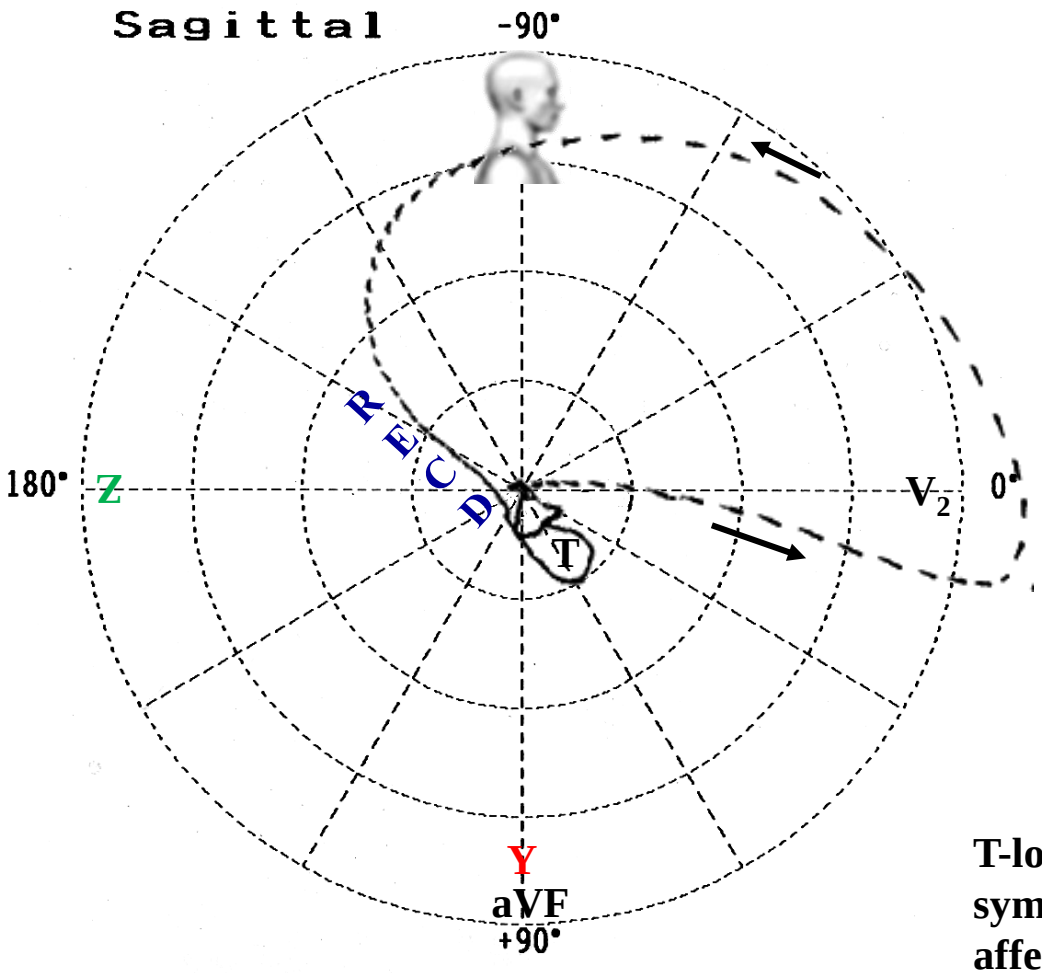

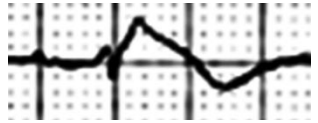

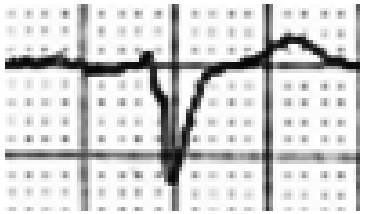

T-loop: Rounded, small, with symmetrical velocity of inscription of afferent and efferent limbs and a 1:1 length/width ratio: Repolarization mechanism.

I) Right anterior subdivision block (RASB)

Type I: It is the variant observed in Brugada syndrome and concealed forms of ARVC. **RECD** near -150° (aVR) "the forgotten lead"

- **Type IA:** QRS loop predominantly located in the left superior quadrant, (SÂQRS with extreme deviation to the left), counterclockwise rotation and **RECD** located in the right superior quadrant. Very similar to LAFB;
- **Type IB:** QRS loop pointed, clockwise or in eight, with the initial portion located in the left inferior quadrant and **RECD** located in the right superior quadrant. SAQRS difficult to determine or shifted to the right;
- **Type IC:** QRS loop of clockwise rotation with SAQRS with no deviation or with a mild shift to the right.

In the three types I the **RECD** is located in the right upper quadrant.

When the anterosuperior subdivision of the right bundle branch, (located in the region of the pulmonary artery infundibulum (RVOT)), is injured, the corresponding unipolar epicardial leads point out the existence of regional delay in the right ventricular activation process, limited to the structures of the ventricular outflow chamber: anterosuperior areas of the right septal mass and high right anterior paraseptal areas. In such areas, R-peak time(or intrisecoide deflection) could be prolonged by 10 ms in average. Additionally, the last ≥30ms of the QRS loop of vectorcardiogram shows conduction delay "**RECD**". In the presence of RASB, the resulting vector of depolarization of the basal regions of the right ventricle (3d vector) is essentially heading upward and right or leftward from -90°, according to the position and rotation of the heart. The electrocardiographic diagnosis of RASB could yield the pattern: S_I S_{II} S_{III} and $AQRS_F$, with the latter shifted upward from the transversal axis between ±180° and 0° (**Type IA**), at the right or left from -90°, with R wave vortex slurring and R-peak time prolongation in I, aVR, V_{3R}, and sometimes in V1, and in the right chest unipolar leads of V_{4R} through V_{9R}, and slurred S waves in V_6, aVF, II and III.

Observation: The loops (P, QRS and T) are fragmented by the action of an oscillator – which cuts the current intermittently for a known period of time, usually each dash has 2 ms (0.0002 s). The goal of this intermittent cut is to know the total duration of the loop in study, which may be estimated by multiplying the number of fragments (in the form of dashes) for the time selected (in our case 2 ms). Additionally , the greater or the lesser distance between dashes indicates the greater or the lesser conduction velocity in the area. Each dash represents a period of 2 ms or 2.5 ms, depending on the calibration of the device. Thus, when they are very close to each other, it indicates the presence of **conduction delay**. To consider the phenomenon as true, it is necessary for it to be evident in at least 2 planes.

Differential diagnosis between Right Superior Divisional Block (RSDB) type IA and Left Anterior Fascicular Block

	RSDB Type IA	LAFB
10 to 20ms initial forces	Directed to left and downward	Directed to right and downward
SIII/SII ratio	SII>SIII	SIII>SII
Final R wave in aVR	Prominent	Maybe low or absent
I and aVL pattern	R or Rs	qR
QRS loop rotation in the frontal plane	Counterclockwise	Counterclockwise
Final 30 to 60 ms of QRS loop	Located on upper right quadrant near -150° with RECD very close dashes = less dromotropism*	Located on upper left quadrant
QRS loop rotation in the frontal plane	Counterclockwise rotation	Counterclockwise rotation ECD on upper left quadrant

Differential diagnosis between Right Superior Divisional Block (RSDB) type IA and Left Anterior Fascicular Block

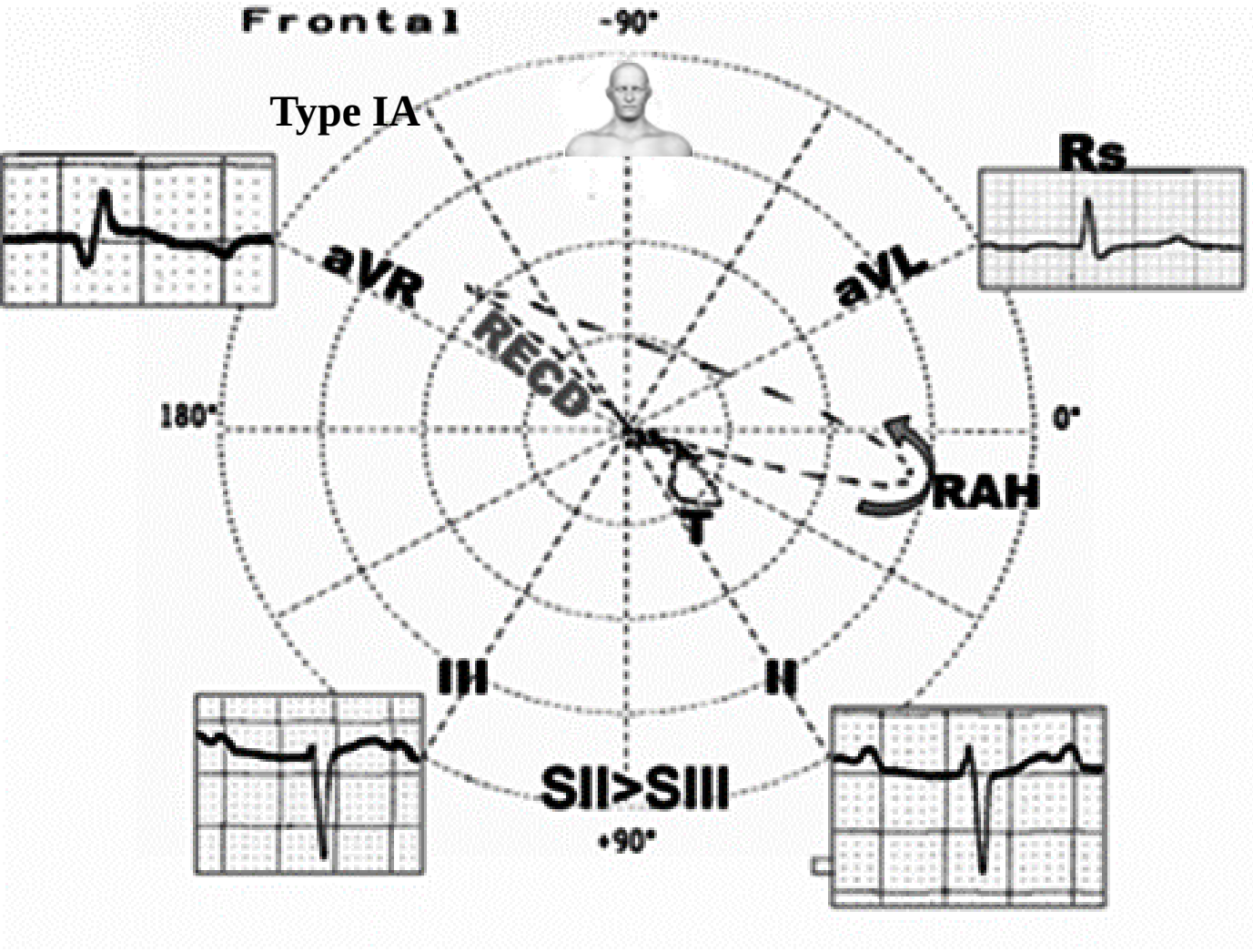

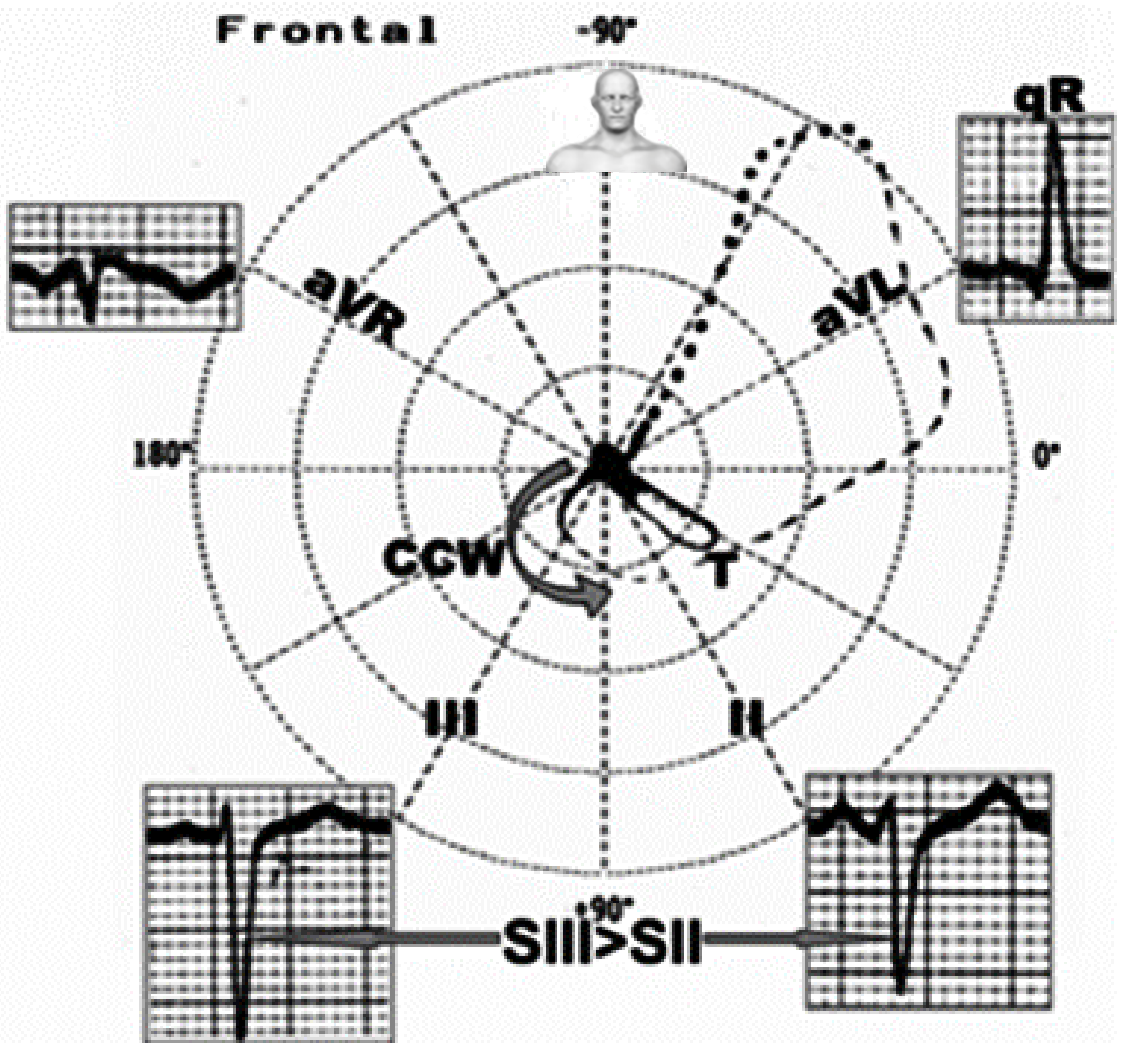

Typical example of Brugada type I and Block of Superior Division of Right Bundle-Branch (BSDRBB) Type IA (pseudo LAFB)

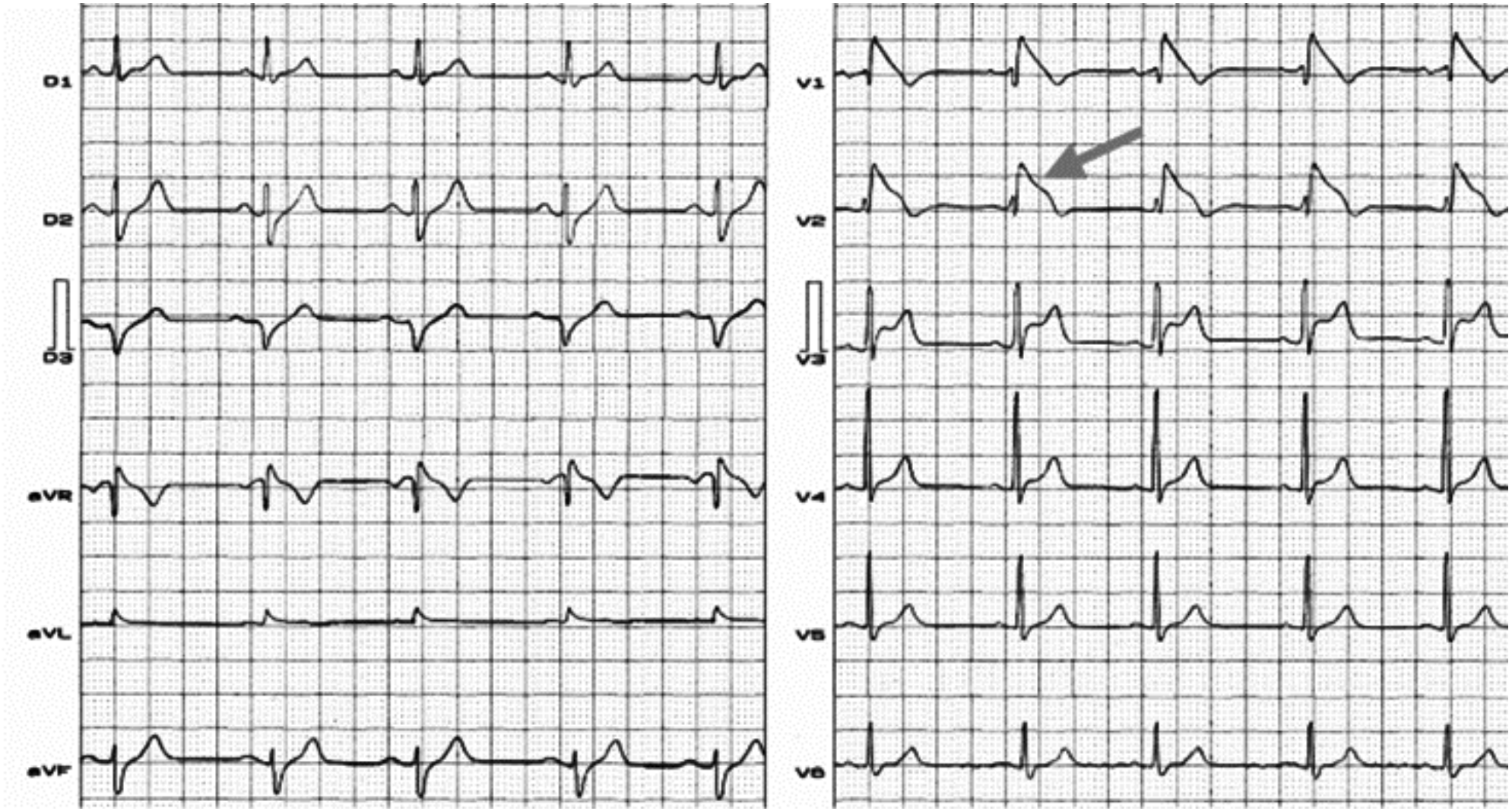

12-lead surface ECG shows a marked axis deviation to the left; SII > SIII and a prominent final R wave of unipolar aVR limb lead and typical type 1 BrP.

Conclusion:

1) Block of Superior Division of Right Bundle-Branch (BSDRBB) Type IA: pseudo LAFB (see explanation in the next example)
2) Type 1 Brugada Pattern.

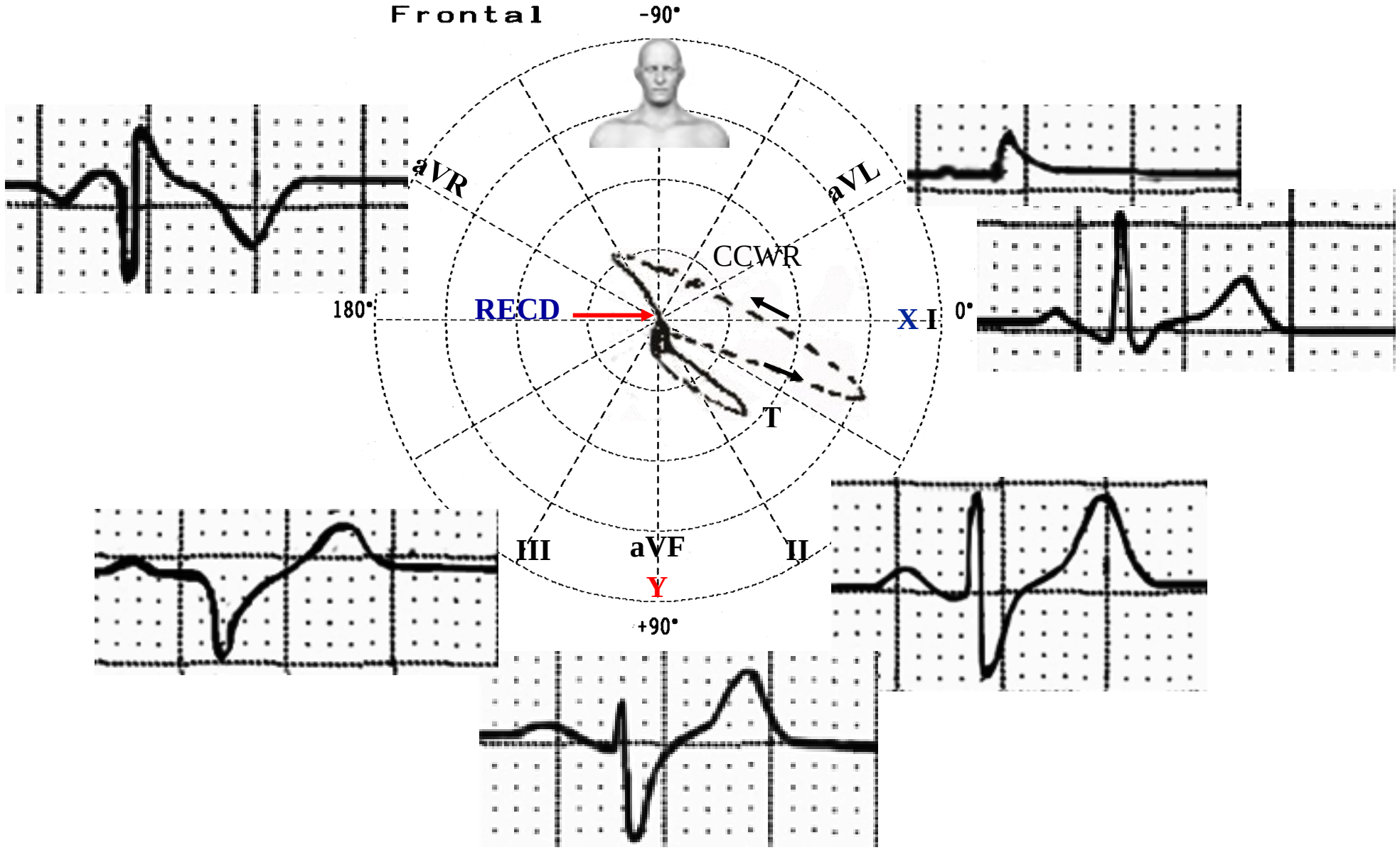

The 10 to 20ms initial forces are directed to left and downward (in LAFB this forces are directed to right and downward). Counterclockwise rotation (CCWR) with extreme left axis deviation, SII>SIII, prominent final R wave in aVR and prolonged R-peak time in this lead.

T-loop: Rounded, small, with symmetrical velocity of inscription of afferent and efferent limbs and a 1:1 length/width ratio: Repolarization mechanism.

RECD on right posterior quadrant: Depolarization mechanism

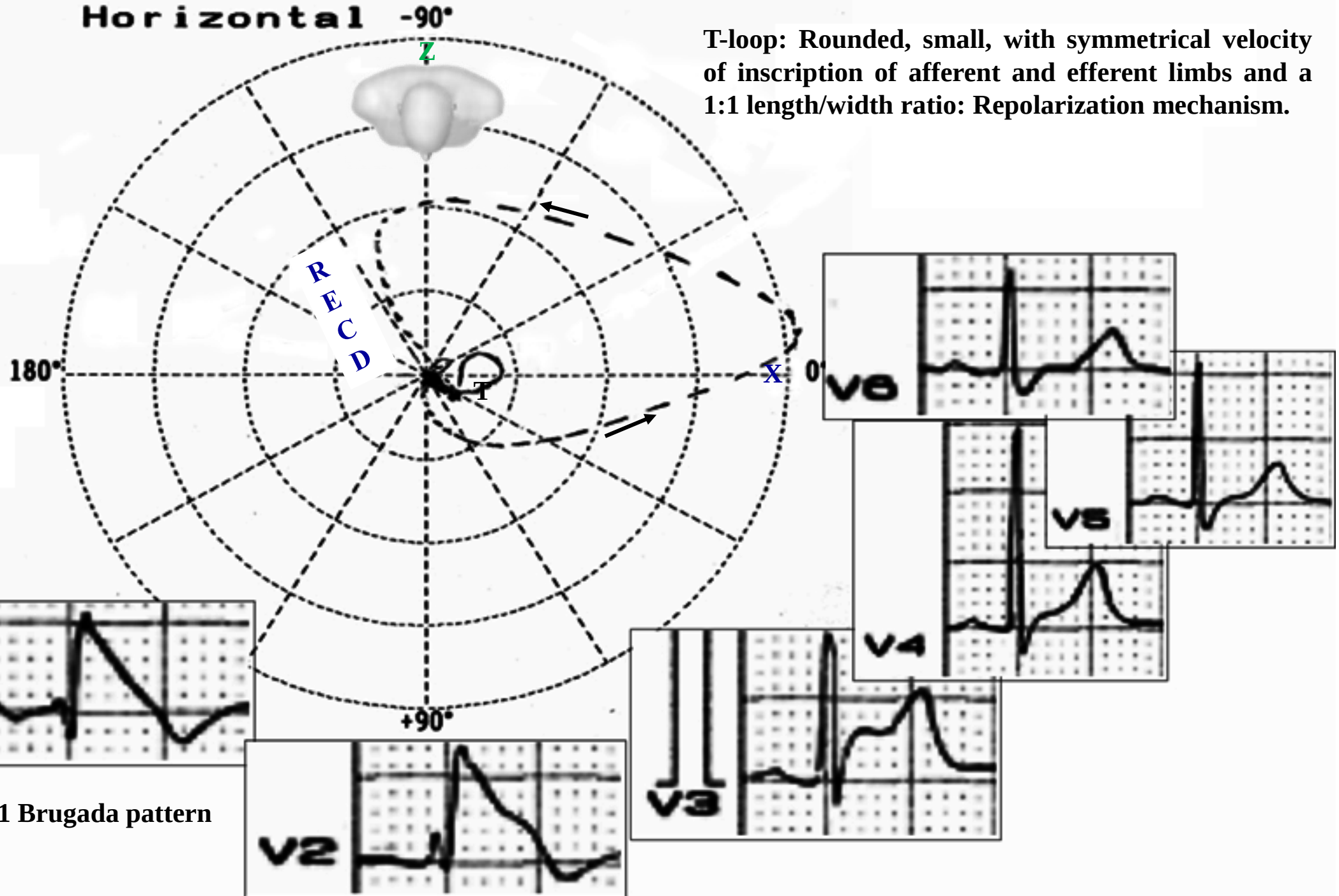

Type 1 Brugada pattern

RECD on posterior superior quadrant: Depolarization mechanism

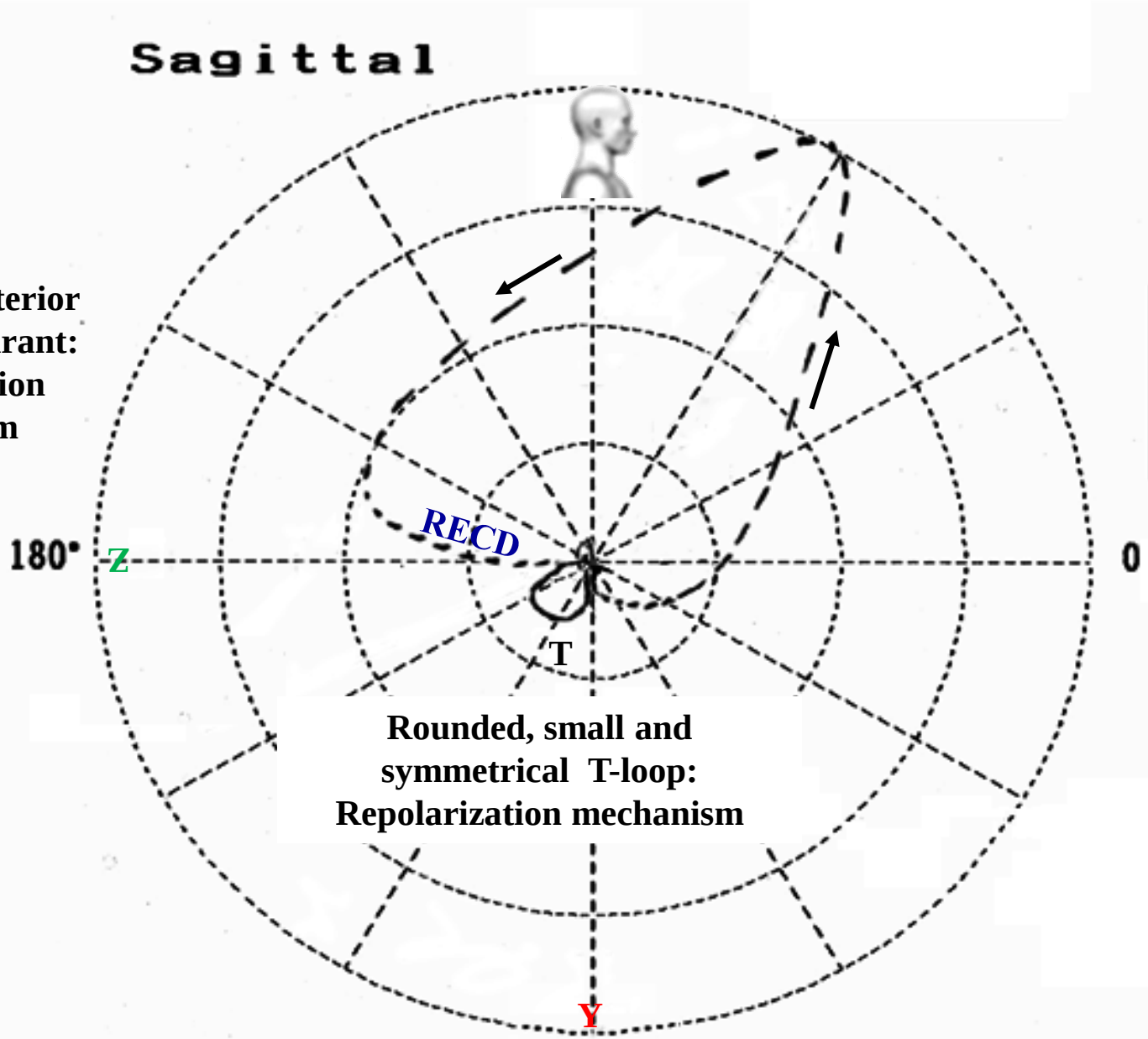

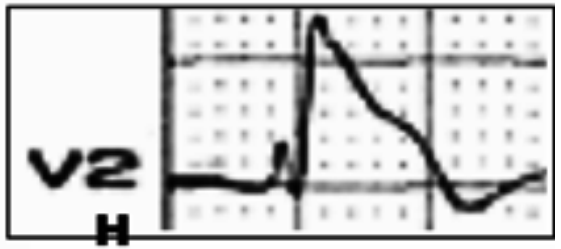

Rounded, small and symmetrical T-loop: Repolarization mechanism

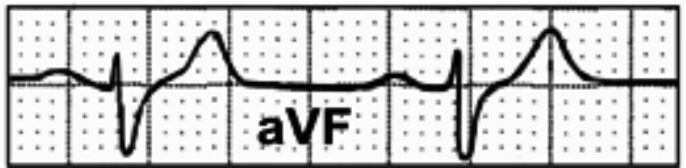

Type II RECD or Right Posteroinferior Subdivision Block (RPSB)

In this variant the **RECD** is located in the right inferior quadrant, in the territory of the inferior fascicle of the right bundle branch or right posterior subdivision block (RPSB) (**de Micheli A 1988**). SÂQRS$_{FP}$: +95°. SI-RII-RIII pattern (RIII < 15 mm). I and aVL: rS, II and III: qR. The descending ramp of R wave is slightly slow. It may present differential diagnosis with LPFB. Surface ECG suggests RPSB or type II RECD when delay and slowness of right ventricular myocardial depolarization signs (R-wave slurring and R-wave peak time prolongation) become evident only in the leads exploring the posterior and mid-inferior lateral regions of the free right ventricular wall. In this case, the resulting vector of homolateral ventricular activation is heading to the right, below and back from its origin point. There is QRS complex slurring in V_{3R} and V_1, also in aVF and in the high right abdominal lead MD, if the cardiac position is horizontal. Likewise, S wave slurring is observed in V_5 and V_6. Further, there should be a significant difference between R-wave peak time from the affected regions and that from the right anteroinferior septal mass (R-wave peak time in V_3 and/or V_4). In absence of right ventricular hypertrophy, such difference should be ≥ 30 ms. This is considered even more significant when the manifestation time of vector 2s is normal: between 20 and 25 ms (healthy hearts or with a single right ventricular dilatation) (**Medrano 1978**). Usually, right chest leads V_{5R}, V_{4R} and V_{3R} explore the posterolateral portions of the right ventricular free wall; while V_3 and V_4 remain facing the interventricular septum (intermediate cardiac position). But in horizontal hearts, it is the low leads (particularly aVF) that explore the low posterolateral regions of the right ventricular free wall. The resulting vector from ventricular activation manifests around 60 ms after the activation starts, and heads ≈ +125° in the frontal plane.

Type II RECD or Right Posteroinferior Subdivision Block (RPSB) ECG/VCG correlation on frontal Plane

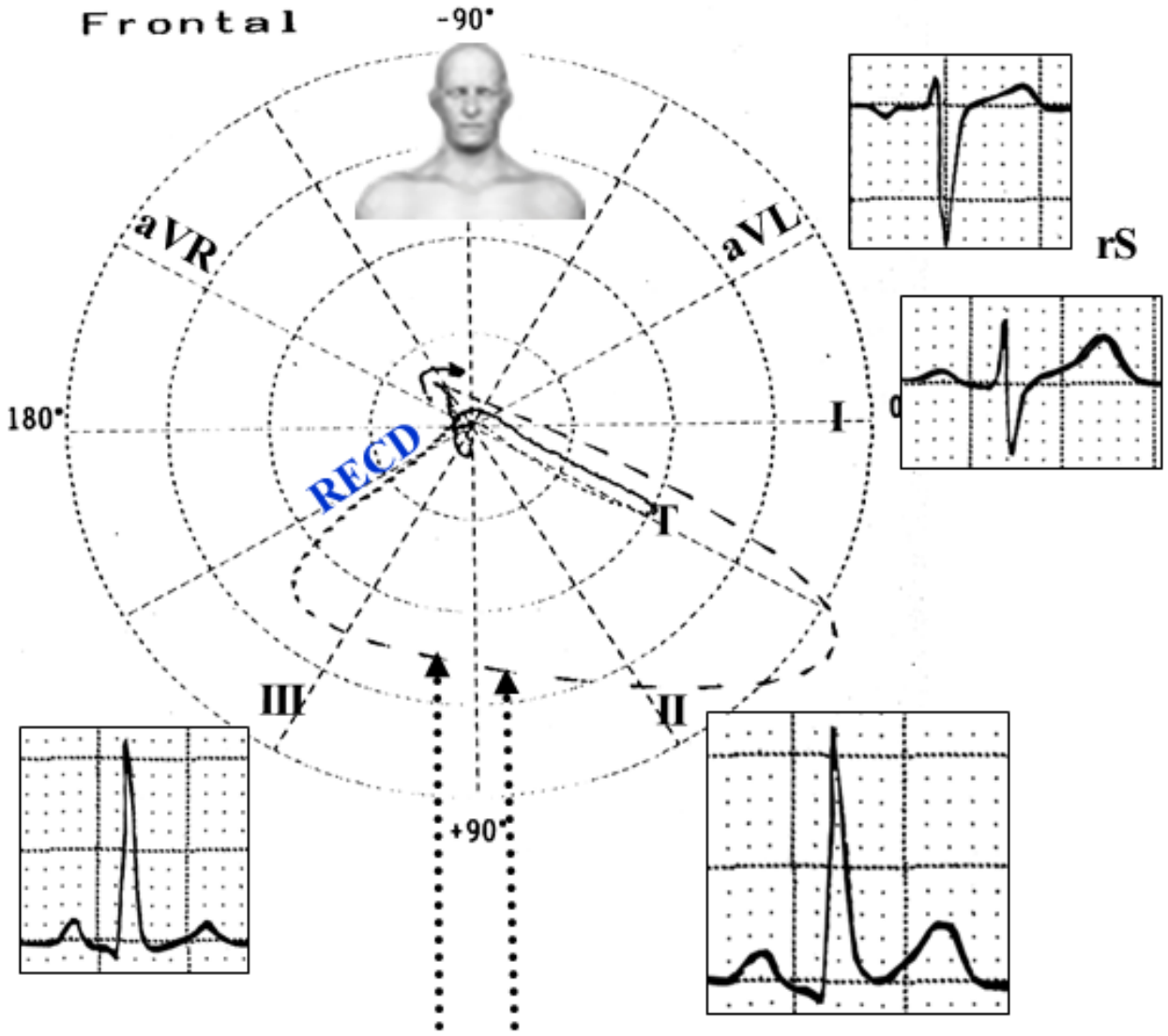

Rapid passage from left to right

Location of RECD in RPSB

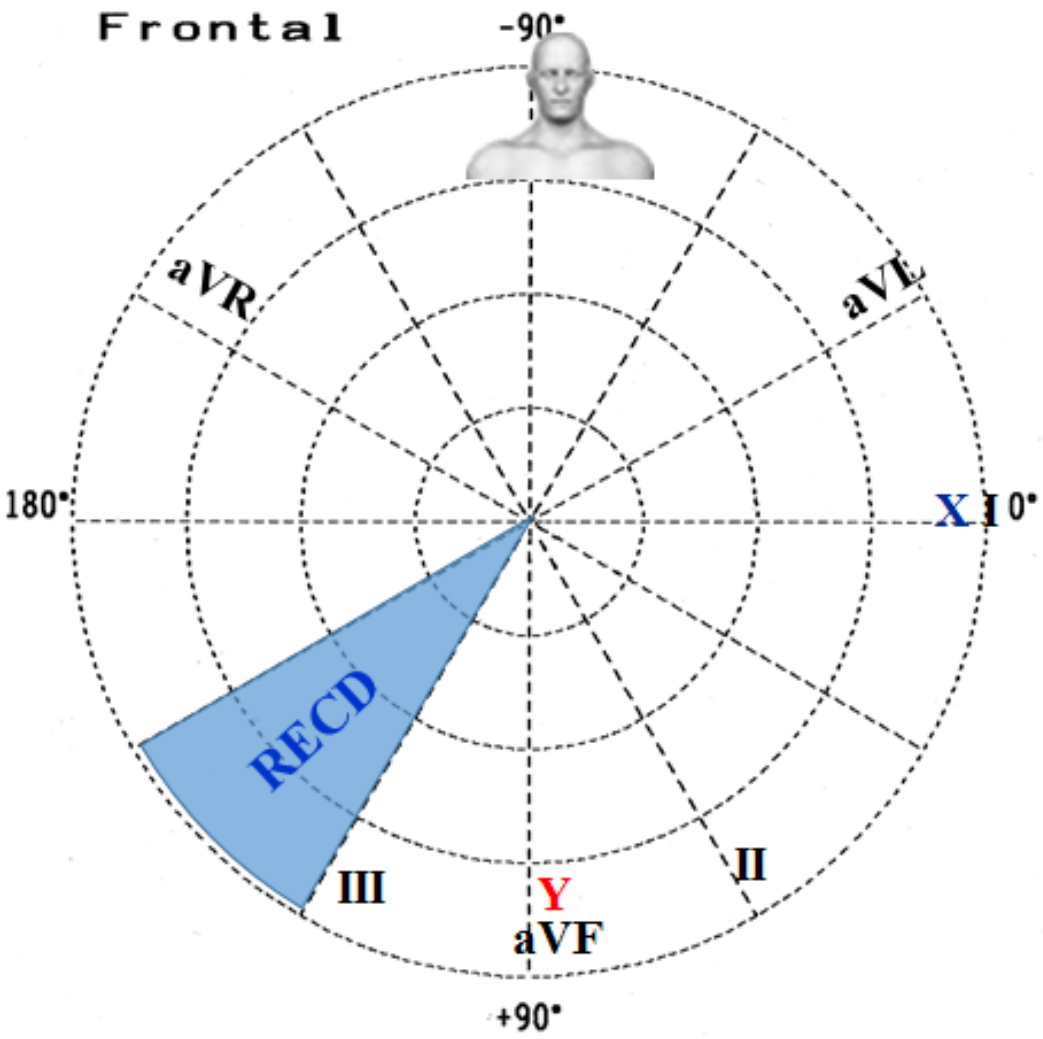

ECG/ VCG features are very similar with the LPFB: See differential diagnosis in next slide table

	Type II RECD or RPSB	LPFB
R-peak time in aVF, V5 and V6	Normal	Increased: > 35 ms (**Rusconi 1980**)
R-peak time in aVL	Normal	Decreased: up to 15 ms.
Aspect of QRS loop in the frontal plane	CWR and with characteristic rapid passage from left to right between 30 and 50 ms.	CWR, aspect of "fat" loop and maximal vector close to + 120°.
Clinical factors that should be excluded	Not stated.	Vertical heart, RVH and lateral infarction.
Association with RBBB		It is the rule
Notch in the descending limb of the R wave in III	No	Characteristic
Middle-final notch in RIII	No	Yes
RII/RIII voltage ratio	RII > RIII	RIII > RII
The q wave in III/ q wave in II ratio	qIII > qII	qIII < qII

Type II RECD or RPSB

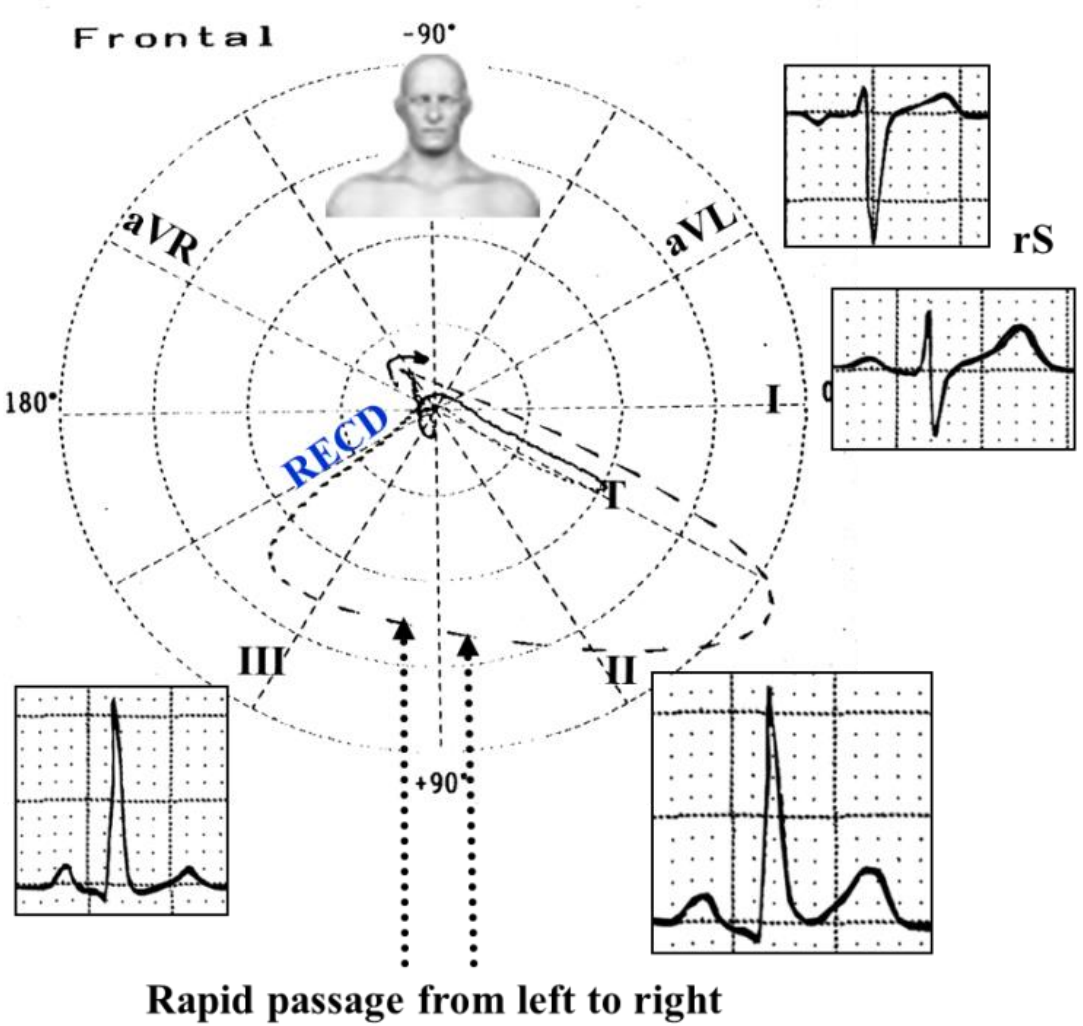

LPFB

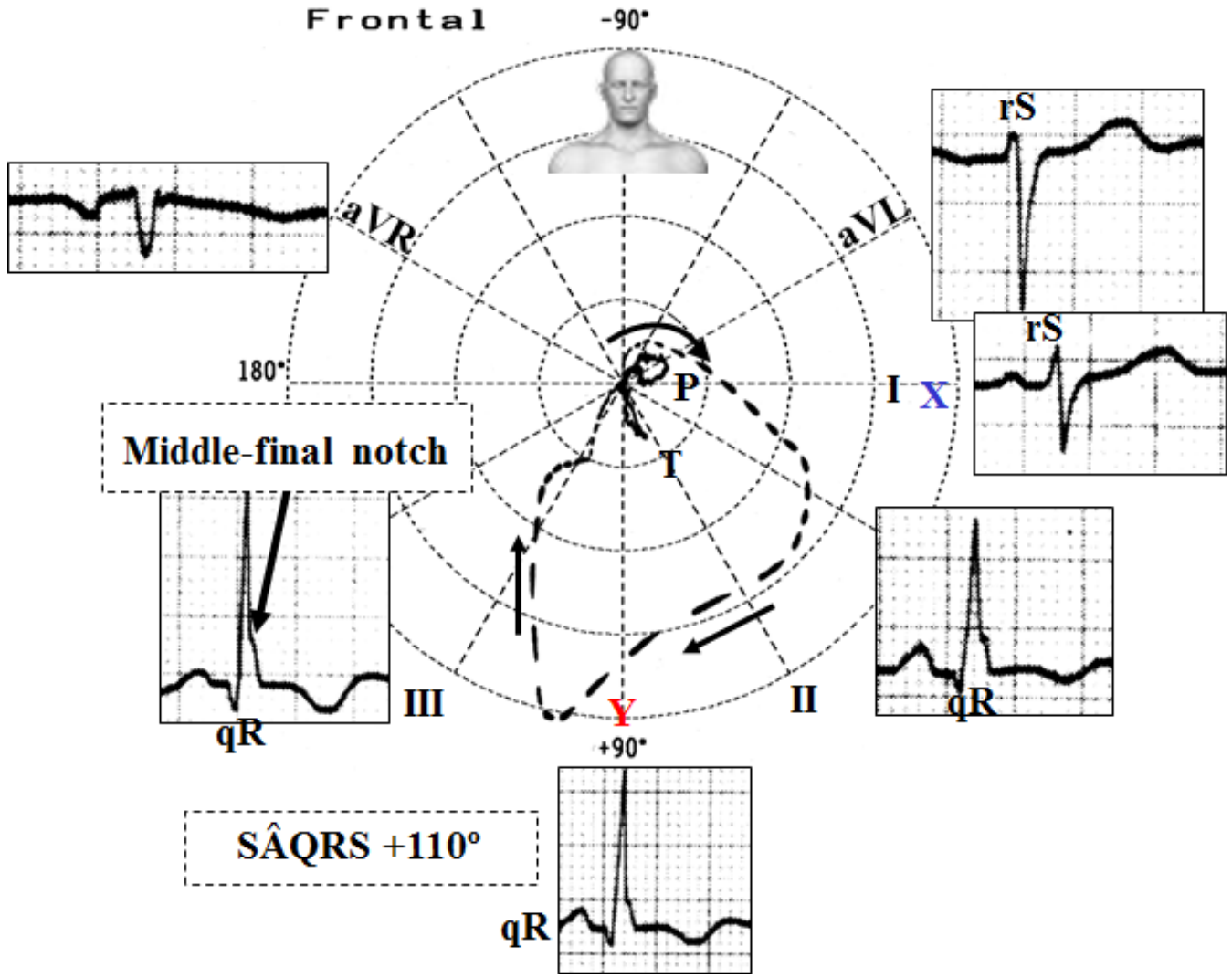

Type III, does it exist?: **RECD** located on the right portion of the 0±180° line, corresponding to the territory of distribution of the hypothetical middle fascicle of the right bundle branch. **RECD** located in the territory of the middle or anterosuperior fascicle of the right bundle branch, i.e. very close of ±180° on X orthogonal lead. It may be called Right Middle Fascicle Block (RMFB). Type III existence is polemic.

Type III

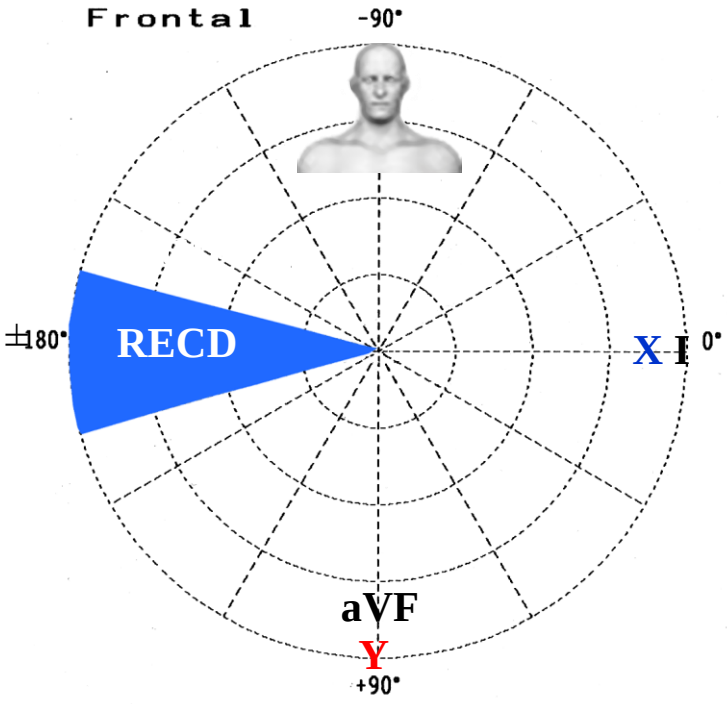

Subtype IIIA: CCWR

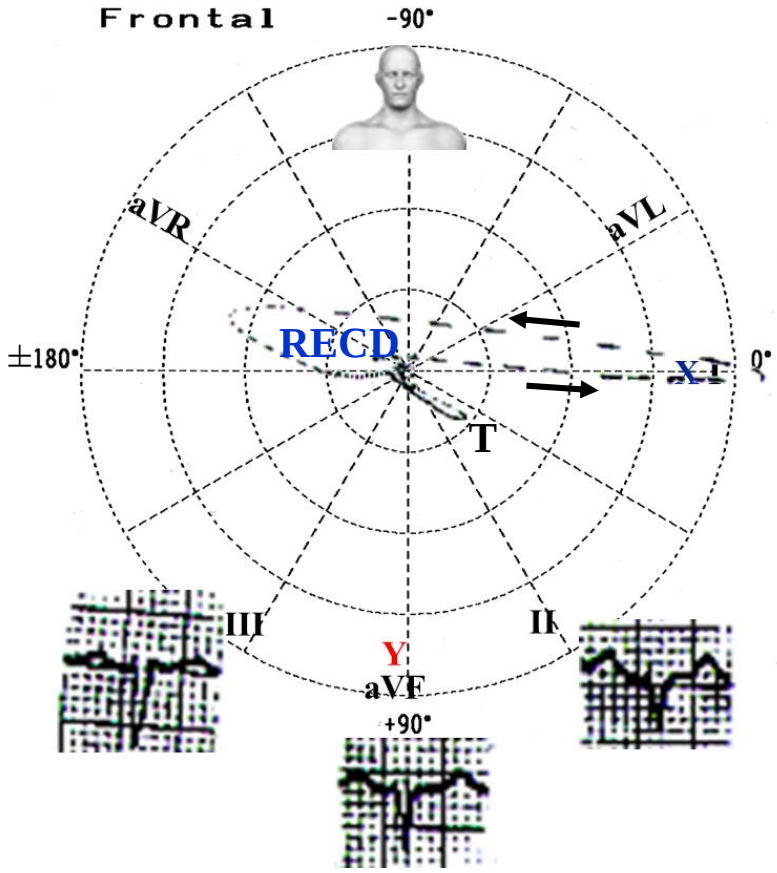

Subtype IIIB: CWR

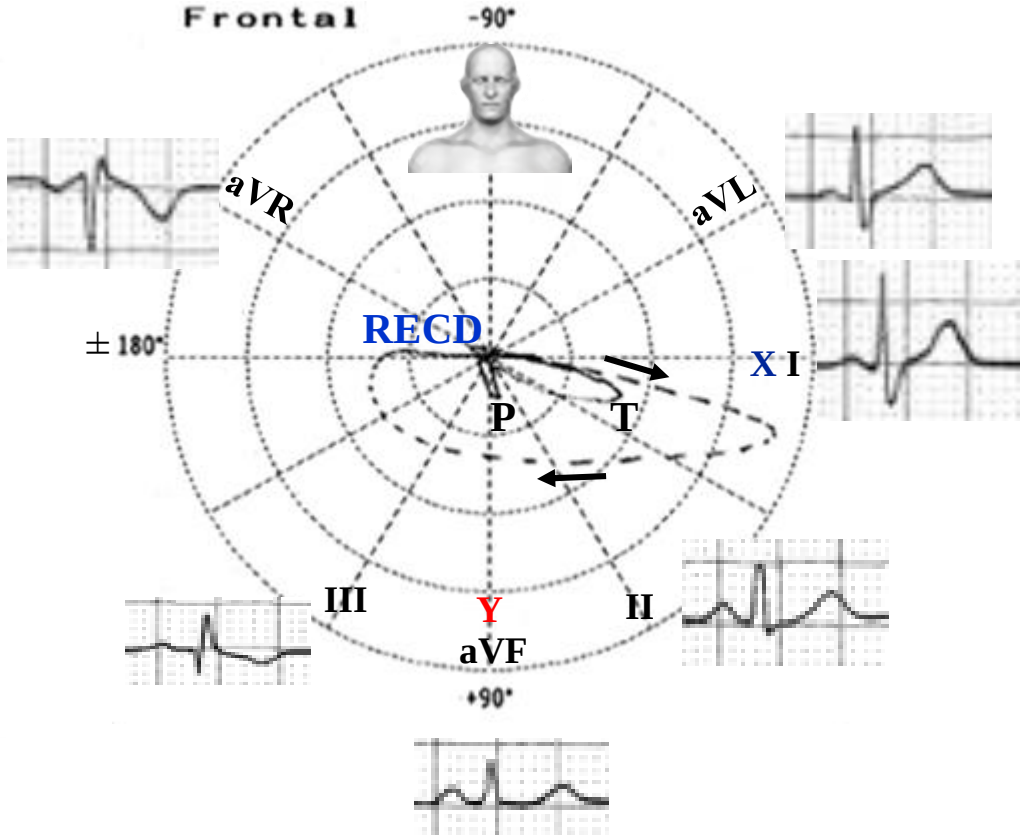

Pseudo inferior myocardial infarction

CCWR: QRS loop with counterclockwise rotation. This subtype has a pattern very similar with myocardial inferior infarction CWR: QRS loop with clockwise rotation

The clinical significance and interest of right divisional or fascicular peripheral right bundle block

I. They may be confused with left fascicular blocks:
   - *Left Anterior Fascicular Block: with the type IA or right superior divisional/fascicular block (RSDB) with counter clock wise rotation on frontal plane) and*
   - *Left Posterior Fascicular Block: with the type II or right inferior divisional/fascicular block (RSDB) on frontal plane.*

II. They may be confused with electrically inactive areas (pseudo electrically inactive areas or pseudo myocardial infarction) both in the anterior and the inferior walls.

III. They may represent the ECG/VCG pattern of Brugada syndrome (**Pérez-Riera 2008**), of one subpopulation of Arrhythmogenic Right Ventricular Cardiomyopathy/Dysplasia(ARVC/D (the so called concealed forms) (**Corrado 1996; Corrado 2001**) and also observed in chronic chagasic cardiomyopathy (**Vichi 1982; Tobias 1986**). Corrado et al investigated members of a single family who possessed the type 1 ECG BrP. Cardiac histopathological examination in the proband revealed myocardial atrophy, transmural fatty replacement, interstitial fibrosis (including fibrosis involving the specialized conducting tissue), although no wall thinning or inflammatory infiltrates associated with classical ARVC were seen. An older sibling had moderate RV dilatation, apical trabecular changes and his right endomyocardial biopsy showed moderate fibrofatty replacement. Some other members of the pedigree had mild to moderate RV and/or RVOT dilatation, wall motion abnormalities and a trabecular pattern on echocardiography. The findings in this family, although not typical of classical ARVC, possess enough pathological features to suggest that there may be a relationship between BrS and ARVC, illustrating the issue of diagnostic classification in the presence of both a typical type 1 ECG and marked structural abnormalities. The suggestion that BrS may actually be a form of ARVC in view of the increasing evidence of structural abnormalities, has been raised. Significant overlap between the two conditions does exist: ajmaline has provoked type 1 changes in ARVC patients (**Peters 2004**), and fibrofatty replacement of cardiac myocytes has been reported in patients diagnosed with BrS (**Zumhagen 2009**).

4. **Abnormal expression of cardiac neural crest cells in heart development** (Elizari 2007) in fact this theory is also eclectic because it admits both mechanisms: depolarization and repolarization. The cardiac neural crest(CNC) cells are a subpopulation of cranial neural crest discovered nearly 33 years ago by ablation of premigratory neural crest. The CNC cells are necessary for normal cardiovascular development.

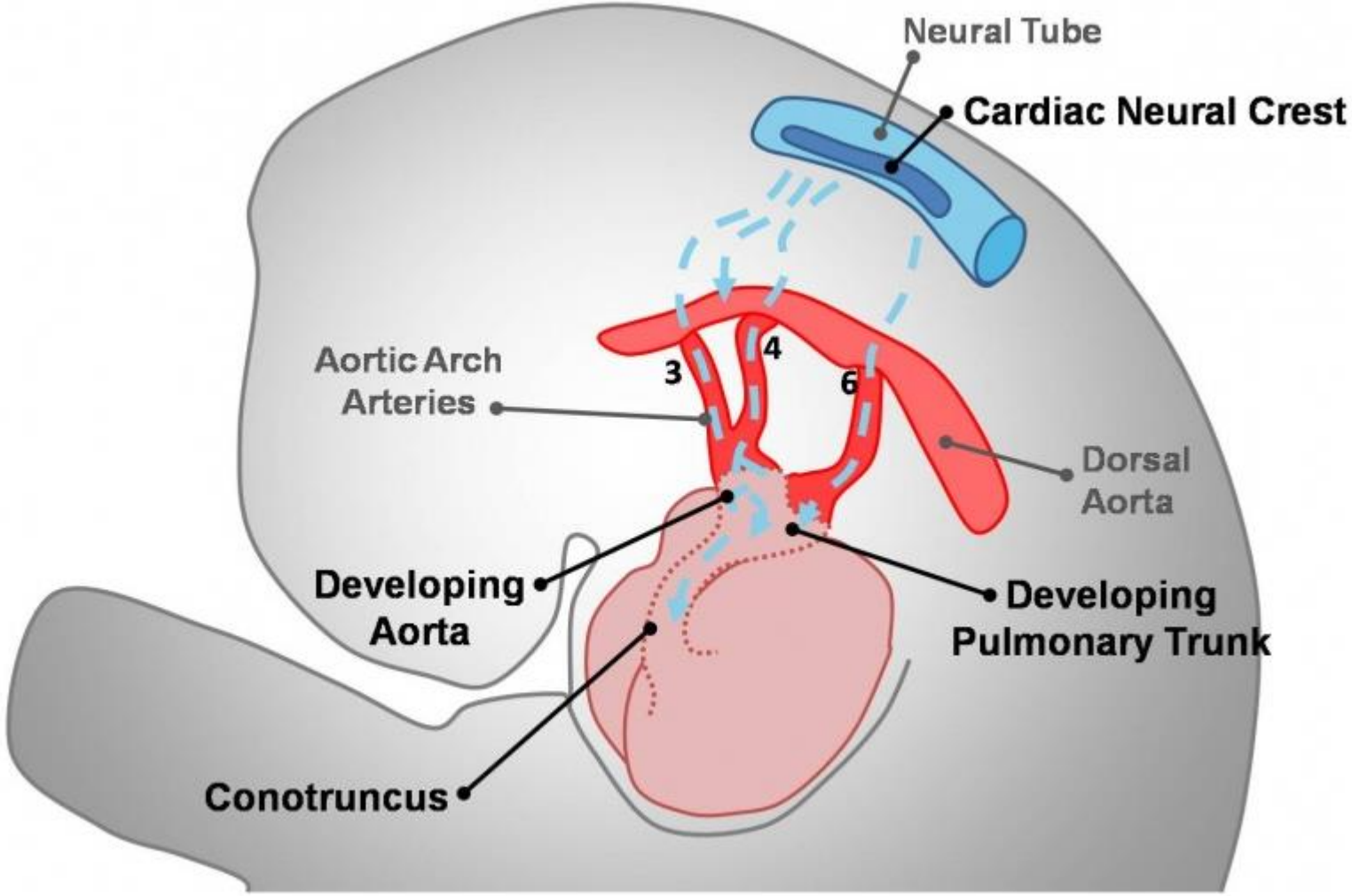

Cardiac neural crest (CNC) cells migrate from the neural tube to the circumpharyngeal ridge (i.e.,circumpharyngeal crest), caudal pharyngeal arches (third, fourth, and sixth), and outflow tract (OFT) just before asymmetrical remodeling of the aortic arch arteries. Some of the CNC cells migrate in and envelop the nascent aortic arch arteries, while others continue to migrate and eventually colonize to later form the aorticopulmonary septum.

Elizari et al (**Elizari 2007**) has been proposed regarding the etiopathogenesis of the BrS linked to the abnormal expression of the CNC on myocardial development of the RVOT. Of the four cardiac chambers, the RV is anatomically, phylogenetically, and developmentally the most complex. Additionally, clinically, it is the most critical chamber because the most complex congenital cardiac anomalies involve the RV, as do the congenital arrhytmogenic syndromes. RVOT formation, which comprises the free wall and the aortopulmonary septum, requires participation of an extracardiac cell source, the CNC. The contribution of the CNC cells to cardiac development was first recognized by Kirby (**Kirby 1983**). In experimental studies, showed the relationship between outflow tract malformations and the disturbed CNC. Kirby´s manuscript showed that ablation of specific points of the premigratory CNC in chicken embryos caused a wide spectrum of outflow tract and great arteries malformations. In mutant and transgenic mice have refined this theory, indicating that "the outflow tract septation is a very vulnerable process" and that "the abnormalities that can be evoked include the myocardium (**Gittenber-de Groot 2000**). Moreover, the neural crest cell death program plays an active role in stimulating outflow tract myocardialization (**Poelmann 1999; van den Hoff 1999**). A population of CNC cells migrates toward the arterial pole of the embryonic heart, and the aortic arch. On the other hand, a second route of migratory CNC cells uses the venous pole as entrance to the heart. These neural crest cells reach the area of the future location of the AV node, His bundle, and beginning of the bundle branches. They are distinguished around the mitral and tricuspid orifices and the pulmonary veins (**Gittenber-de Groot 2000**; **Poelmann 1999**). Neural crest cells also contribute to the development of part of the atrial tissues that play an important role in closing the primary atrial septal foramen and septation of the AV canal. Likewise, they are involved in morphogenesis of the pulmonary veins. Thus, eventual abnormalities in this developmental process may be correlated with the fact that a proportion of patients with BrS exhibit paroxysmal AF and other supraventricular arrhythmias (**Antzelevitch 2005**). Consequently, it is reasonable to postulate that the arrhytmogenic substratum in BrS should not be restricted to the ventricular level and may well also account for the occurrence of supraventricular arrhythmias. Among other molecules, the connexins (Cxs), particularly Cx 43, are known to be strongly involved in neural crest cell migration and are expressed in adult working myocardium. Cx 43 function may be of critical importance in downstream events involving migration of neural crest cells and that heart defects, when present, involve the RV (**Ewart 1997**). Slower or faster migration of neural crest in vitro and in situ was directly correlated with overexpression or underexpression of Cx43 (**Waldo 1999**). Quantification by immunofluorescence has demonstrated significantly lower expression of Cx 43 in subepicardial compared with deeper layers, thus creating and contributing to transmural heterogeneity (**Poelzing 2004**). It has also been postulated that mistiming of CNC migration or malfunction of the crest cells as a consequence of altered gap junctional communications may have profound effects on tissue remodeling depending on CNC cells (**Söhl 2004**). Cx43 contribute to the propagation proprieties of the cardiac impulse. Transmural distribution of Cx43 is heterogeneous, being twice as abundant in midmyocardium and endocardium compared with epicardium (**Yamada 2004**). It was proposed that the basis for BrS was an abnormal transmural repolarization in the RVOT due to heterogeneous loss of the cardiomyocyte AP dome in the epicardium.

However, electrophysiological, imaging, and histopathological studies have identified subtle structural abnormalities in patients with BrS. Myocardial fibrosis has been suggested by abnormal, low-voltage, fractionated electrograms localized to the RVOT at the epicardium (**Zhang 2016**). Ablation at these sites has eliminated the type 1 BrP and successfully reduced arrhythmic events, as was seen in a previous experimental model.

A study of SCD cases associated the type 1 ECG with ARV. Furthermore, SCD cases with a familial diagnosis of BrS showed structural abnormalities that were insufficient to fulfill the diagnostic criteria for cardiomyopathy or myocarditis. Other myocardial anomalies have been reported in selected cases. Therefore, there is significant debate about the underlying substrate in BrS. To resolve this controversy, Nademme et al (**Nademanee 2015**) tested the hypothesis that BrS is associated with fibrosis in the RVOT and altered expression of the gap junction protein connexin-43 (Cx43), which may be critical for correct cellular migration and maintenance of RVOT zonation. These authors observed that BrS is associated with epicardial surface and interstitial fibrosis and reduced gap junction expression in the RVOT. This collocates to abnormal potentials, and their ablation abolishes the BrS phenotype and life-threatening arrhythmias. BrS is also associated with increased collagen throughout the heart. Abnormal myocardial structure and conduction are therefore responsible for BrS. Lesser expression of Cx43 and, hence, gap junctional impairments in the epicardium may contribute to heterogeneous electrophysiologic properties throughout the ventricular wall favoring both transmural repolarization heterogeneity and slower dromotropic velocity in the RVOT epicardium. The effect of such heterogeneity would influence both repolarization and depolarization proprieties (**Smits 2002**). Abnormal myocardialization dependent on CNC expression in the RVOT might also explain repolarization heterogeneities underlying the phenotype of BrS. Additionally, The heterogeneous expression of Cx43 in the RVOT area may serve as substrate for idiopathic ventricular arrhythmia (**Ou 2005**). Inhomogeneous transmural and regional Cx43 distribution in the RVOT may lead to conduction slowing and late activation of the RVOT in BrS. The wide spectrum in the severity or magnitude of ECG and clinical manifestations of BrS must correlate with the existence of a wide spectrum in the severity of underlying cellular abnormalities in the RVOT. Similarly, the well-known dynamic changes of the Brugada phenotype should be interpreted as the consequence of the interaction between the magnitude of the pathophysiologic compromise of the substrate and the strength of the triggers. A pre-ECG alteration very close to threshold may readily shift from unapparent to manifest or vice versa. The fact that Na^+ channel blockers exacerbate repolarization changes and depress conduction, increasing QRS duration to a grater extent in patients with BrS than in controls, suggests the presence of a Na^+ channel and/or a gap junctional disorder, In an area with scarce, poor devoid of, Purkinje fibers as it happens in the RVOT, a reduced Na^+ current under the effect of a Na^+ -channel blocking drug and a poorer distribution of gap junctions in the RVOT may lead to slow conduction contributing to the ECG/VCG and electrophysiologic manifestations of BrS. The exact manner in which abnormal expression of the CNC affect ionic current and/or gap junctions should be explored. It can be hypothesized that repolarization gradients causing ST-SE occur not only between the epicardium and endocardium

but also between the RVOT ad normal surrounding myocardium.

The unequal distribution of repolarizing forces between the epicardium and subendocardial layers due to stronger I_{to} expression in epicardium than in endocardium might also apply between the RVOT and surrounding normal myocardium.

In patients with BrS, arrhythmias typically originate in the RVOT. The RVOT develops from the slowly conducting embryonic outflow tract. The slowly conducting embryonic phenotype is maintained in the fetal and adult RVOT and is unmasked when cardiac Na^+ channel function is reduced (**Boukens 2013**).

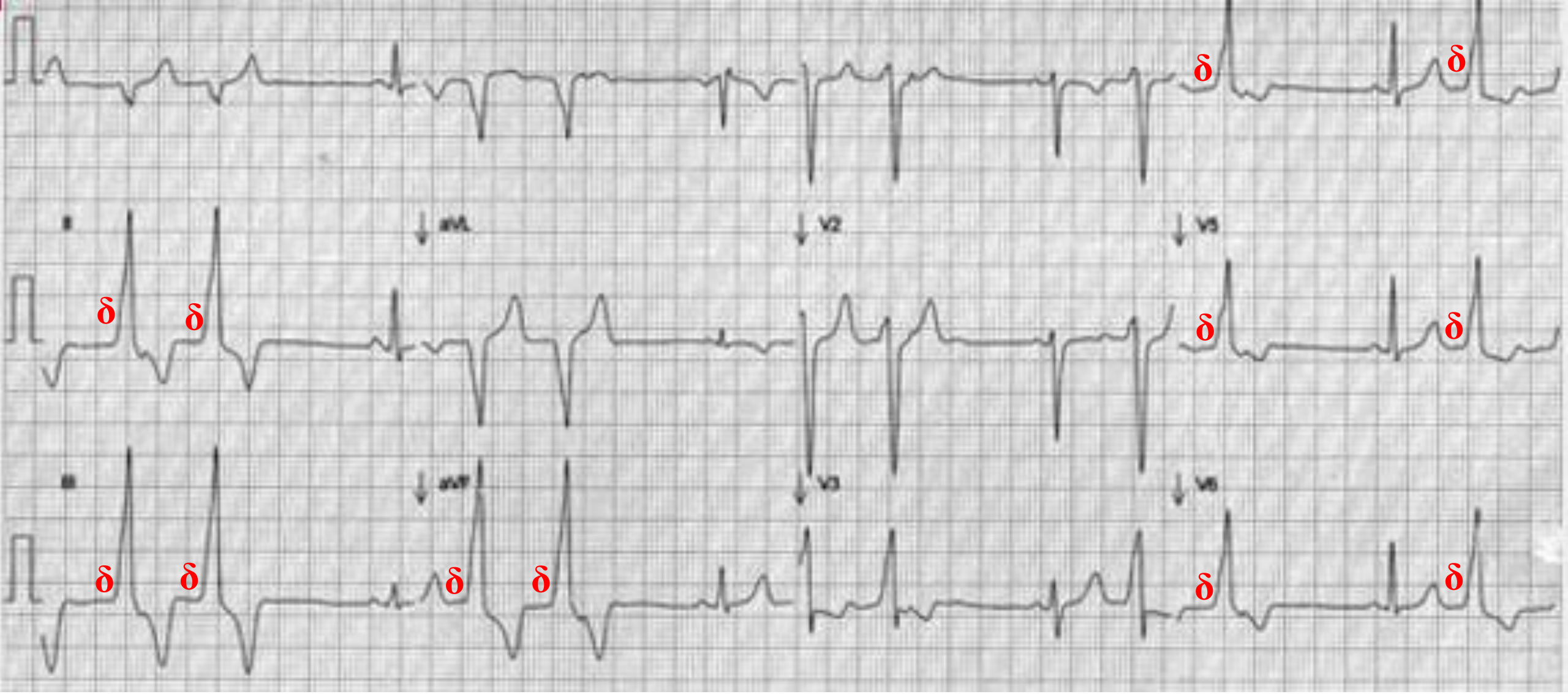

A 12-lead ECG of PVCs originating in the left coronary cusp/aortic sinus of Valsalva (ASV). Note that the QRS morphology in the limb leads is nearly the same as in the before example. However, the precordial ECG leads are markedly different. There is a broad but small r-wave in V_1 and V_2, and the transition from small to large R-wave is from V_2 to V_3. Although that could still be from the right side, a left-sided site is more likely, and intracardiac mapping and ablation confirmed a left ASV site. Pseudo delta wave is registered suggesting epicardial focus.

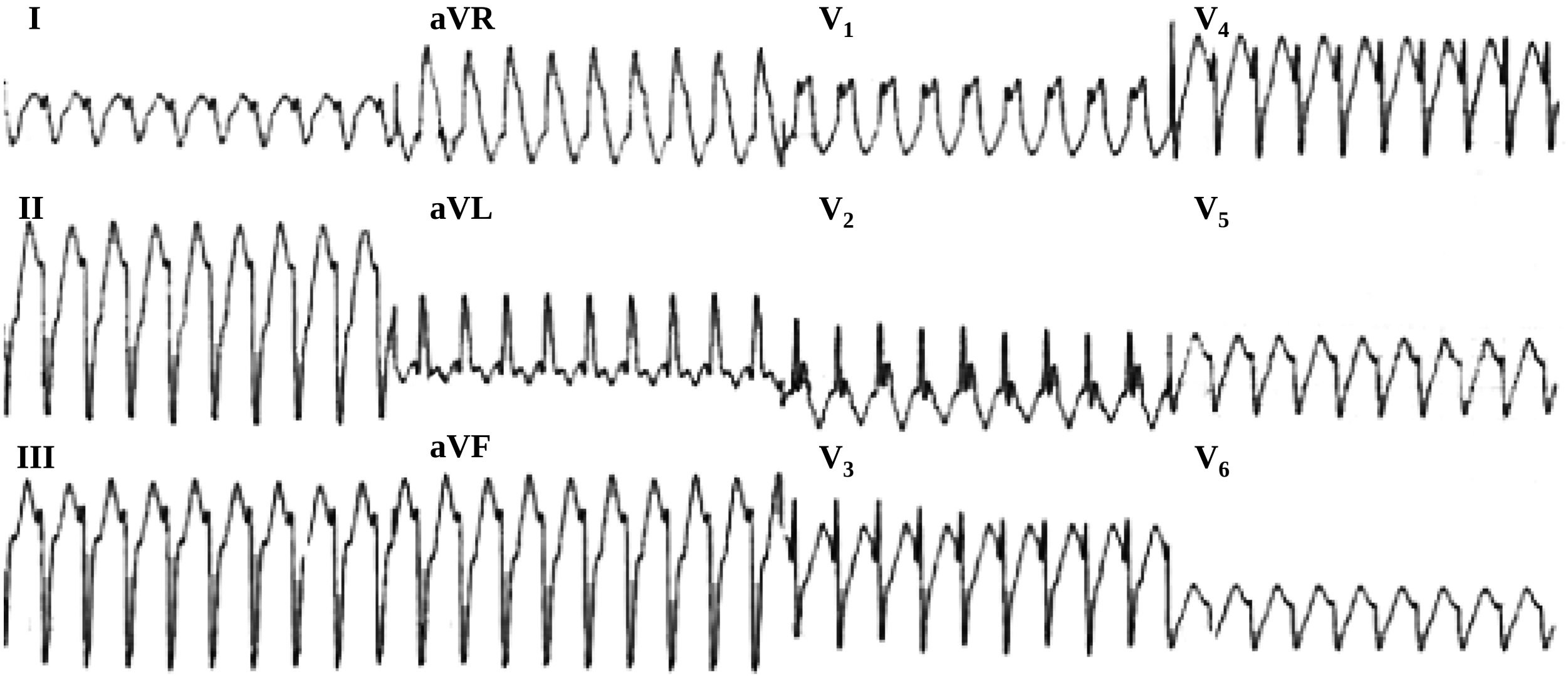

12-Lead ECG of Idiopathic Left VT: note that there is a RBBB pattern with a superior axis. This type of tachycardia has a site of origin near the left posterior fascicle.

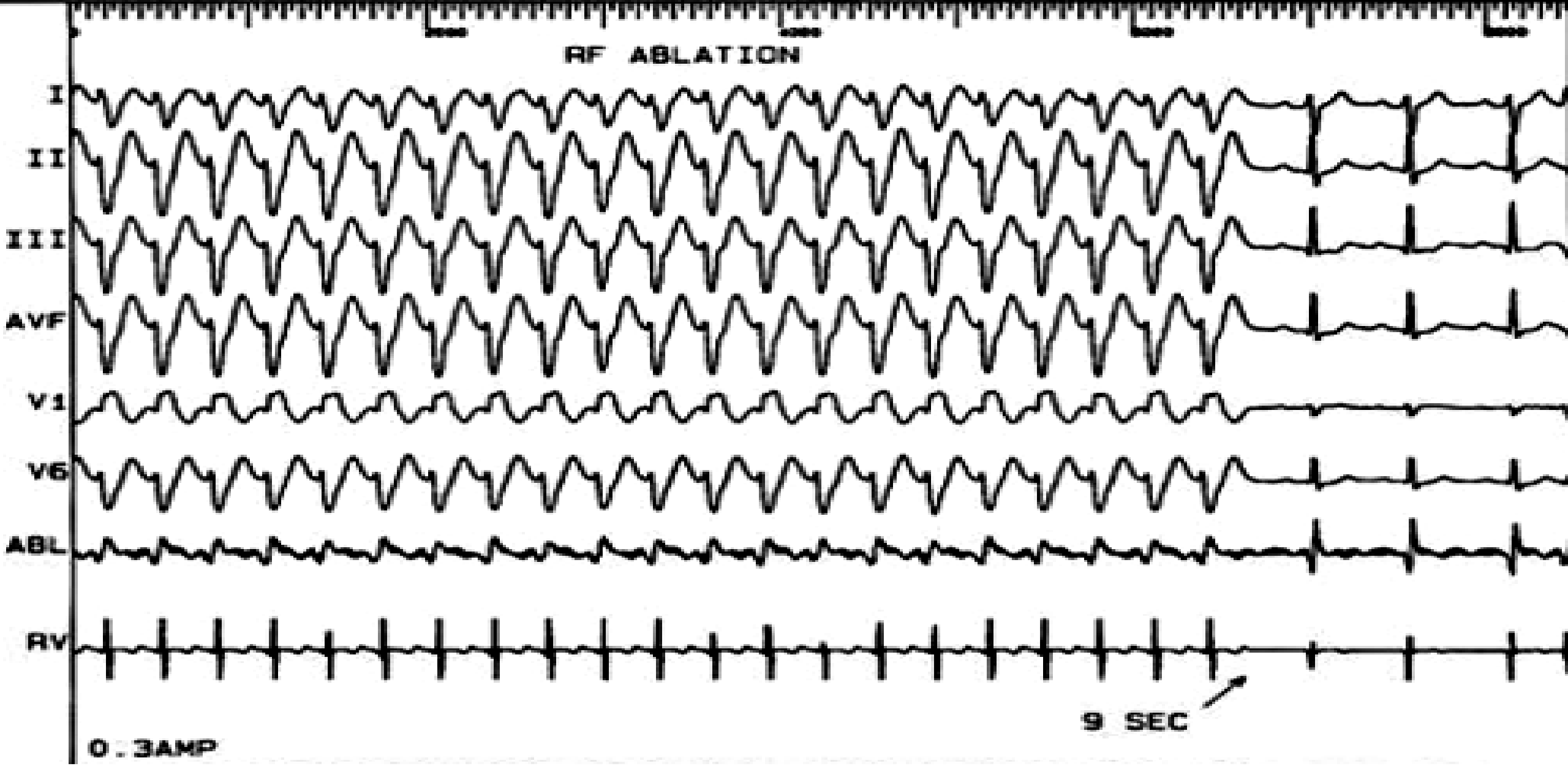

RFCA of idiopathic left VT: simultaneous tracings are ECG leads I, II, III, aVF, V_1, and V_6; intracardiac tracings from the ablation catheter near the LV posterior fascicle (Abl) and at the RV apex; and the energy delivery tracing (Current). Note that at 9 s after onset of 0.3 AMP, the tachycardia terminates. After this ablation, the VT was no longer inducible.

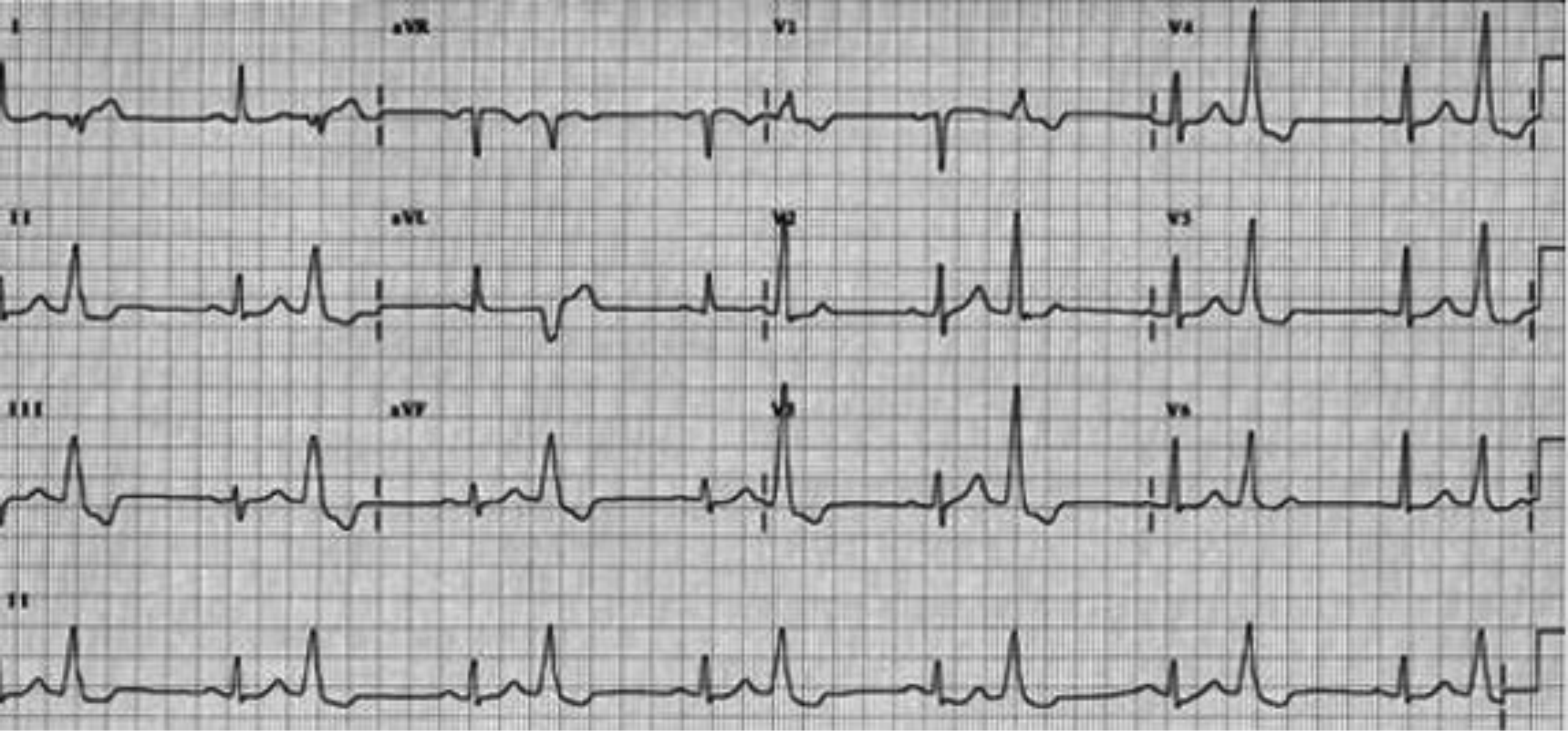

On this 12-lead ECG of PVCs originating from the LV epicardium at the anterior base, the QRS complexes show RBBB morphology in V_1 and upright R waves in ECG leads II, III, and aVF (inferior axis). Key is the broad, pseudodelta-wave appearance of the QRS complexes in the precordial leads that has been described with sites of origin on the mitral annulus and the ventricular epicardium. The site of origin was confirmed at mapping and ablation.

The BrS is characterized by coving ST-SE in right precordial leads V_1 to V_3 (≥2 mm in 2 of these 3 leads are diagnostic) followed by negative symmetrical T wave , and clinical presentation with syncope or cardiac arrest This pattern can be spontaneously present or provoked by sodium-channel–blocking agents such as ajmaline, flecainide, or procainamide The syndrome manifests predominantly in men in the third and fourth decades of life. The typical ECG pattern can be transient and may only be detected during long-term ECG monitoring. BrS has also been linked to SCD in young men in Southeast Asia and has several local names, including Lai Tai ("died during sleep") in Thailand. Patients with BrS are also prone to AF and SN dysfunction. Although different genes involved in BrS have been described, SCN5A gene mutations (BrS1) that lead to a loss of function of cardiac sodium channel (NaV 1.5) account for the vast majority of genotyped cases. However, even in patients with the typical BrS ECG pattern, a positive genotype is obtained only a minority (13%). BrS1 and LQT3 share SCN5A mutations as their basis, and overlapping phenotypes of BrS and LQT3 have been reported.

Genes Implicated in Brugada Syndrome

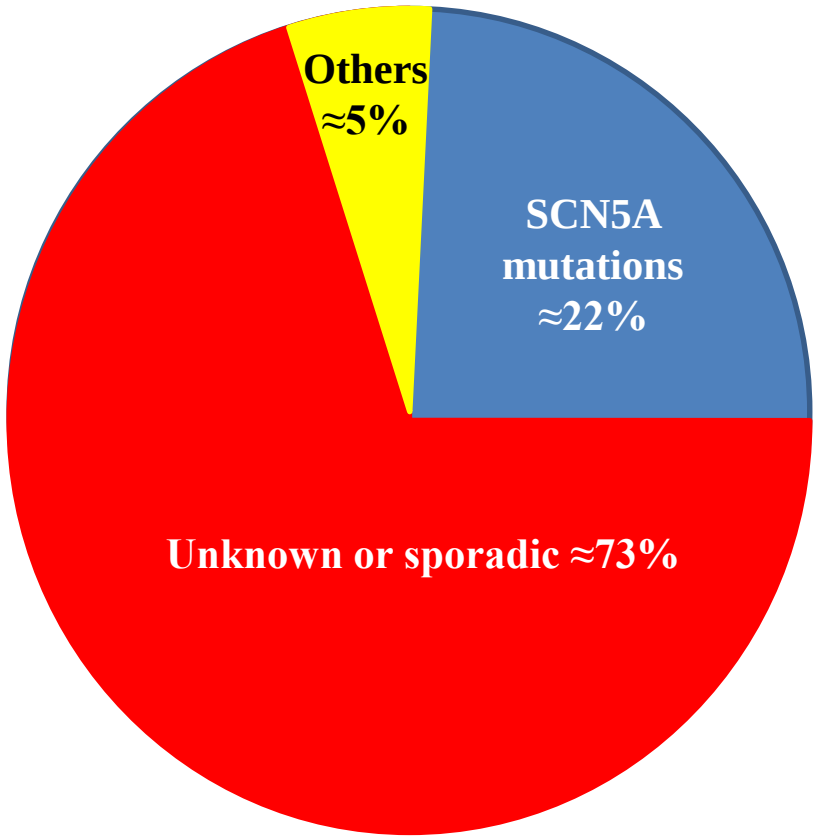

Multiple cardiac phenotypes that are associated with SCN5A mutations (Veltmann 2016)

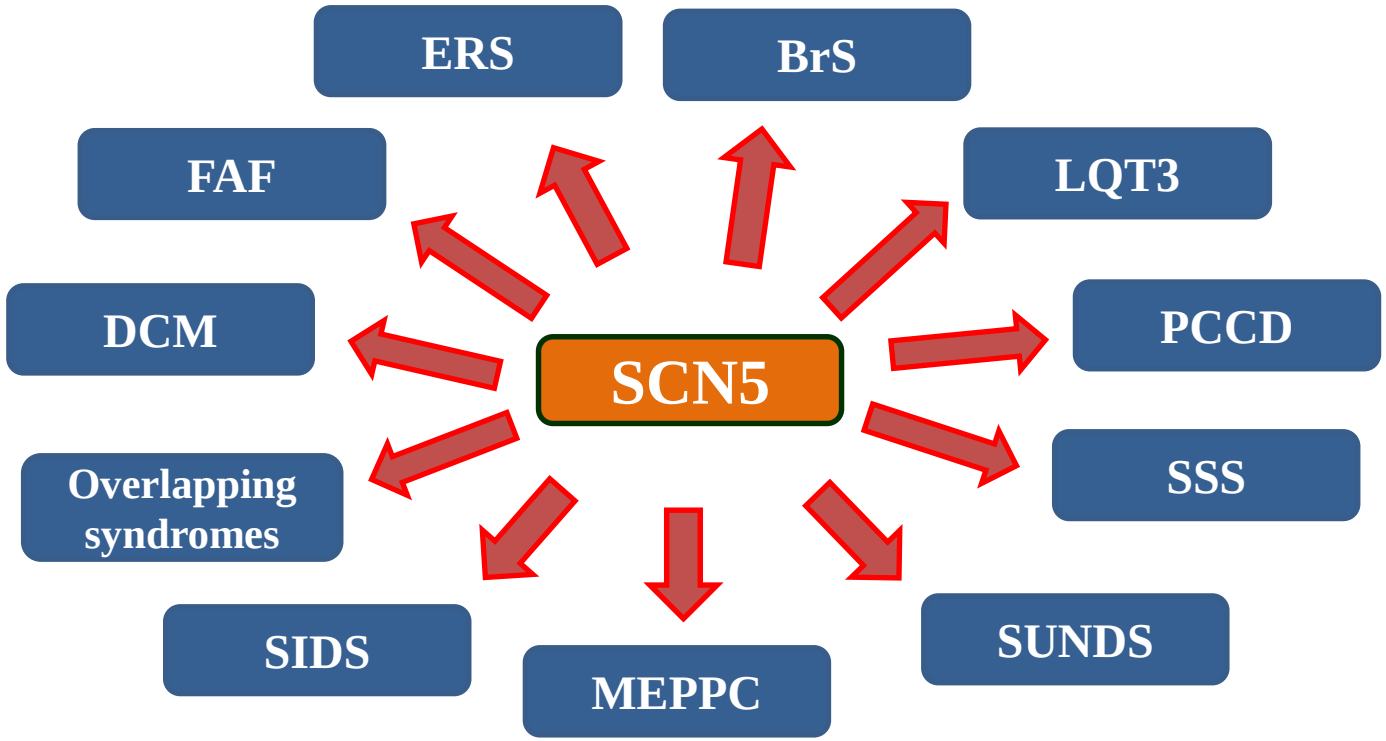

Sodium channel mutation in SCN5A gene and its phenotypes

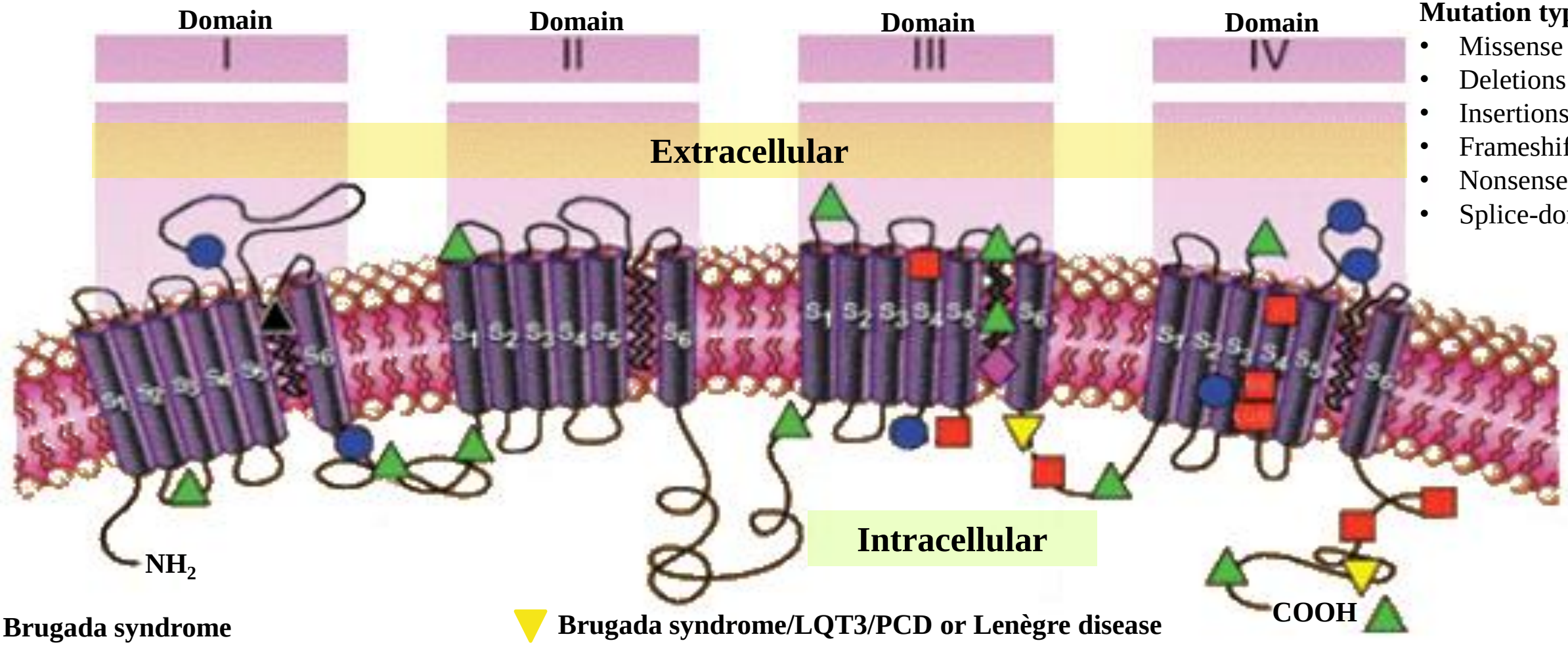

The predicted secondary structure of the cardiac sodium channel and locations of mutations causing the BrS, LQT3, Lenègre disease, overpaying syndromes and atrial standing . The channel consists of four putative transmembrane domains (I–IV), with each domain containing six transmembrane segments (S1–S6 BrS mutations green triangles, LQT3 red square, Lenègre disease blue circles, overlapying BrS and Lenègre disease trapezoid pink and black triangle atrial standing.

Structure of the sodium channel

The Na^+ channel acts in phase 0 of depolarization (P wave & QRS)

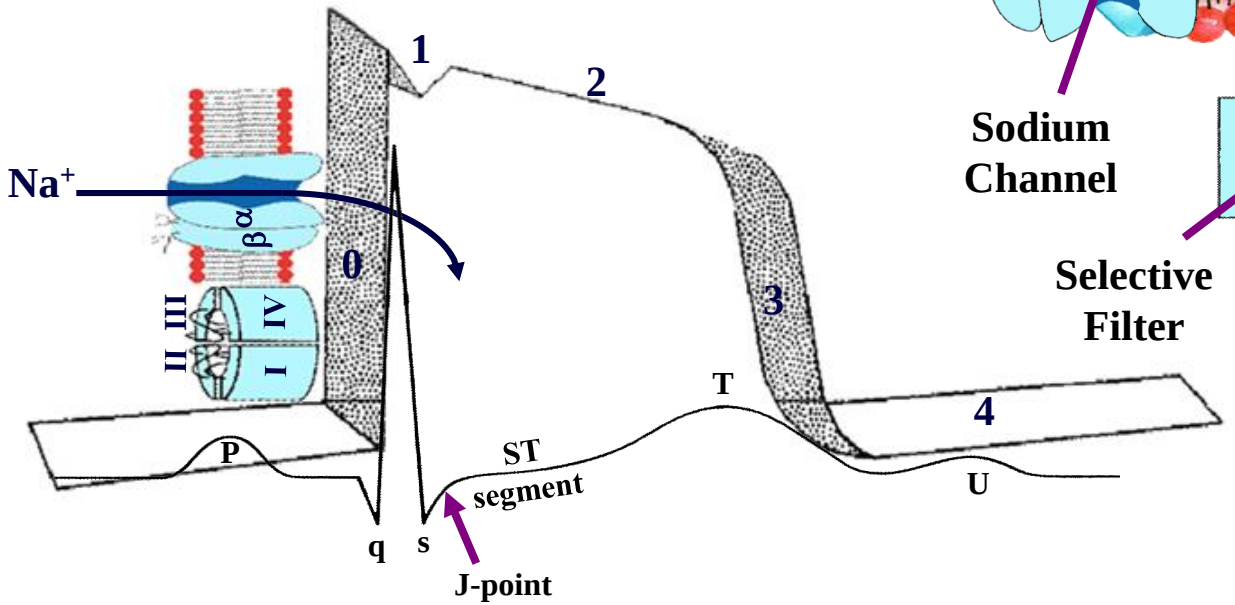

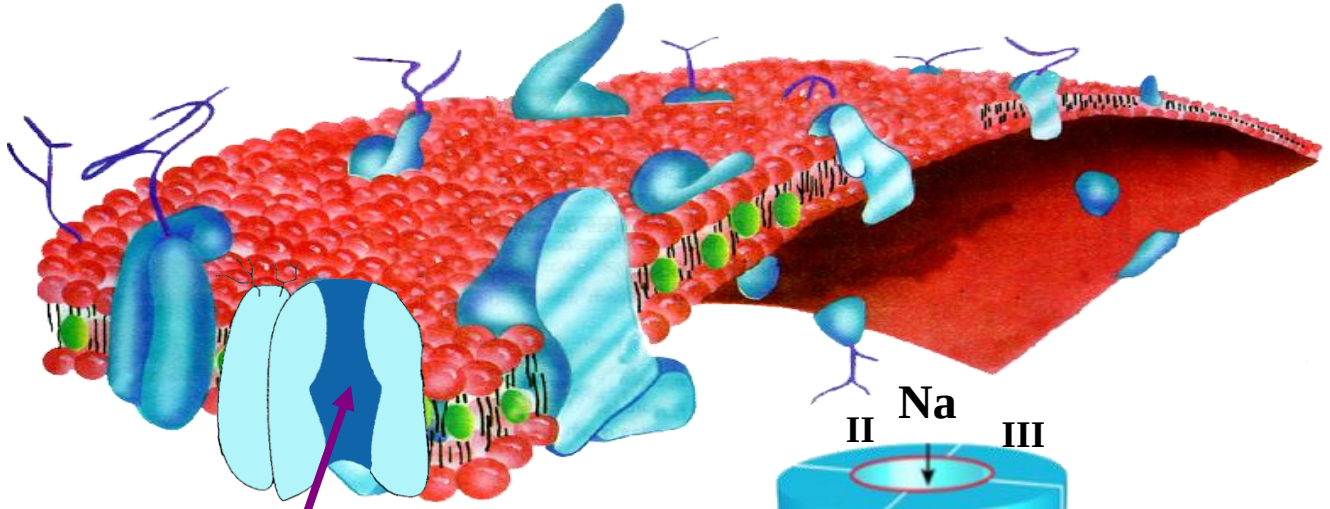

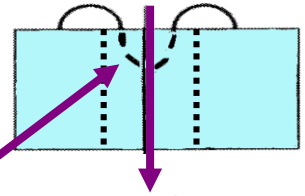

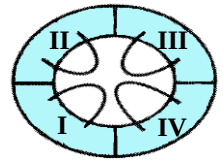

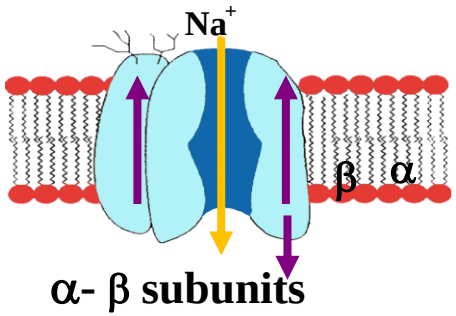

Characteristics of the Na^+ channel. This is a protein structure, formed by four modules that surround a central pore. This channel has a main structure, called α and other surrounding accessory ones called β1 and β-2. This channel is very important in stimulus conduction and cell activation. Inherited mutations in SCN5A, the gene encoding the cardiac Na^+ channel, provoke life-threatening cardiac arrhythmias, often by modifying these voltage-dependent conformational changes. $Na_v1.5$ consists of four domains (DI–DIV), each containing six transmembrane segments (S1–S6); S4 segments are positively charged and act as voltage sensors.

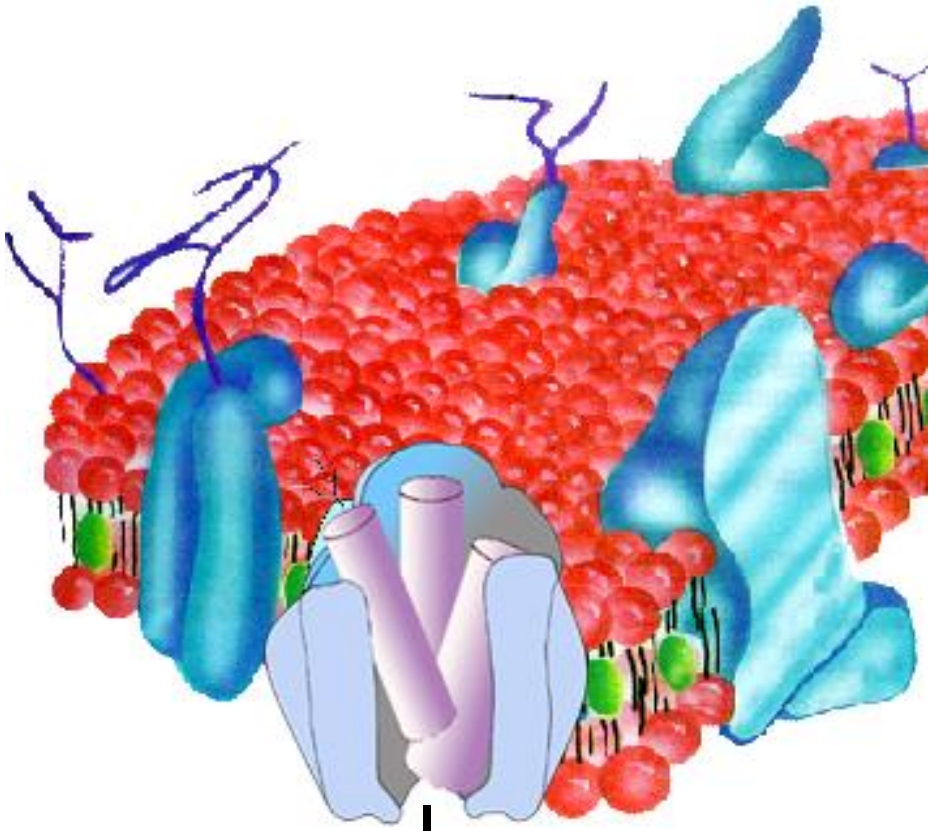

STATES OF THE SODIUM CHANNEL

CLOSED

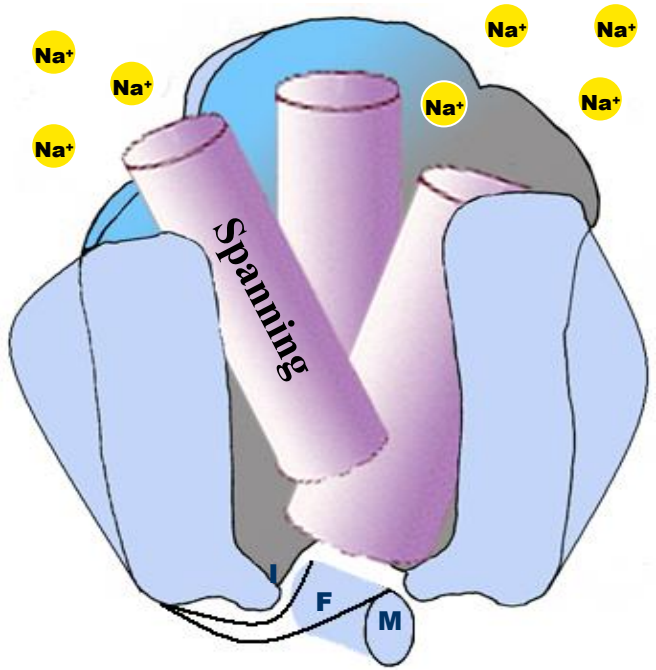

OPEN

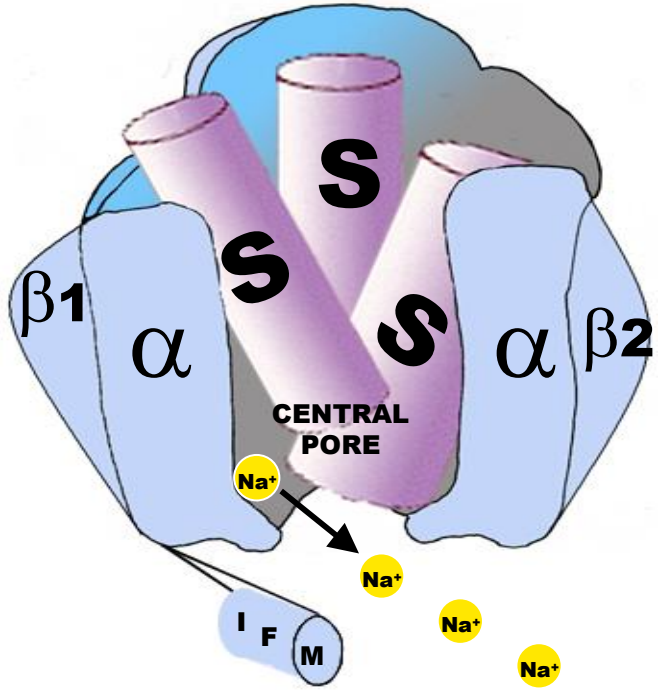

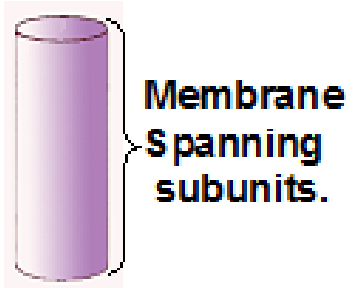

The critical residue (Phe1489F) is shown as occluding the intracellular mouth of the pore.

Transmembrane APs from epicardium, endocardium and midmyocardium (M cells): repolarization mechanism

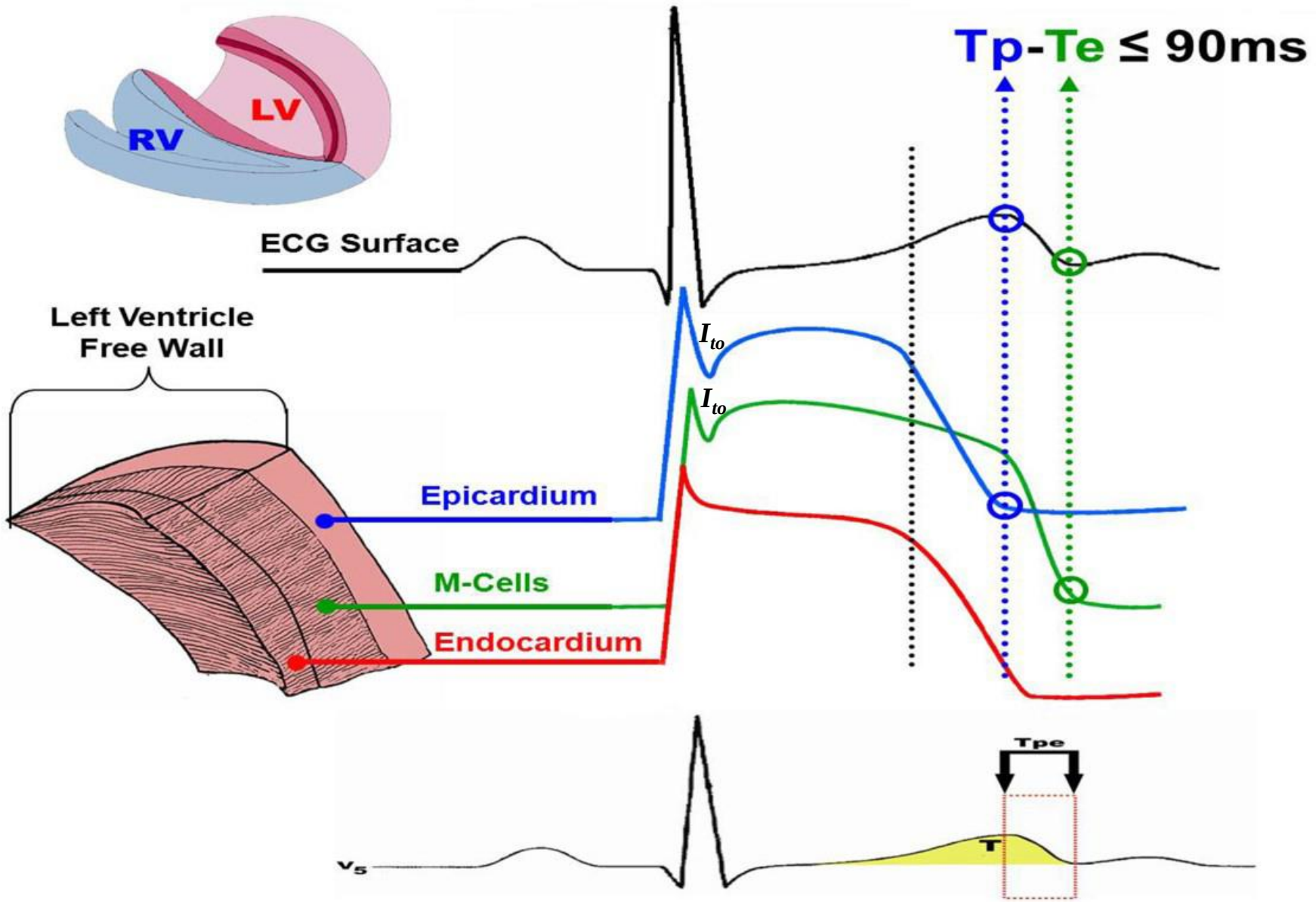

A prominent AP notch in the epicardium mediated by I_{to} channels is responsible for the appearance of J wave on the ECG of BrS, IVF and o.

References

1. Antzelevitch C: Molecular biology and cellular mechanisms of Brugada and long QT syndromes in infants and young children. J Electrocardiol 2001;34(Suppl):177-81.
2. Antzelevitch C, Brugada P, Borggrefe M, et al. Brugada syndrome: report of the second consensus conference. Heart Rhythm.2005; 2(4): 429-40.
3. Antzelevitch C. Brugada syndrome. Pacing Clin Electrophysiol. 2006; 29 (10): 1130-59.
4. Bezzina CR, Barc J, Mizusawa Y, et al. Common variants at SCN5A-SCN10A and HEY2 are associated with Brugada syndrome, a rare disease with high risk of sudden cardiac death. Nat Genet. 2013;45(9):1044-9.
5. Boukens BJ, Sylva M, de Gier-de Vries C, et al. Reduced sodium channel function unmasks residual embryonic slow conduction in the adult right ventricular outflow tract. Circ Res. 2013;113(2):137-41.
6. Bueno-Orovio A, Cherry EM, Evans SJ, Fenton FH. Basis for the Induction of Tissue-Level Phase-2 Reentry as a Repolarization Disorder in the Brugada Syndrome. Biomed Res Int. 2015;2015:197586.
7. Burashnikov A, Antzelevitch C. Late-phase 3 EAD. A unique mechanism contributing to initiation of atrial fibrillation. Pacing Clin Electrophysiol. 2006;29(3):290-5.
8. Calò L, Giustetto C, Martino A, et al. A New Electrocardiographic Marker of Sudden Death in Brugada Syndrome: The S-Wave in Lead I.J Am Coll Cardiol. 2016;67(12):1427-40.
9. Conte G, de Asmundis C, Sieira J, et al. Prevalence and Clinical Impact of Early Repolarization Pattern and QRS-Fragmentation in High-Risk Patients With Brugada Syndrome. Circ J. 2016;80(10):2109-16.
10. Coronel R, Casini S, Koopmann TT et al. Right ventricular fibrosis and conduction delay in a patient with clinical signs of Brugada syndrome: a combined electrophysiological, genetic, histopathologic, and computational study. Circulation 2005;112(18):2769-77.
11. Corrado D, Nava A, Buja G, et al. Familial cardiomyopathy underlies syndrome of right bundle branch block, ST segment elevation and sudden death. J Am Coll Cardiol. 1996;27(2):443-8.
12. Corrado D, Basso C, Buja G, Nava A, Rossi L, Thiene G. Right bundle branch block, right precordial st-segment elevation, and sudden death in young people. Circulation. 2001;103(5):710-7.
13. de Micheli A, Medrano GA. Diagnosis of the myocardial inactivatable zone in the presence of right and bilateral intraventricular blocks. Arch Inst Cardiol Mex. 1988;58(6):575-86.

14. Dinckal MH, Davutoglu V, Akdemir I, et al. Incessant monomorphic ventricular tachycardia during febrile illness in a patient with Brugada syndrome: Fatal electrical storm. 2003;5(3):257-61.
15. Elizari MV, Levi R, Acunzo RS, et al. Abnormal expression of cardiac neural crest cells in heart development: a different hypothesis for the etiopathogenesis of Brugada syndrome. Heart Rhythm. 2007;4(3):359-65.
16. Ewart JL, Cohen MF, Meyer RA, et al. Heart and neural tube defects in transgenic mice overexpressing the Cx43 gap junction gene. Development. 1997;124(7):1281-92.
17. Frigo G, Rampazzo A, Bauce B, et al. Homozygous SCN5A mutation in Brugada syndrome with monomorphic ventricular tachycardia and structural heart abnormalities. Europace. 2007;9(6):391-7.
18. Gittenber-de Groot AC, Poelmann RE. Normal and abnormal cardiac development. In: Moller I, Hoffman J Churchill CC, editors. Pediatric Cardiovascular medicine. New York: Churchill Livingstone; 2000. P. 3-20.
19. Gomes J, Finlay M, Ahmed AK, et al. Electrophysiological abnormalities precede overt structural changes in arrhythmogenic right ventricular cardiomyopathy due to mutations in desmoplakin-A combined murine and human study. Eur Heart J. 2012;33(15):1942-53.
20. Haïssaguerre M, Extramiana M, Hocini M et al. Mapping and ablation of ventricular fibrillation associated with long-QT and Brugada syndromes. Circulation 2003;108(8):925-8.
21. Hoogendijk MG, Opthof T, Postema PG, et al. The Brugada ECG pattern: a marker of channelopathy, structural heart disease, or neither? Toward a unifying mechanism of the Brugada syndrome. Circ Arrhythm Electrophysiol. 2010;3(3):283-90.
22. Kawamura M, Gerstenfeld EP, Vedantham V, et al. Idiopathic ventricular arrhythmia originating from the cardiac crux or inferior septum: epicardial idiopathic ventricular arrhythmia. Circ Arrhythm Electrophysiol. 2014;7(6):1152-8.
23. Kirby ML, Gale TF, Stewart DE. Neural crest cells contribute to normal aorticopulmonary septation. Science. 1983;220(4601):1059-61.
24. Kusano KF, Taniyama M, Nakamura K. Atrial fibrillation in patients with Brugada syndrome relationships of gene mutation, electrophysiology, and clinical backgrounds. J Am Coll Cardiol. 2008;51(12):1169-75
25. Lambiase PD, Ahmed AK, Ciaccio EJ, et al. High-density substrate mapping in Brugada syndrome: combined role of conduction and repolarization heterogeneities in arrhythmogenesis. Circulation. 2009;120(2):106-17, 1-4.
26. Letsas KP, Weber R, Astheimer K, et al. Predictors of atrial tachyarrhythmias in subjects with type 1 ECG pattern of Brugada syndrome. Pacing Clin Electrophysiol. 2009;32(4):500-5.
27. Letsas KP, Asvestas D, Vlachos K, et al. Electrocardiographic characteristics of premature ventricular contractions in subjects with type 1 pattern of Brugada syndrome. J Electrocardiol. 2014;47(3):351-5.

28. Luna Filho B, Bocanegra JA, Pfeferman A, Andrade JL, Martinez Filho EE. Fascicular block of the His bundle: critical approach for its identification. Arq Bras Cardiol. 1989;53(5):261-5.
29. Medrano GA, Attie F, Castro A, de Micheli A, Morún Simão C. Electrocardiograma en el niño normal. Arch Inst Cardiol Mex 1978;48(2):320–34.
30. Morita H, Zipes DP, Fukushima-Kusano K et al. Repolarization heterogeneity in the right ventricular outflow tract: correlation with ventricular arrhythmias in Brugada patients and in an in vitro canine Brugada model. Heart Rhythm. 2008;5:725-33.
31. Nademanee K, Veerakul G, Chandanamattha P, et al. Prevention of ventricular fibrillation episodes in Brugada syndrome by catheter ablation over the anterior right ventricular outflow tract epicardium. Circulation 2011;123(12):1270-9.
32. Olde Nordkamp LR, Wilde AA, Tijssen JG, Knops RE, van Dessel PF, de Groot JR. The ICD for primary prevention in patients with inherited cardiac diseases: indications, use, and outcome: a comparison with secondary prevention. Circ Arrhythm Electrophysiol. 2013;6:91-100.
33. Osher HL, Wolff L. Electrocardiographic pattern simulating acute myocardial injury. Am J Med Sci. 1953;226(5):541–5.
34. Ou B, Nakagawa M, Kajimoto M, et al. Heterogeneous expression of connexin 43 in the myocardium of rabbit right ventricular outflow tract. Life Sci. 2005;77(1):52-9.
35. Pastore CA, Pinho JA, Pinho C, et al. II Diretrizes da sociedade brasileira de cardiologia sobre análise e emissão de laudos eletrocardiográficos. Arq Bras Cardiol. 2016;106(4 Suppl 1):1-23.
36. Patterson E, Po SS, Scherlag BJ, Lazzara R. Triggered firing in pulmonary veins initiated by in vitro autonomic nerve stimulation. Heart Rhythm. 2005;2(6):624-31.
37. Patterson E, Lazzara R, Szabo B, et al. Sodium-calcium exchange initiated by the Ca2+ transient: an arrhythmia trigger within pulmonary veins. J Am Coll Cardiol. 2006;47(6):1196-206.
38. Pérez Riera AR, Ferreira C, Schapachnik E. Value of 12 Lead ECG and Derived Methodologies in the Diagnosis of Brugada Disease. Chapter 7 In The Brugada Syndrome From Bench to Bedside. Edited By: Charles Antzelevitch. Blackwell Publishing; 2005.
39. Pérez Riera AR, Filho CF, Uchida AH, Zhang L, Antzelevitch C, Schapachnik E, Dubner S, Ferreira C. Study of the extent of the information of cardiologists from São Paulo city, Brazil, regarding a low-prevalence entity: Brugada syndrome. Ann Noninvasive Electrocardiol. 2008;13(4):352-63.
40. Peréz-Riera AR, Ferreira Filho C, International VCG Investigators Group. Do patients with electrocardiographic Brugada type 1 pattern have associated right bundle branch block? A comparative vectorcardiographic study. Europace. 2012;14(6):889-97.

41. Peters S, T.M., Denecke S, Koehler B, Results of ajmaline testing in patients with arrhythmogenic right ventricular dysplasia-cardiomyopathy. Int J Cardiol. 2004;95(2-3):207-10.
42. Pinar-Bermudez E, Garcia-Alberola A, Martinez Sanchez J, et al. Spontaneous sustained monomorphic ventricular tachycardia after administration of ajmaline in a patient with Brugada syndrome. Pacing Clin Electrophysiol 2000;23(3):407-9.
43. Pitzalis MV, Anaclerio M, Iacoviello M, et al. QT-interval prolongation in right precordial leads: an additional electrocardiographic hallmark of Brugada syndrome. J Am Coll Cardiol. 2003;42(9):1632-7.
44. Poelmann RE, Gittenberger-de Groot AC. A subpopulation of apoptosis-prone cardiac neural crest cells targets to the venous pole: multiple functions in heart development? Dev Biol. 1999;207(2):271-86.
45. Poelzing S, Akar FG, Baron E, Rosenbaum DS. Heterogeneous connexin43 expression produces electrophysiological heterogeneities across ventricular wall. Am J Physiol Hear Circ Phisiol. 2004;286(5):H2001-9.
46. Rodríguez-Mañero M, de Asmundis C, Sacher F, et al. T-Wave Oversensing in Patients With Brugada Syndrome: True Bipolar Versus Integrated Bipolar Implantable Cardioverter Defibrillator Leads: Multicenter Retrospective Study. 2015;8(4):792-8
47. Rodríguez-Mañero M, Sacher F, de Asmundis C, et al. Monomorphic ventricular tachycardia in patients with Brugada syndrome: A multicenter retrospective study. Heart Rhythm. 2016;13(3):669-82.
48. Rossenbacker T, Priori SG. The Brugada syndrome. Curr Opin Cardiol. 2007;22(3):163-70.
49. Rusconi L, Nava A, Sermasi S, Antonioli GE. The left posterior fascicular block: is the diagnosis possible only by ECG? G Ital Cardiol. 1980;10(9):1129-34.
50. Sacher F, Probst V, Iesaka Y et al. Outcome after implantation of a cardioverter-defibrillator in patients with Brugada syndrome: a multicenter study. 2006;114(22):2317-24.
51. Sacher F, Jesel L, Jais P, Haïssaguerre M. Insight into the mechanism of Brugada syndrome: epicardial substrate and modification during ajmaline testing. Heart Rhythm. 2014;11(4):732-4.
52. Sastry BK, Narasimhan C, Soma Raju B. Brugada syndrome with monomorphic ventricular tachycardia in a one-year-old child. Indian Heart J. 2001;53(2):203-5.
53. Schott JJ, Alshinawi C, Kyndt F, et al. Cardiac conduction defects associate with mutations in SCN5A. Nat Genet. 1999;23(1):20-1.
54. Shimada M, Miyazaki T, Miyoshi S, et al. Sustained monomorphic ventricular tachycardia in a patient with Brugada syndrome. Jpn Circ J. 1996;60(6):364-70.

55. Smits JP, Eckardt L, Probst V, et al. Genotype-phenotype relationship in Brugada syndrome: electrocardiographic features differentiate SCN5A-related patients from non-SCN5A-related patients. J Am Coll Cardiol. 2002;40(2):350-6.
56. Söhl G, Willecke K. Gap junctions and the connexin protein family. Cardiovasc Res. 2004;62(2):228-32.
57. Tobias NM, Pastore CA, Moffa PJ, et al. Divisional blocks of the right branch in Chagas' cardiomyopathy. Arq Bras Cardiol. 1986;47(6):387-91.
58. van den Hoff MJ, Moorman AF, Ruijter JM, et al. Myocardialization of the cardiac outflow tract. Dev Biol. 1999;212(2):477-90.
59. Veltmann C, Barajas-Martinez H, Wolpert C, et al. Further Insights in the Most Common SCN5A Mutation Causing Overlapping Phenotype of Long QT Syndrome, Brugada Syndrome, and Conduction Defect. J Am Heart Assoc. 2016;5(7). pii: e003379.
60. Vichi FL, Romero LC, Arévalo JR. The prevalence of branch and left fascicular blocks in the bundle of His in Chagas' cardiomyopathy. Arq Bras Cardiol. 1982;39(2):87-8.
61. Waldo KL, Lo CW, Kirby ML. Connexin 43 expression reflects neural crest patterns during cardiovascular development. Dev Biol. 1999;208(2):307-23.
62. Yamada KA, Kanter EM, Green KG, Saffitz JE. Transmural distribution of connexins in rodent hearts. J Cardiovasc Electrophysiol. 2004;15(6):710-5.
63. Zhang P, Tung R, Zhang Z, et al. Characterization of the epicardial substrate for catheter ablation of brugada syndrome. Heart Rhythm. 2016;13(11):2151-8.
64. Zumhagen S, Spieker T, Rolinck J, et al. Absence of pathognomonic or inflammatory patterns in cardiac biopsies from patients with Brugada syndrome. Circ Arrhythm Electrophysiol. 2009;2(1):16-23.